

**VASCULARISED BONE TISSUE ENGINEERING:
ENDOTHELIAL PROGENITOR CELLS AND HUMAN MESENCHYMAL STEM
CELLS COCULTURE IN 3D HONEYCOMB SCAFFOLDS AND THE EFFECT OF
BI-ROTATIONAL BIOREACTOR AND HYPOXIC MICROENVIRONMENT**

LIU YUCHUN

B.Eng.(Hons), NUS

**A THESIS SUBMITTED
FOR THE DEGREE OF DOCTOR OF PHILOSOPHY**

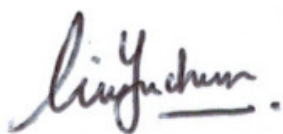
**DEPARTMENT OF MECHANICAL ENGINEERING
NATIONAL UNIVERSITY OF SINGAPORE**

2012

Declaration

I hereby declare that this thesis is my original work and it has been written by me in its entirety. I have duly acknowledged all the sources of information which have been used in the thesis.

This thesis has also not been submitted for any degree in any university previously.

A handwritten signature in black ink, appearing to read 'Liu Yuchun', with a horizontal line underneath the name.

Liu Yuchun

18 December 2012

Acknowledgements

It is a pleasure recalling the past few delightful years of my PhD journey as I pen down the names of many people whom I would like to thank for making this PhD thesis possible.

First and foremost, I owe my deepest gratitude to my two supervisors Prof Teoh Swee-Hin and A/Prof Jerry Chan. I would like to thank them for their constant sharing of knowledge and ideas, their patience and understanding, and the many hours they have each dedicated to sit down with me in person to guide and advise me in scientific thinking, planning, writing and making presentations. Their supervision in combination was like the Yin and Yang put together that completed me, developing me personally and scientifically. I am also indebted to them for the many opportunities that they have laid out for my exploration during the time of my PhD journey, exposing me to various aspects of research and the life of academia. It was in their selflessness and enthusiasm that I found inspiration and encouragement that stretched me beyond limits I never imagined I could achieve.

I am also grateful to Prof Mahesh Choolani and Dr Chui Chee Kong for their support during my postgraduate studies, as well as many fellow colleagues especially Mark, Citra, Yanti, Zhiyong, Sonia, Eddy, Niraja, Lay Geok, Daren, Priya, Aniza, Erin, Zuyong, Qinyuan, Lim Jing, Wang Zhuo, Julie, Joan, Yiping, Chin Wen (and many others!) for their camaraderie and advice – they have all been a great help to me. I would also like to thank the administrative staff, Ms Sharen Teo (Mechanical Engineering) and Ms Ginny Chen (Obstetrics & Gynaecology) laboratories for their kind assistance these years.

It has been a pleasure to work on a collaborative project under the guidance of Prof Roger Kamm, who has made available his support in many ways. I am extremely grateful to his kind supervision and the various opportunities he had provided me with, allowing me great exposure to various research projects, discussions and ideas outside of my scope of PhD work. It was also a great honour for me to work in his laboratory in Massachusetts Institute of Technology. A big thank you to his laboratory mates, especially Kenichi and Yannis, as well as the administrative staff for providing such a stimulating and friendly working environment!

To the staff of the Cels Vivarium, especially Dr Enoka, Jeremy and James, thank you for taking such great care of my experimental animals; To the NUHS delivery suite for their assistance with sample collection; To the other collaborators whom I have interacted with at Singapore-MIT Alliance for Research and Technology (the many post-docs, graduate students and intern students!), Singapore Polytechnic and QuinXell (especially Dr Lau, Mr Chong, Mr Foo, Yhee Cheng, Huilun and their FYP students), my two RJC students Rebecca and Grace, thank you so much for your kind assistance and friendship. To my undergraduate Bioengineering friends, especially Xiuli, thank you for providing valuable advice and experimental help whenever needed. My gratitude list continues to run long...

Most importantly, I would like to thank my family and Raye for their constant care and love that I have felt in many ways; for their guidance, unwavering support, words of wisdom and encouragement that kept me strong and motivated during both good times and tough times. With gratitude and love, I dedicate this PhD thesis to them.

This work was funded National Medical Research Council of Singapore (NMRC/1179/2008 and NMRC/1268/2010).

Preface – International Publications, Conferences and Awards

Nothing is impossible, the word itself says “I’m Possible”!

~Audrey Hepburn

Preface – International Publications, Conferences and Awards

International Journal Publications

First-authorship

1. **Yuchun Liu**, Swee-Hin Teoh, Mark S K Chong, Eddy S M Lee, Citra N Z Mattar, Nau'shil Kaur Randhawa, Zhi Yong Zhang, Reinhold J. Medina Benavente, Roger D Kamm, Nicholas M Fisk, Mahesh Choolani, Jerry K Y Chan. Vasculogenic and Osteogenesis-Enhancing Potential of Human Umbilical Cord Blood Endothelial Colony-Forming Cells. **Stem Cells**. 2012 Sep;30(9):1911-24
- Featured Top Story in Cord Blood News, Connexion, July 2012
2. **Yuchun Liu**, Swee-Hin Teoh, Mark Chong, Chen-Hua Yeow, Roger D, Kamm; Mahesh Choolani; Jerry K Y Chan. Enhanced Vasculogenic Induction Upon Biaxial Bioreactor Stimulation of Mesenchymal Stem Cells and Endothelial Progenitor Cells Cocultures in 3D Honeycomb Scaffolds for Vascularised Bone Tissue Engineering. **Tissue Engineering Part (A)**. 2012 Oct 26. doi:10.1089/ten.TEA.2012.0187
3. **Yuchun Liu**, Jerry KY Chan, Swee-Hin Teoh. Review on Vascularised Bone Tissue Engineering Strategies: Focus on Coculture Systems. **Journal of Tissue Engineering and Regenerative Medicine**. 2012 Nov 19. doi: 10.1002/term.1617
4. **Yuchun Liu** and Swee-Hin Teoh. Development of Next Generation Scaffolds for Successful Vascularised Bone Tissue Engineering. **Biotechnology Advances**. 2012 Nov 9. doi: 10.1016/j.biotechadv.2012.10.003

Co-authorship

1. Ji-Hoon Bae, Hae-Ryong Song, Hak-Jun Kim, Hong-Chul Lim, Jung-Ho Park, **Yuchun Liu**, Swee-Hin Teoh. Discontinuous release of Bone Morphogenetic Protein-2 (BMP-2) loaded within interconnected pores of honeycombed-like polycaprolactone scaffold promotes bone healing in a large bone defect of rabbit ulna. **Tissue Engineering Part (A)**. 2011 Oct;17(19-20):2389-97
2. Choong Kim, Seok Chung, **Yuchun Liu**, Min-Cheol Kim, Jerry K. Y. Chan, H. Harry Asada and Roger D. Kamm. In vitro angiogenesis assay for the study of cell encapsulation therapy. **Lab on the Chip**. 2012 Aug 21;12(16):2942-50
3. Kenichi Funamoto, Ioannis Zervantonakis, **Yuchun Liu**, Christopher Ochs, Choong Kim, Roger Kamm. A Novel Microfluidic Platform for High-Resolution Imaging of a Three-Dimensional Cell Culture under a Controlled Hypoxic Environment. **Lab on the Chip**. 2012 Nov 21;12(22):4855-63

Conferences and Meetings

Y Liu, WS Chong, TT Foo, YC Chng, MA Choolani, J Chan, SH Teoh. In vitro maturation of large hfMSC-PCL/TCP bone tissue engineered construct through long term culture in a biaxial perfusion flow bioreactor. Joint meeting: International Conference on Materials for Advanced Technologies (ICMAT) and International Union of Materials Research Societies – International Conference in Asia (IUMRS-ICA), 28 June – 3 July 2009, Singapore.

Y Liu, SK Chong, Z Zhang, M Choolani, J Chan, SH Teoh. Generation of vascular networks within osteogenic tissue engineered constructs through the coculture of umbilical cord derived endothelial progenitor cells and fetal bone marrow derived mesenchymal stem cells. 7th Singapore International Congress of O&G (SICOG), 26-29 August 2009, Singapore.

Y Liu, SK Chong, Z Zhang, M Choolani, SH Teoh, J Chan. Generation of vascular networks within bone tissue engineered constructs through the coculture of umbilical cord derived endothelial progenitor cells and fetal mesenchymal stem cells. National Healthcare Group (NHG) Annual Scientific Congress, 16-17 October 2009, Singapore.

Attended 6th World Congress of Biomechanics (WCB), 1-6 August 2010, Singapore.

Attended Singapore-Australia Joint Symposium on Stem Cells and Bioimaging, 24-25 May 2010, Singapore.

Y Liu, SH Teoh, SK Chong, Z Zhang, MA Choolani, J Chan. Human endothelial progenitor stem cells accelerates and potentiates the osteogenic response of bone marrow derived human fetal mesenchymal stem cells through paracrine signalling mechanisms. International Society for Stem Cell Research (ISSCR), 16-19 June 2010, San Francisco, USA.

Attended Global Enterprise for Micro-Mechanics and Molecular Medicine (GEM4), 25-31 July 2010, Singapore.

Y Liu, SH Teoh, SK Chong, Z Zhang, M Choolani, J Chan. Human endothelial progenitor stem cells enhances osteogenic response of bone marrow derived human fetal mesenchymal stem cells through paracrine signalling mechanisms *in vitro* and induces neovasclogenesis *in vivo* prior to bone repair. Tissue Engineering and Regenerative Medicine International Society (TERMIS-AP), 15-17 September 2010, Singapore.

Y Liu, J Chan, SK Chong, Z Zhang, MA Choolani, SH Teoh. Coculture of human endothelial progenitor stem cells and bone marrow-derived human fetal mesenchymal stem cells potentiates osteogenesis through paracrine activity *in vitro* and induces neovasclogenesis within tissue engineered bone grafts *in vivo*. International Bone-Tissue-Engineering Congress (Bone-Tec), 7-10 October 2010, Hannover, Germany.

Y Liu, SH Teoh, SK Chong, Z Zhang, M Choolani, J Chan. Human endothelial progenitor cells & bone marrow-derived human fetal mesenchymal stem cells potentiate osteogenesis via paracrine activity & induce neovasclogenesis in tissue engineered bone grafts. SingHealth Duke-NUS Scientific Congress, 15-16 October

2010, Singapore.

Y Liu, SH Teoh, SK Chong, R Kamm, Z Zhang, M Choolani, J Chan. Role of EPC in vascularised bone tissue engineering. International Society for Stem Cell Research (ISSCR), 15-18 June 2011, Toronto, Canada.

Y Liu, J Chan, SK Chong, Z Zhang, M Choolani, SH Teoh. Cellular interactions of endothelial progenitor cells and mesenchymal stem cells for vascularised bone tissue engineering. Tissue Engineering and Regenerative Medicine International Society (TERMIS-AP), 3-5 August 2011, Singapore.

Y Liu, SK Chong, SH Teoh, Z Zhang, M Choolani, J Chan. Role of EPC: vasculogenic and osteogenic regulator of msc for bone tissue engineering. 8th Singapore International Congress of O&G (SICOG), 25-27 August 2011, Singapore.

Y Liu, SH Teoh, SK Chong, R Kamm, M Choolani, J Chan. Cellular interactions of EPC with MSC: An osteogenic and vasculogenic enhancer for vascularised bone tissue engineering. Stem Cell Biology, 20-24 September 2011, Cold Spring Harbour, New York.

Y Liu, J Chan, SK Chong, Z Zhang, M Choolani, SH Teoh. Vascularised bone tissue engineering using a coculture of endothelial progenitor cells and mesenchymal stem cells. 3rd Asian Biomaterials Congress, 15-17 September 2011, Busan, Korea.

Y Liu, J Chan, R Kamm, SK Chong, M Choolani, SH Teoh. Revolutionary approach to cell cultures: culturing fresh bone marrow aspirates in hypoxia enhances osteogenic differentiation of human fetal mesenchymal stem cells. International Bone-Tissue-Engineering Congress (Bone-Tec), 13-16 October 2011, Hannover, Germany.

Y Liu, J Chan, R Kamm, SK Chong, M Choolani, Z Zhang, SH Teoh. Generating Vascularised Tissue-Engineered Bone Grafts: Endothelial Progenitor Cells in Vasculogenic and Osteogenic Priming of Human Fetal Mesenchymal Stem Cells. International Bone-Tissue-Engineering Congress (Bone-Tec), 13-16 October 2011, Hannover, Germany.

Y Liu, J Chan, R Kamm, SK Chong, M Choolani, SH Teoh. A coculture approach towards increasing vascularisation in bone tissue engineered grafts. 4th International Conference on the Development of Biomedical Engineering (BME4), Regenerative Medicine Conference, 8-10 January 2012, Ho Chi Minh City, Vietnam.

Y Liu. Building vascularised bone tissue-engineered grafts. "Speak Out For Engineering" by Institution of Mechanical Engineers (ImechE, Local Heats), 2 February 2012, Singapore.

Y Liu. Building vascularised bone tissue-engineered grafts. "Speak Out For Engineering" by Institution of Mechanical Engineers (ImechE, Oceania and Asia Regional Heats,), 21 April 2012, Singapore.

Y Liu, J Chan, R Kamm, SK Chong, M Choolani, SH Teoh. Revolutionary approach to cell cultures: culturing fresh bone marrow aspirates in hypoxia enhances osteogenic differentiation of human fetal mesenchymal stem cells. University Obstetrics & Gynaecology Congress (UOGC), 25-27 May 2012, Singapore.

SK Chong, Y Liu, Z Zhang, D Sandikin, C Mattar, M Choolani, J Chan. Human Fetal

Mesenchymal Stem Cells and Endothelial Progenitor Cells for the Generation of Engineered Bone Grafts: A Pre-clinical Study. University Obstetrics & Gynaecology Congress (UOGC), 25-27 May 2012, Singapore.

Z Wang, Y Liu, WS Chong, TT F, SH Teoh. Enhanced osteogenesis of human mesenchymal stem cells under the continuous compressive force by a novel biaxial bioreactor system. World Biomaterials Congress (WBC), 1-5 June 2012, Chengdu, China.

Y Liu, SH Teoh, SK Chong, MA Choolani, J Chan. Mimicking the bone-marrow niche: continuous culture of fresh bone marrow aspirates in hypoxia enhances osteogenic differentiation of human fetal mesenchymal stem cells. International Society for Stem Cell Research (ISSCR), 13-16 June 2012, Yokohama Japan.

Y Liu, J Chan, SK Chong, M Choolani, SH Teoh. The importance of continuous hypoxic exposure for the culture of human fetal mesenchymal stem cells in bone tissue engineering applications. 3rd Tissue Engineering and Regenerative Medicine International Society (TERMIS) World Congress, 5-8 September 2012, Vienna, Austria.

K Funamoto, IK Zervantonakis, Y Liu, R Kamm. Oxygen Tension Control in a Microfluidic Device for Cell Culture. 9th International Conference on Flow Dynamics (ICFD), 19-21 September 2012, Sendai, Japan.

K Funamoto, IK Zervantonakis, Y Liu, CJ Ochs, R Kamm. Computational Simulation to Create Low Oxygen Tension in a Microfluidic Device for Cell Culture. 9th International Conference on Flow Dynamics (ICFD), 19-21 September 2012, Sendai, Japan.

Y Liu. Perfusion Biaxial Rotary Bioreactor for Vascularised Bone Tissue Engineering, 2012 Bioreactor & Growth Environments for Tissue Engineering Training Course, 5-7 November 2012, Keele, United Kingdom.

FS Goh, Y Liu, SH Teoh. Effect of Desferrioxamine on Cytocompatibility, Angiogenesis and Bone Forming Ability of Mesenchymal Stem Cells. International Conference on Cellular & Molecular Bioengineering (ICCMB3), 8-10 Dec 2012, Singapore.

XY Lim, Y Liu, SH Teoh. Effects of Strontium on the Proliferation and Bone Forming Capacity of Human Fetal Mesenchymal Stem Cells Seeded onto Scaffolds. International Conference on Cellular & Molecular Bioengineering (ICCMB3), 8-10 Dec 2012, Singapore.

R Akhilandeshwari, Y Liu, J Lim, SH Teoh. Determination of Compressive Range of Scaffolds for Bone Tissue Engineering in Biaxial Bioreactor. International Conference on Cellular & Molecular Bioengineering (ICCMB3), 8-10 Dec 2012, Singapore.

Y Liu, J Chan, SH Teoh. Vascularised Bone Tissue Engineering. International Conference on Cellular & Molecular Bioengineering (ICCMB3), 8-10 Dec 2012, Singapore.

Awards

2009 - Best Poster Award at ICMAT, Singapore

2010 - Top 10 selected Best Posters, Translational Research Category at
SingHealth Duke-NUS Scientific Congress 2010, Singapore

2010 - Best Poster Award at Bone-Tec, Hannover, Germany

2011 - Travel Award at ISSCR, Toronto, Canada

2011 - Best Young Scientist Award at Bone-Tec 2011, Hannover, Germany

2011 - World's Fastest Cell at the 1st World Cell Race held at the American Society
for Cell Biology, Denver, Colorado.

Submitted the human fetal bone marrow derived mesenchymal stem cells on behalf
of the team, which came in first with a cellular speed record of 5.2 microns per
minute amongst 70 other submissions globally.

2012 - Travel Award at ISSCR, Yokohama, Japan

2012 - 1st Prize, "Speak Out For Engineering" Local Heats by Institution of
Mechanical Engineers

2012 - 2nd Prize, "Speak Out For Engineering" Regional Heats (Oceania and Asia)
by Institution of Mechanical Engineers

2012 - S Arulkumaran Young Investigator (Scientist) at University Obstetrics &
Gynaecology Congress 2012, Singapore

Table of Contents

| | |
|--|-------|
| Declaration | i |
| Acknowledgements | ii |
| Preface – International Publications, Conferences and Awards | v |
| International Journal Publications | v |
| First-authorship | v |
| Co-authorship | vi |
| Conferences and Meetings | vii |
| Awards | x |
| Table of Contents | xi |
| Summary | xv |
| List of Tables | xvi |
| List of Figures | xviii |
| List of Symbols | xxiv |
| Chapter 1 – Introduction | 2 |
| 1.1 Bone Grafts and Current Unmet Needs | 2 |
| 1.2 Non-union Fractures | 2 |
| 1.3 Current Strategies for Bone Repair | 3 |
| 1.3.1 Autologous Grafts | 4 |
| 1.3.2 Allogenic Grafts | 4 |
| 1.3.3 Synthetic Grafts | 5 |
| 1.4 Bone Tissue Engineering | 5 |
| 1.4.1 Limitations in Bone Tissue Engineering | 6 |
| 1.5 Importance of Vascularisation | 7 |
| 1.5.1 Vascularisation in Bone Tissue Engineering | 7 |
| 1.5.2 Vascularisation in Natural Bone Repair Processes | 8 |
| 1.5.3 Periosteum and Its Vasculature | 9 |
| 1.6 Motivation of Study | 10 |
| 1.7 Proposed Approach | 11 |
| 1.7.1 Vascularised BTE – A Mimicry of Natural Bone Tissue | 11 |
| 1.7.2 Aims and Hypotheses | 12 |
| 1.7.2.1 Main Aim | 12 |
| 1.7.2.2 Hypothesis 1 | 13 |
| 1.7.2.3 Hypothesis 2 | 13 |
| 1.7.2.4 Hypothesis 3 | 13 |
| 1.7.3 Novelty and Clinical Implications | 13 |
| Chapter 2 – Literature Review | 16 |
| 2.1 The Skeletal System | 16 |
| 2.2 Anatomy of Bone | 16 |
| 2.3 Composition of Bone | 18 |
| 2.3.1 Bone Cells | 18 |
| 2.3.2 Bone Matrix | 19 |
| 2.4 Natural Bone Forming Process | 20 |
| 2.4.1 Endochondral Ossification | 20 |
| 2.4.2 Distraction Osteogenesis | 21 |
| 2.5 Physiological Microenvironment of Bone | 22 |
| 2.5.1 Biomechanical Cues | 23 |
| 2.5.2 Oxygen Tension Cues | 24 |
| 2.5.3 Biochemical Cues | 26 |
| 2.6 Bone Tissue Engineering | 30 |
| 2.6.1 Four-Stage Bone Formation in Bone Tissue Engineering | 30 |
| 2.6.2 Strategies in Bone Tissue Engineering | 32 |

| | |
|---|----|
| 2.6.2.1 Growth Factors Approach | 32 |
| 2.6.2.2 Cell-Based Approach | 34 |
| 2.7 Vascularisation Strategies in Bone Tissue Engineering | 34 |
| 2.7.1 'Smart'-scaffolds and Growth Factors | 36 |
| 2.7.2 Prevascularisation Techniques | 37 |
| 2.7.2.1 <i>In Vivo</i> Prevascularisation | 38 |
| 2.7.2.2 <i>In Vitro</i> Prevascularisation | 38 |
| 2.8 Components of Bone Tissue Engineering | 39 |
| 2.8.1 Scaffolds | 40 |
| 2.8.1.1 Biomaterial Selection | 42 |
| 2.8.1.2 Polycaprolactone | 43 |
| 2.8.1.3 Tri-calcium Phosphate | 44 |
| 2.8.1.4 Proposed Scaffold – Polycaprolactone/Tri-calcium Phosphate Composite | 44 |
| 2.8.2 Cellular Sources | 46 |
| 2.8.2.1 Osteogenic Cells | 46 |
| 2.8.2.2 Mesenchymal Stem Cells | 48 |
| 2.8.2.3 Mesenchymal Stem Cells in Bone Tissue Engineering | 49 |
| 2.8.2.4 Proposed Cell Type – Human Fetal Mesenchymal Stem Cells | 50 |
| 2.8.2.5 Endothelial Cell Types | 51 |
| 2.8.2.6 Endothelial Progenitor Cells | 52 |
| 2.8.2.7 Endothelial Progenitor Cells in Fracture Healing | 53 |
| 2.8.2.8 Proposed Endothelial Cell Type – Umbilical Cord Blood-Endothelial Progenitor Cells | 54 |
| 2.8.3 Bioreactor | 56 |
| 2.8.3.1 Proposed Bioreactor – Perfusion Biaxial Bioreactor | 57 |
| 2.8.4 Hypoxia in the Natural Physiology | 60 |
| 2.8.4.1 Hypoxia and Mesenchymal Stem Cells | 60 |
| 2.8.4.2 Hypoxia and Bone Repair | 61 |
| 2.9 Coculture Systems | 62 |
| 2.9.1 Trends in Coculture Systems | 62 |
| 2.9.2 Cocultures in Vascularised Bone Tissue Engineering | 63 |
| 2.9.3 Considerations for Coculture Systems | 67 |
| 2.9.3.1 Choice of Media | 67 |
| 2.9.3.2 Seeding Methodology | 70 |
| Chapter 3 - Materials and Methods | 74 |
| 3.1 Samples, Animals and Ethics | 74 |
| 3.2 Cells | 74 |
| 3.2.1 Cell Isolation, Culture and Characterisation | 74 |
| 3.2.1.1 Human Fetal Bone Marrow Derived Mesenchymal Stem Cells | 74 |
| 3.2.1.2 Human Umbilical Cord Blood Derived Endothelial Progenitor Cells | 75 |
| 3.2.2 Lentiviral-Transduction of hfMSC and EPC | 76 |
| 3.3 Flow Cytometry | 76 |
| 3.4 Multilineage Differentiation | 77 |
| 3.4.1 Adipogenic Differentiation | 77 |
| 3.4.2 Chondrogenic Differentiation | 77 |
| 3.4.3 Osteogenic Differentiation | 77 |
| 3.5 Preparation of EPC Conditioned Media | 77 |
| 3.6 Osteogenic Assays | 78 |
| 3.6.1 Calcium Assay | 78 |
| 3.6.2 Alkaline Phosphatase Assay | 78 |
| 3.6.3 Von Kossa Staining | 78 |
| 3.7 Antibody Array and Microarray Scanning | 79 |
| 3.8 Microarray Analysis of Gene Expression | 79 |
| 3.9 Quantitative Polymerase Chain Reaction Analysis | 80 |

| | |
|--|-----|
| 3.10 Cellular Viability Assay | 81 |
| 3.11 Growth Kinetics and Colony-Forming Unit-Fibroblasts Assay | 81 |
| 3.12 Preparation of Cellular-Scaffold Constructs | 82 |
| 3.12.1 Scaffold Fabrication and Treatment | 82 |
| 3.12.2 Cell Loading..... | 82 |
| 3.13 Bioreactor Setup..... | 83 |
| 3.14 Imaging..... | 83 |
| 3.14.1 Phase Contrast Light Microscopy..... | 83 |
| 3.14.2 Confocal Microscope | 84 |
| 3.14.3 Scanning Electron Microscope..... | 84 |
| 3.14.4 Micro-Computed Tomography | 84 |
| 3.15 Animal Work | 84 |
| 3.15.1 Subcutaneous Implantations in Mice..... | 84 |
| 3.15.2 Microfil Perfusion | 85 |
| 3.15.3 Histology..... | 85 |
| 3.15.3.1 Capillary Density Analysis | 86 |
| 3.15.4 Immunohistochemistry | 86 |
| 3.15.4.1 Human:Mouse Chimerism..... | 86 |
| 3.15.4.2 Staining of CD31 Structures..... | 86 |
| 3.15.4.3 Osteopontin Staining..... | 87 |
| 3.15.5 Image Analysis | 87 |
| 3.15.5.1 ImageJ Software | 87 |
| 3.15.5.2 Imaris Software | 87 |
| 3.16 Statistical Analysis..... | 87 |
| Chapter 4 – Coculture of Human Umbilical Cord Blood Endothelial Colony-Forming Cells with Human Fetal Mesenchymal Stem Cells for the Generation of Vascularised BTE Grafts | 89 |
| 4.1 Abstract..... | 89 |
| 4.2 Introduction..... | 90 |
| 4.3 Experimental Approach | 91 |
| 4.4 Results | 91 |
| 4.4.1 Cell Characterisation..... | 91 |
| 4.4.1.1 Human Fetal Mesenchymal Stem Cells..... | 91 |
| 4.4.1.2 Endothelial Progenitor Cells..... | 93 |
| 4.4.2 Optimal Media for Osteogenic Differentiation of Coculture In Vitro..... | 94 |
| 4.4.3 Optimal Coculture Ratio for Osteogenic Differentiation In Vitro | 96 |
| 4.4.4 Mechanism of Action of EPC for Osteogenic Potentiation..... | 98 |
| 4.4.5 Identity of EPC Secretome..... | 101 |
| 4.4.6 Osteogenic and Angiogenic Capacity of UCB versus PB-EPC..... | 104 |
| 4.4.7 In Vitro Vessel Forming Ability of EPC/hfMSC Cocultures | 106 |
| 4.4.8 In Vivo Vasculogenesis of EPC/hfMSC Cocultures | 108 |
| 4.4.9 Ectopic Bone Forming Ability of EPC/hfMSC Cocultures | 112 |
| 4.5 Discussion | 113 |
| 4.6 Conclusion..... | 119 |
| Chapter 5 – Dynamic Biaxial Bioreactor Culture for <i>In Vitro</i> Maturation of Vascularised BTE Coculture Grafts | 121 |
| 5.1 Abstract..... | 121 |
| 5.2 Introduction..... | 122 |
| 5.3 Experimental Approach | 124 |
| 5.4 Results | 124 |
| 5.4.1 Effect of Biaxial Bioreactor Culture on <i>In Vitro</i> Vessel Formation | 124 |
| 5.4.2 Effect of Biaxial Bioreactor Culture on Mineralisation <i>In Vitro</i> | 126 |
| 5.4.3 Effect of Biaxial Bioreactor Culture on Bone Formation and Vasculogenesis <i>In Vivo</i> | 128 |

| | |
|---|-----|
| 5.4.4 Effect of Biaxial Bioreactor Culture on Cell Viability and Human:Mouse Chimerism | 130 |
| 5.5 Discussion | 131 |
| 5.6 Conclusion..... | 135 |
| Chapter 6 – Culture Methodologies of hfMSC Under Hypoxia for the Enhancement of Growth Kinetics and Osteogenic Differentiation..... | 137 |
| 6.1 Abstract | 137 |
| 6.2 Introduction..... | 138 |
| 6.3 Experimental Approach | 139 |
| 6.4 Results | 140 |
| 6.4.1 Effect of Hypoxia ^{short-term} on hfMSC Growth Kinetics | 140 |
| 6.4.2 Effect of Hypoxia ^{short-term} on the Osteogenic Differentiation of hfMSC..... | 141 |
| 6.4.3 Effects of Hypoxia ^{precondition} on Retaining hfMSC Properties | 144 |
| 6.4.4 Ex Vivo Expansion in Hypoxia ^{continuous} on hfMSC Growth Kinetics..... | 146 |
| 6.4.5 Ex Vivo Expansion in Hypoxia ^{continuous} on the Osteogenic Differentiation of hfMSC | 147 |
| 6.5 Discussion | 148 |
| 6.6 Conclusion..... | 152 |
| Chapter 7 – Conclusion, Considerations and Future Work | 154 |
| 7.1 Conclusion..... | 154 |
| 7.2 Considerations and Future Work | 155 |
| 7.2.1 Cells: Improving Expansion and Differentiation via Hypoxic Isolation Methods | 156 |
| 7.2.1.1 Endothelial Progenitor Cells..... | 156 |
| 7.2.1.2 Human Fetal Mesenchymal Stem Cells | 161 |
| 7.3.1 Cocultures and their Mechanisms | 162 |
| 7.3.2 Cocultures in Hypoxia | 163 |
| 7.3.3 Coculture Patterning via Bioprinting | 163 |
| 7.4 Bioreactor Development and Optimisation..... | 165 |
| 7.4.1 Optimisation of Timing of Biomechanical Exposure | 165 |
| 7.4.2 Scale-Down Bioreactors | 165 |
| 7.4.3 Introduction of Low Oxygen Tensions into Bioreactor | 166 |
| 7.5 Imaging Tools: High Resolution Tracking of Vessel and Bone Formation | 167 |
| 7.5.1 In Vivo Time-Lapse Tracking in Animal Models..... | 167 |
| 7.5.2 In Vitro Studies in Microfluidic Devices | 168 |
| 7.6 Clinical Feasibility | 169 |
| 7.6.1 Large Orthotopic Animal Models | 169 |
| 7.6.2 Cord Blood Banking..... | 170 |
| 7.7 Regulatory Approval for Clinical Translation | 170 |
| Bibliography | 173 |
| Appendix | 189 |

Summary

Poor angiogenesis impairs bone regeneration, limiting the clinical translation of bone tissue engineered (BTE) grafts for the repair of large defects. In this project, vasculogenic endothelial progenitor cells (EPC) cocultured with osteogenic human fetal mesenchymal stem cells (hfMSC) potentiated its osteogenic differentiation *in vitro* through paracrine signalling and formed an *in vitro* vascular network in the three dimensional honeycomb polycaprolactone/tri-calcium phosphate composite scaffolds. Upon subcutaneous implantation, EPC/hfMSC showed enhanced vascularity and consequentially, improved osteogenicity *in vivo*. Biomechanical stimulation of EPC/hfMSC-grafts in a biaxial bioreactor resulted in increased cell viability, more robust bone formation and increased vasculogenesis compared to its implanted static-cultured coculture. In addition, the maintenance of hfMSC under continuous hypoxic microenvironment upon cell isolation demonstrated enhanced colony-forming ability and osteogenic potential. This thesis explores the use of a coculture of stem cells, in conjunction with bioresorbable scaffolds, bioreactor technologies and a low oxygen microenvironment for the generation of voluminous bone grafts that are capable of rapid vascularisation for facilitating bone repair.

List of Tables

- Table 1-1** Characteristics of the different types of non-union fractures include avascular and vascular non-unions.
- Table 1-2** Proposed BTE approach and the choice of each individual BTE component, including the choice of cells, scaffolds, bioreactor and microenvironment oxygen tensions.
- Table 2-1** Endochondral ossification involves four main stages, namely the inflammatory phase, soft callus fibrocartilagenous formation, hard callus formation and bone remodelling.
- Table 2-2** The process of distraction osteogenesis involves three stages, namely latency, distraction and consolidation.
- Table 2-3** (A-B) Comparison between the natural fracture healing and distraction osteogenesis processes and their various microenvironmental cues that contribute to vascular and bone formation, including the relative up and down expressions of molecular regulators involved in various stages of bone repair and distraction osteogenesis.
- Table 2-4** Four-staged bone forming process relating to the structural bone, its mechanical properties and vessel formation over time of healing; + indicates the relative intensity.
- Table 2-5** A summary of the advantages and disadvantages of *in vitro* and *in vivo* prevascularisation strategies.
- Table 2-6** Basic criteria and considerations when designing a scaffold for use in BTE applications.
- Table 2-7** PCL/TCP scaffold design and its characteristics as reported in literature data.
- Table 2-8** Comparison of different cellular sources, including MSC for their potential in BTE applications.
- Table 2-9** Summary of the main characteristics of mature endothelial cells and its progenitor cells.
- Table 2-10** Comparison between UCB and adult PB-EPC in terms of its colony emergence, growth and vessel forming ability.
- Table 2-11** Comparison of the advantages and disadvantages of the various modes of commonly used bioreactors.
- Table 2-12** (A-B) Citation analysis on the utility of cocultures in tissue engineering and bone tissue engineering respectively, as well as the leading institutions and experts.
- Table 2-13** Summary of various animal models used for implantation of coculture systems in vascularised BTE. * Denotes an orthotopic

implantation in the animal model

| | |
|-------------------|--|
| Table 2-14 | Maintenance of coculture systems in BTE, including media used, coculture ratios and the seeding methodology, with coculture in direct contact unless otherwise stated. |
| Table 2-15 | Advantages and disadvantages of various seeding methodologies of cocultures in vascularised BTE. |
| Table 4-1 | The different media types and their respective constituents are used for identifying the optimal media for directing osteogenic differentiation of the coculture. |
| Table 4-2 | (A) Top highest concentration of proteins found within EPC ^{CM} , of which angiogenic cytokines and other (B) bone related morphogens belonging to the TGF- β superfamily are featured prominently. |
| Table S1 | (A-B) Top 10 most highly expressed osteogenic and angiogenic genes in EPC (n=3 biological replicates) which were expressed in fold terms over the median gene expression (median gene expression = 4.59) include members of the TGF β family such as SMAD1,2,3 and 5, IL6 and the secreted osteogenic stimulants BMP 1,2,4,6,7,8). |
| Table S2 | Microarray data for upregulated osteogenic genes above median value of 4.59, along with relevant heat map colour indicator. |
| Table S3 | Microarray data of upregulated angiogenic genes above median value of 4.59, along with relevant heat map colour indicator. |
| Table S4 | Human Cytokine Antibody Array and its normalised values against the positive control, a biotinylated protein as indicated by the manufacturer. |
| Table S5 | Osteogenesis Genes (shown for 1 UCB x 3 PB), fold difference between UCB-EPC and PB-EPC (n=3), LN2 Values given for UCB and PB-EPC. |
| Table S6 | Angiogenesis Genes (shown for 1 UCB x 3 PB), fold difference between UCB-EPC and PB-EPC (n=3), LN2 Values given for UCB and PB-EPC. |

List of Figures

- Figure 1-1** Four key technologies used in tissue engineering include cells and their biomolecules, scaffolds, bioreactors and imaging tools.
- Figure 1-2** Graphical analysis of the total number of publications and citations on BTE in the past 20 years (Web of Science, 2012).
- Figure 1-3** Three-dimensional rendering of computed tomography scans. (A) Mice femurs showed impairment of fracture repair upon soluble, neutralising VEGF receptor (Fit-IgG) treatment as compared to its controls after 7 days. Callus (blue) and cortical bone (peach). (B) VEGF stimulated repair of a rabbit segmental defect upon exogenous VEGF-treatment (250µg) compared to its placebo on 28 days.
- Figure 1-4** Vascularisation as a key component for successful BTE as well as other areas of tissue engineering where vascularisation is needed.
- Figure 2-1** Anatomy of the long bone and microstructure of vascularised bone tissue and the comparative porosity of compact bone and spongy bone.
- Figure 2-2** A schematic of the hierarchical structure of bone from a sub-nanostructure of collagen molecules to a nanostructure of cylindrically arranged microfibrils to lamellar layers forming the macrostructure of cortical bone.
- Figure 2-3** Vascularised bone anatomy and microenvironmental influences such as biomechanical, microarchitectural and low oxygen tension cues.
- Figure 2-4** (A) Under hypoxic conditions, the HIF-1 α subunit accumulates and is stabilised, allowing it to translocate into the nucleus for dimerisation with the HIF-1 β subunit, forming the HIF-1 complex. This initiates the upregulation of several angiogenic genes and secretion of growth factors. *Figure reproduced from Carmeliet and Jain (Carmeliet and Jain 2000)*. (B) Sprouting of the endothelial cells is induced, resulting in tip cells migrating towards the hypoxic stimulus, with stalk cells following behind. New vascular network forms with the emergence of various branch points overtime.
- Figure 2-5** Growth factor delivery systems and their various entrapment methodologies. Non-covalent strategies include (A-C) physical entrapment released by diffusion with or without degradation of delivery system (D-E) adsorption through physiochemical interactions with material or receptor-proteins (F) ion complexation of growth factors with oppositely charged molecules or *via* (G) covalent means through direct coupling or *via* a bifunctional linker.
- Figure 2-6** Conceptual illustration of cell viability and cell death within the thick scaffold graft towards its core where cells are found more than 200µm away from the blood vessel supply.

- Figure 2-7** Diagrammatic representation of porous scaffold constructs (A) encapsulated with growth factors and its time-dependent control release (B) surface functionalised with growth factors either *via* physical adsorption or covalent immobilisation methods.
- Figure 2-8** An example of an *in vivo* prevascularisation technique. The implant is grown inside the latissimus dorsi muscle, followed by subsequent transplantation in the mandible.
- Figure 2-9** Graphical representation of the molecular weight loss of the 3D scaffold with respect to the growth and remodelling of the tissue-engineered constructs over time.
- Figure 2-10** Illustration of a scaffold with a trabecular-like honeycomb structure and high porosity that allows for vascular infiltration, mass transport and new tissue formation. (Right-hand image) Scanning electron microscopy shows a honeycomb polycaprolactone/tri-calcium phosphate scaffold, with an average pore size within the range of 500µm.
- Figure 2-11** Micro-computed tomography imaging of PCL/TCP composite scaffold showing fine TCP granules interspersed randomly within the polymer matrix.
- Figure 2-12** The process of mesengensis illustrates the ability of MSC to undergo defined differentiate into various cellular lineages, including bone.
- Figure 2-13** hfMSC constructs showed formation of an extensive vasculature network with functional union repair after 12 weeks as compared to little vasculature in the defect region of acellular constructs.
- Figure 2-14** Mechanisms of angiogenesis and vasculogenesis. (a) Sprouting angiogenesis from a pre-existing vessel through the secretion of matrix metalloproteases that degrade the vascular basement membrane, allowing endothelial cells to migrate and form a new vessel branch. (b) EPC forms a vascular plexus, deposits matrix and forms a lumen resulting in the formation of immature capillaries.
- Figure 2-15** The perfusion biaxial bioreactor has two rotational axes (indicated by blue block arrows), with scaffolds pinned and fixed in place while the bioreactor rotates.
- Figure 3-1** (A) Macroscopic view and (B) SEM imaging of the PCL/TCP scaffolds shows a high porosity with an approximate pore size of 500µm and honeycomb microarchitecture.
- Figure 3-2** The perfusion biaxial bioreactor has two rotational axes (indicated by pink block arrows), with scaffolds pinned and fixed in place while the bioreactor rotates.
- Figure 3-3** Diagrammatic representations of scaffold-constructs upon subcutaneous implantations at the dorsal surface of the NOD/SCID mice.
- Figure 4-1** (A) hfMSC had a spindle-like morphology and underwent tri-lineage

differentiation. This was confirmed by Oil-red-O staining for intracytoplasmic vacuoles of neutral fat; Alcian Blue staining showed the presence of glycosaminoglycan in cartilages upon culture in a micro-mass pellet form; von Kossa stains (black) for extracellular calcium deposition. (B) Immunophenotypic characterisation of hfMSC using flow cytometry showed high expression of MSC markers such as (A-C) CD73, CD90, CD105 and did not express hematopoietic and endothelial markers such as (D-F) CD14, CD34 and CD45.

Figure 4-2 Characterisation of UCB-EPC. (Top row from left to right) PCLM of EPC demonstrated typical cobblestone morphology of endothelial cells. EPC differentiated and formed networks when plated on Matrigel. Immunostaining demonstrated expression of (Bottom row from left to right) CD31, von Willebrand Factor, acLDL uptake (red) and VE Cadherin, indicating endothelial phenotype and function. Cell nuclei were counterstained with PI (red) and DAPI (blue) accordingly.

Figure 4-3 BM is necessary to induce osteogenic differentiation of hfMSC. (A) hfMSC laid down extracellular minerals when cultured in BM, while cell debris was observed with EPC in BM. Cells cultured in EGM10 and b-EGM10 did not demonstrate mineralisation. (B) hfMSC cultured in BM showed dark Von Kossa stains for calcium crystals but none in the other study groups. (C) This was confirmed by quantitative calcium assays with only hfMSC grown in BM laying down significant amounts of calcium. All assays were performed on Day 14.

Figure 4-4 EPC/hfMSC in coculture induces earlier osteogenic differentiation of hfMSC. (A) EPC/hfMSC groups in varying ratios displayed earlier mineralisation compared to EPC and hfMSC monocultures. (B) Quantitative ALP measurements with EPC/hfMSC (1:1) demonstrated the earliest ALP peak activity on Day 7. (C) EPC/hfMSC (1:1) cocultures laid down the most calcium on Day 14. “****” ($p < 0.001$).

Figure 4-5 Dose dependent effect of soluble factors in EPCCM enhanced osteogenic differentiation of hfMSC. (A) hfMSC cultured in EPCCM (1:1) and EPCCM (1:10) demonstrated earlier and more extensive mineralisation than when cultured in BM. (B) Greater Von Kossa staining were observed in EPCCM (1:1) and EPCCM (1:10) compared to BM at Day 14 of osteogenic differentiation. (C) EPC^{CM} (1:1) and EPC^{CM} (1:10) displayed higher (2.2 fold and 1.8 fold respectively) peak of ALP activity than BM. (D) Calcium deposited in EPC^{CM} (1:1) and EPC^{CM} (1:10) was consistently higher (1.5 fold and 1.4 fold respectively) than BM in all time points. (E) ALP levels were consistently higher in BM than in basal media, D10, with the coculture displaying highest levels on Day 14. (F) Both hfMSC and EPC/hfMSC cocultures required osteogenic supplements to induce osteogenic differentiation, which was potentiated with coculture, with deposition of calcium after 14 days of induction, further confirmed by Von Kossa staining (G). “****” ($p < 0.001$)

Figure 4-6 Semi-quantitative analysis of EPC^{CM} using the Human Cytokine Antibody Array, where 118 secreted proteins found within EPC^{CM}.

- Figure 4-7** UCB versus adult PB-EPC taken from Medina *et al* (Medina *et al.* 2010) demonstrated higher expression levels of key osteogenic and angiogenic genes using (A) Transcriptomic microarray analysis and (B) qPCR.
- Figure 4-8** EPC potentiate osteogenic programming of hfMSC and *in vitro* tubule formation in the presence of bone inducing components (A) GFP-labelled EPC showed better survival when cultured in BM than in D10. (B) Coculture of GFP-EPC and H2B-RFP-hfMSC (Red fluorescence nuclear staining) resulted in the formation of EPC islets (white arrowheads), leading eventually to the development of tubular structures (yellow arrows) by Day 7 (C) Formation of GFP-EPC vessel-like structures with complex branching points was observed when EPC/hfMSC were cocultured over 14 days within a 3D culture system within a macroporous scaffold.
- Figure 4-9** *In vivo* neovasculogenesis and ectopic bone formation. A) Increased vascularisation of the EPC/hfMSC scaffolds evident three weeks after implantation, as seen after Microfil perfusion (blue vessels). (B) At eight weeks, human blood vessels stained with human specific CD31 (green) were seen coursing through EPC/hfMSC scaffolds but not hfMSC scaffolds. These human vessels can be seen enmeshed with murine vessels (stained red with murine CD31 antibody) as evident in a 50 μm section [merged and stacked confocal images (C)]. EPC/hfMSC scaffolds contained a 2.2 fold ($p=0.001$) higher density of host-derived murine-CD31 positive vessels (red) compared to hfMSC scaffolds (arrows indicating area of human-murine vasculature junctures) (D), while human vessels constituted 30.2% of the total vessel area within the construct (E). (F) Immunostaining with human Lamins A/C demonstrated high levels of chimerism in both scaffolds, with a trend towards lower human cell chimerism in EPC/hfMSC scaffolds compared with hfMSC scaffolds.
- Figure 4-10** (A-B) Von Kossa staining of the implants showed darker level of staining (Scaffold regions has been denoted as S) and a slightly higher level of calcium deposited in EPC/hfMSC scaffolds compared to hfMSC scaffold. “*” ($p<0.05$)
- Figure 5-1** (A) Vessel-like networks were formed only under static conditions of both 2D (white arrows) and 3D cultures on Day 7, but not in dynamic bioreactor cultures or when EPC were cultured alone. (B-C) An extensive *in vitro* vessel network was formed in the statically-cultured EPC/hfMSC cocultures which were observed to increase with scaffold depth on Day 7.
- Figure 5-2** Dynamic bioreactor culture of EPC/hfMSC-constructs induced greater mineralisation compared to static culture. (A) Higher levels of mineralisation were observed within the pores of dynamically-cultured scaffolds by PCLM on Day 14. SEM also showed more prominent network of extracellular matrix formation. (B) Dynamically-cultured constructs showed 1.7 fold higher levels of calcium deposited across all time points compared to static culture ($p<0.001$). (C) FDA/PI staining of EPC/hfMSC cocultures were seen to maintain a high level of viability in both static and dynamic culture as indicated by the live:dead cell ratio (green:red) on Day 14.

- Figure 5-3** Dynamic bioreactor culture induced greater vascularisation and new bone formation in implanted EPC/hfMSC-constructs as compared to statically-cultured constructs. (A) Masson's Trichrome staining showed denser and more compact tissue formation, with greater number of capillary structures containing red blood cells (black arrows) in the core of dynamically-cultured sections on Week 4. Higher levels of pre-mineralising collagen (blue stains) with perfused luminal structures are found at the edges of the scaffold, with capillary density 1.2 and 2.3 fold higher than static and acellular groups respectively ($p>0.05$; $p<0.01$) (B) Micro-CT analysis of the scaffold volume showed presence of a capillary network formation within the central pores of dynamically-cultured scaffolds as compared to static and acellular scaffolds on Week 8, which showed no observable differences (C) Von Kossa staining showed greater regions of ectopic mineralisation (black stains indicated by white arrows; scaffolds were indicated by 'S') and a larger area of rabbit anti-human osteopontin staining in dynamically-cultured constructs compared to static-constructs on Week 8.
- Figure 5-4** Confocal imaging of histological sections showed 1.4 fold ($p<0.001$) higher human:mouse chimerism upon anti-human lamins A/C staining on Week 8.
- Figure 6-1** (A-B) Growth kinetics of hfMSC showed higher cell proliferation upon 2% O₂ culture, with 1.4 fold higher cell numbers on Day 6 and 4.0 fold higher CFU-F capabilities on Day 14 ($p<0.01$) when cultured in 2% O₂ compared to 21% O₂.
- Figure 6-2** Osteogenic differentiation capabilities of hfMSC cultured in 2% and 21% O₂. (A) Light microscopy images of mineral deposition showed inhibition in 2% O₂ compared to 21% O₂ cultures, (B) with 3.1 fold lower calcium deposition on Day 14 ($p<0.001$).
- Figure 6-3** *In vivo* subcutaneous mice studies of hypoxia^{short-term}-treated hfMSC constructs for 2 days (A) Human specific Lamins A/C staining showed no significant differences in hfMSC viability in both groups on Week 8 ($p>0.05$). (B) Murine specific CD31 staining showed slight increase in angiogenic potential in hypoxia compared to normoxia-cultured scaffolds on Week 8 ($p>0.05$). (C) Masson's Trichrome staining showed new bone formation around the periphery of the pores of the hypoxic cultured scaffolds, with the presence of dense pre-mineralising collagenous tissue as compared to normoxia-cultured scaffolds on Week 8.
- Figure 6-4** (A) Cell proliferation assay showed highest proliferation in hypoxia, which dropped to a level comparable to normoxic cultures upon switching from 2% to 21% O₂. (B) Photographs of crystal violet-stained colonies of hfMSC cultured under 2% and 21% O₂, with and without O₂ switching at different time points.
- Figure 6-5** (A) Photographs of crystal violet stained hfMSC colonies for different gestational samples, seeded at different MNC densities and stained at different time points as indicated (n=3), found to be 6.5 fold higher under continuous hypoxia exposure (n=1; $p<0.05$). (B) Cell

proliferation assay of hfMSC showed similar proliferative capacity in the first 6 days of culture (n=1).

- Figure 6-6** (A-B) Osteogenic assays of fresh BM-aspirates cultured in 2% and 21% O₂. Light microscopy images show greater mineralisation, with 2.9 fold higher calcium deposition in continuous 2% O₂ compared to 21% O₂ on Day 14 ($p < 0.001$) (n=1).
- Figure 7-1** Future work for the development of current coculture systems will encompass the four key technologies in tissue engineering, including cells and their biomolecules, scaffolds, bioreactors and imaging tools.
- Figure 7-2** Earlier emergence of EPC colonies formed by Day 10 under continuous hypoxic conditions, with none observed under normoxia (B) Cell proliferation assay of EPC showed 1.3-1.8 fold higher proliferative capacity in the first 7 days of culture.
- Figure 7-3** (A, C) Experimental work-flow of cellular-treatment before and during Matrigel assay and (B, D) quantification of quantification of branch points of vessel networks formed. (B) HUVEC cultured in 2% O₂ during differentiation on Matrigel showed highest *in vitro* vessel-forming ability, exhibiting 7.1-13.3 fold higher branch points than when in 21% O₂ ($p < 0.001$). No significant difference was noted when cells were preconditioned before being laid onto Matrigel (D) Untreated cells incubated in hypoxia during differentiation overnight, resulting in 1.7 fold higher branch points formation ($p < 0.001$).

List of Symbols

| | |
|-----------------|--|
| 2D | Two-dimensional |
| 3D | Three-dimensional |
| AAALAC | Association for Assessment and Accreditation of Laboratory Animal Care |
| Dil acLDL | Dil complex acetylated Low Density Lipoprotein |
| ALP | Alkaline Phosphatase |
| ANOVA | Analysis of Variance |
| BESTT | BMP-2 Evaluation in Surgery for Tibial Trauma |
| BM | Bone Media |
| BM-MSC | Bone-marrow derived MSC |
| BMP | Bone Morphogenetic Protein |
| BSA | Bovine Serum Albumin |
| BTE | Bone Tissue Engineering |
| cDNA | complementary Deoxyribonucleic Acid |
| CFU-F | Colony-Forming Unit-Fibroblasts |
| cGMP | Current Good Manufacturing Practices |
| CM | Conditioned Media |
| CO ₂ | Carbon Dioxide |
| CSD | Critical-Sized Defect |
| DAPI | 4',6-diamidino-2-phenylindole |
| DMEM | Dulbecco's Modified Eagle's Medium |
| EC | Endothelial Cell |
| ECM | Extracellular Matrix |
| EGF | Endothelial Growth Factor |
| EGM | Endothelial Growth Media |
| EPC | Endothelial Progenitor Cell |
| ESC | Embryonic Stem Cell |
| FBS | Fetal Bovine Serum |
| FDA | Fluorescein Diacetate |
| FGF | Fibroblast Growth Factor |
| GCOS | GeneChip Operating Software |

| | |
|----------------|--|
| GFP | Green Fluorescent Protein |
| H&E | Hematoxylin and Eosin |
| HA | Hydroxyapatite |
| HDMEC | Human Dermal Microvascular Endothelial Cell |
| hfMSC | Human Fetal Mesenchymal Stem Cell |
| HIF | Hypoxia-Inducible Factor |
| HUVEC | Human Umbilical Vein Endothelial Cell |
| IGF | Insulin Growth Factor |
| IL | Interleukin |
| IMDM | Iscove's Modified Dulbecco's Media |
| IgG | Immunoglobulin G |
| iPSC | Induced Pluripotent Stem Cell |
| MCP | Monocyte Chemotactic Protein |
| MG-63 | Osteosarcoma cell line |
| Micro-CT | Micro-Computed Tomography |
| MIP | Macrophage Inflammatory Protein |
| MNC | Mononuclear Cell |
| mRNA | messenger Ribonucleic Acid |
| MSC | Mesenchymal Stem Cell |
| MT | Masson's Trichrome |
| MVEC | Microvascular Endothelial Cell |
| NaOH | Sodium Hydroxide |
| NOD SCID | Obese Diabetic Severe Combined Immunodeficient |
| O ₂ | Oxygen |
| OB | Osteoblast |
| OCT | Optimal Cutting Temperature |
| PB | Peripheral Blood |
| PBS | Phosphate-Buffered Saline |
| PCL | Polycaprolactone |
| PDGH | Platelet-Derived Growth Factor |
| PGA | Polyglycolide |
| PI | Propidium Iodide |

| | |
|--------------|--|
| PLLA | Poly lactide |
| qPCR | Quantitative Polymerase Chain Reaction |
| RFP | Red Fluorescent Protein |
| RNA | Ribonucleic Acid |
| SEM | Scanning Electron Microscopy |
| siRNA | Small Interfering Ribonucleic Acid |
| TGF | Transforming Growth Factor |
| TIMP | Tissue Inhibitor of Metalloproteinase |
| TU | Transducing Unit |
| UCB-EPC | Umbilical Cord Blood derived Endothelial Progenitor Cell |
| VEGF | Vascular Endothelial Growth Factor |
| vWF | von Willebrand Factor |
| w/v | weight per volume |
| α MEM | Alpha Minimum Essential Medium |
| β -TCP | β -Tri-calcium Phosphate |

Chapter 1 – Introduction

Happiness does not come from doing easy work but from the afterglow of satisfaction that comes after the achievement of a difficult task that demanded our best ~ Theodore Issac Rubin

Chapter 1 – Introduction

1.1 Bone Grafts and Current Unmet Needs

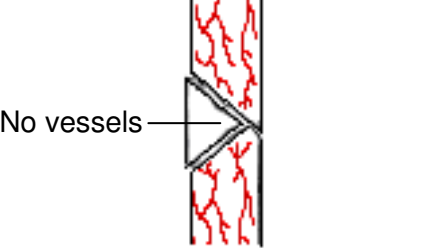
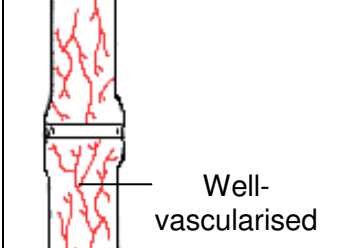
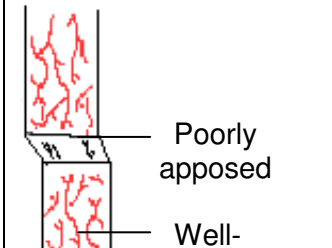
Bone is the second most transplanted tissue in the world, with the number of fractures per annum on the rise due to increasingly active lifestyles, accidents and aging. Recent advancements in new technologies for orthopaedic treatments of bone injuries have shown considerably favourable outcomes. However, in cases where there is extensive loss of bone due to trauma, post-tumour resection or inflammation, the repair for such large non-union fractures still remains a significant clinical problem. Globally, it has been estimated that approximately 15 million fracture cases occurs annually (O'Keefe and Mao 2011), of which up to 10% are complicated by non-union (Praemer *et al.* 1992; Salgado *et al.* 2004). Currently, most grafts utilised for bone repair suffer from a lack of integration with the host bone, and hence result in non-unions (Muramatsu *et al.* 2003; Soucacos *et al.* 2006) with late graft fracture occurring as high as 60% at 10 years (Wheeler and Enneking 2005). Thus, there is an urgent need for new therapeutic strategies for bone repair to meet the increasing demand, with an estimated market potential of \$3.3 billion by 2013 for bone grafts and its substitutes in the markets of United States alone (Frost&Sullivan 2007).

1.2 Non-union Fractures

In addressing the challenges faced by current clinical therapies for the repair of large bone defects, it is important to first understand bone physiology and the underlying reasons that result in these non-unions. Typically, non-unions are fractures that fail to heal after 6 months and can be caused by different factors including surgical expertise, pathological conditions and/or fracture types that vary between patients. Non-union fractures can be broadly categorised as hypertrophic, oligotrophic and atrophic non-unions which are primarily a result of insufficient mechanical

stabilisation, poor fracture apposition and poor vascularity respectively. **Table 1-1** compares the characteristics of both types of avascular and vascular non-unions and their associated strategy for successful bone repair.

Table 1-1: Characteristics of the different types of non-union fractures include avascular and vascular non-unions (Tseng *et al.* 2008). *Figure adapted from Mosby et al (Mosby 2003).*

| Avascular Non-Union | Vascular Non-Union | |
|--|---|---|
| | Hypertrophic | Oligotrophic |
| <ul style="list-style-type: none"> • Lack of blood supply • No callus formation • No bone growth • Resorption at bone ends | <ul style="list-style-type: none"> • Adequate blood supply and callus formation • Inadequate mechanical stabilisation | <ul style="list-style-type: none"> • Minimal callus formation • Fracture fragments not properly apposed |
| Require bone graft with vascularity | Require external or internal fixation | Require bone graft and proper fixation |
|  <p>No vessels</p> <p>Eg. Comminuted (Necrotic fragment)</p> |  <p>Well-vascularised</p> <p>Eg. Horse hoof</p> |  <p>Poorly apposed</p> <p>Well-vascularised</p> |

1.3 Current Strategies for Bone Repair

Currently, bone grafting strategies such as autologous grafts, allografts and synthetic grafts are used to address these clinical needs. Despite their widespread clinical utility, these strategies are subjected to limited success particularly for the repair of large bone defects. The advantages and disadvantages of each strategy are discussed in the next section.

1.3.1 Autologous Grafts

Autologous bone grafting is taking bone chips from a secondary site of the patient's own body, with the iliac crest as the most common donor site, often taken in the form of trabecular bone. This remains as the gold standard for bone repair because it provides an osteoconductive matrix, osteogenic cells and an osteoinductive environment necessary for bone regeneration (Rose and Oreffo 2002) and will not cause any immunoreactions (Schroeder and Mosheiff 2011). However, a limited supply for harvest, donor site morbidity (Laurie *et al.* 1984), varying osteogenic graft potential depending on the age and health status of the patient, as well as the difficulty in graft shaping for filling of defect sites hamper its use. The need for two surgeries on the same patient also increases the cost and risk of infection (Fowler *et al.* 1995; Goulet *et al.* 1997; Tseng *et al.* 2008).

1.3.2 Allogenic Grafts

To overcome issues of harvesting and limited tissue quantities, allografts have been used as an alternative, where bone is taken from another patient's body. However, this strategy introduces possibilities of potential graft rejection by the host immune system and disease transmission from donor to host (Rose and Oreffo 2002). The use of allografts have also been reported to result in poorer bone healing due to reduced cellularity and vascularity upon processing (Damien and Parsons 1991; Lane *et al.* 1999) and do not provide the necessary osteoinductive signals upon sterilisation as compared to autologous grafts (Oklund *et al.* 1986). Other complications of allografts segments are associated with incomplete resorption, resulting in fatigue failure and infections (Thompson *et al.* 1993).

1.3.3 Synthetic Grafts

Synthetic grafts such as metals and ceramics are subjected to fatigue, fracture, toxicity and wear over time, without the possibility of remodelling which is a critical part of the bone healing process (Salgado *et al.* 2004). Metals for example, have excellent mechanical properties but are unable to integrate with the host bone. Ceramics are brittle and has a high Young's modulus (Teoh 2004) and low tensile strength, thus not suited for use in locations that undergo significant torsion, bending or shear stress (Yaszemski 1994).

1.4 Bone Tissue Engineering

To overcome the issues encountered in current strategies, bone tissue engineering (BTE) has emerged as an alternative for fracture repairs. Tissue engineering is “an interdisciplinary field of research that applies the principles of engineering and the life sciences towards the development of biological substitutes that restore, maintain, or improve tissue function” (Langer and Vacanti 1993). Briefly, this strategy involves an appropriate combination of cells and their biomolecules such as growth factors, scaffolds, bioreactor culture systems, allowing for intercellular communications and cell-biomaterial interactions towards achieving a therapeutic response. This will be accompanied by various imaging tools to determine the success of the tissue engineering strategy (**Figure 1-1**).

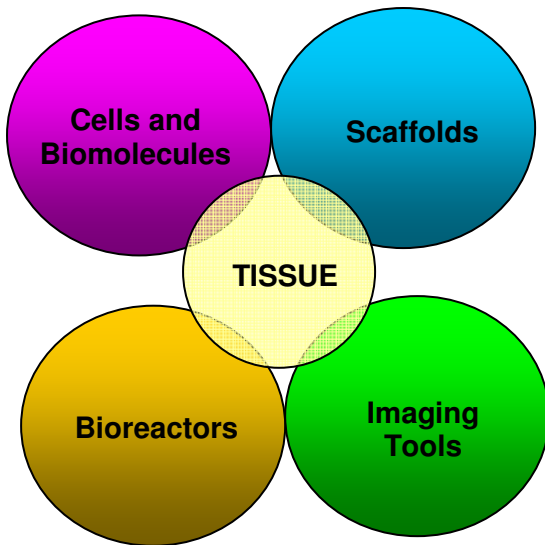


Figure 1-1: Four key technologies used in tissue engineering include cells and their biomolecules, scaffolds, bioreactors and imaging tools.

1.4.1 Limitations in Bone Tissue Engineering

Since the introduction of BTE over the past two decades, there has been an exponential increase in the number of investigations in the area of BTE, with close to 10,000 publications and more than 200,000 citations in this growing field (**Figure 1-2**; Web of Science, 2012).

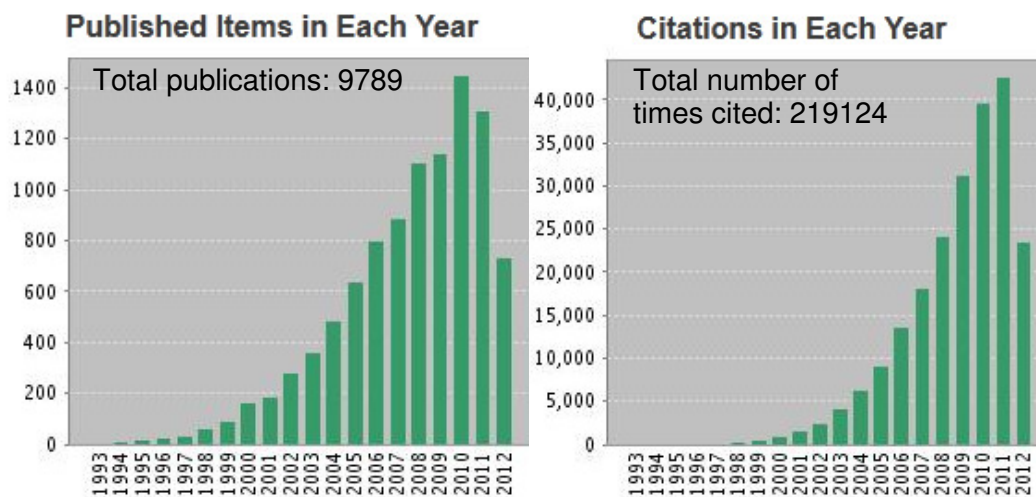


Figure 1-2: Graphical analysis of the total number of publications and citations on BTE in the past 20 years (Web of Science, 2012).

Despite several groups having reported considerable success in their approach in the regeneration of bone in various animal segmental models (Bruder *et al.* 1998; Arinzeh *et al.* 2003; Zhu *et al.* 2006; Rai *et al.* 2007; Bae *et al.* 2011; Kolambkar *et al.* 2011), few have reported clinical success (Meijer *et al.* 2007). Current BTE constructs suffer from a lack of sufficient vascularity within larger grafts due to slow spontaneous vessel ingrowth (Clark 1939), hence resulting in cellular necrosis especially at the core and eventual failure of the BTE graft over time (Ko *et al.* 2007). A pilot cell-based clinical study for the treatment of large bone defects (Quarto *et al.* 2001) has shown vascularisation in the grafted region at 6.5 years post-surgery (Marcacci *et al.* 2007). However, most studies still lack clear data demonstrating evidence of early vasculature development within the graft necessary for cell survival, and eventual integration and long term remodelling. Therefore, apart from ensuring the converging use of osteoconductive matrices, osteoinductive signals and osteogenic cells in sufficient numbers, ensuring an adequate vascular supply is crucial for successful bone repair in large defects. Challenges relating to achieving adequate vascularisation within synthetic bone grafts remain a major concern (Cancedda *et al.* 2007), hence limiting the introduction of BTE into the clinical setting.

1.5 Importance of Vascularisation

1.5.1 Vascularisation in Bone Tissue Engineering

The importance of angiogenesis has been documented as early as the 1700s by Hunter (Haller 1763) and Haller (Hunter and Palmer 1840), but was however not recognised as an important aspect of bone healing until the 19th century where Trueta suggested that “vascular stimulating factors” present at the sites of bone damage initiate osteogenesis (Trueta and Buhr 1963). This has since been verified by many experimental studies which demonstrate a need for an adequate vascular supply in order for bone regeneration to succeed (Carano and Filvaroff 2003;

Kanczler and Oreffo 2008). For example, endogenous vascular endothelial growth factor (VEGF) has been shown to be essential for endochondral bone formation (Gerber *et al.* 1999; Street *et al.* 2002; Zelzer *et al.* 2002). Inhibition of VEGF via a soluble neutralising VEGF receptor during endochondral and intramembranous ossification led to decreased angiogenesis, with reduced callus mineralisation and bone formation in a femoral fracture and tibia cortical bone defect in mice respectively (**Figure 1-3A**). Conversely, an exogenous VEGF supply accelerated bone bridging across a critical-sized defect (CSD) in rabbit radius, suggesting the distinct roles of VEGF as an angiogenic factor in promoting bone healing (**Figure 1-3B**) (Street *et al.* 2002). Optimal healing of the defect region is found to be heavily reliant upon adequate vascularisation, hence suggesting the integral role of blood vessels for bone regeneration.

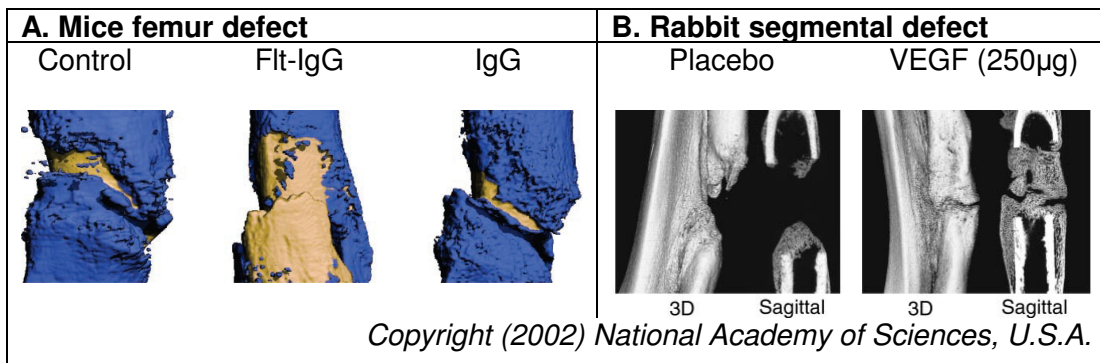


Figure 1-3: Three-dimensional rendering of computed tomography scans. (A) Mice femurs showed impairment of fracture repair upon soluble, neutralising VEGF receptor (Flt-IgG) treatment as compared to its controls after 7 days. Callus (blue) and cortical bone (peach). (B) VEGF stimulated repair of a rabbit segmental defect upon exogenous VEGF-treatment (250µg) compared to its placebo on 28 days. *Figures reproduced from Street et al (Street et al. 2002).*

1.5.2 Vascularisation in Natural Bone Repair Processes

In the natural physiology, bone repair processes such as endochondral and intramembranous ossification occur in the proximity of a vascular network. Briefly, endochondral bone formation develops via a cartilage model where subsequent

osteogenesis and mineralisation of the cartilaginous callus relies on the extent of vascularisation. This process will be discussed in greater detail in Chapter 2. In comparison, intramembranous ossification is a non-cartilaginous process that is involved in the natural healing of bone fractures. Here, the presence of blood vessels is necessary for directing the differentiation of mesenchymal stem cells into osteoblasts at the fracture site (Kanczler and Oreffo 2008).

1.5.3 Periosteum and Its Vasculature

The periosteum, a highly vascularised thin bilayered tissue membrane covering the bone surfaces, is also found to play a crucial role during fracture healing (Bullens *et al.* 2010). The highly vascularised periosteum consists of a network of microvasculature resides in the outer fibrous layer of the periosteum which is known as the intrinsic periosteal system (Simpson 1985). Other periosteal-associated vessel systems includes the musculo-osteal and fascio-osteal vessels which connect the muscles and periosteum (Colnot 2009), while the cortical capillary anastomoses are linked to the intramedullary circulation in the bone cortex (Simpson 1985).

During a fracture, the outer cambium layer of the activated periosteum is responsible for driving the initiation of osteogenesis and angiogenesis for bone repair, and direct the differentiation of stem cells into bone lineage (Tran Van *et al.* 1982). Experimentally, the osteogenic and angiogenic potency of the periosteum has been investigated in various *in vitro* and *in vivo* studies, showing revitalisation of allografts or enhancement in bone regeneration (Melcher and Accursi 1971; Tran Van *et al.* 1982; Jacobsen 1997; Lemperle *et al.* 1998; Runyan *et al.* 2010). Conversely, the absence of a periosteum in fracture healing was demonstrated to result in decreased fracture healing capacity (Utvag *et al.* 1996; Ozaki *et al.* 2000; Colnot 2009; Bullens

et al. 2010). For example, Shimizu *et al.* reported no new bone formation when periosteum was removed completely from the rat calvarial bone, while new bone was observed on the parietal bone surface on Week 3 in areas in direct contact with the periosteum (Shimizu *et al.* 2001).

From the natural physiological repair of the bone tissue and its anatomy, it is evident that blood vessels play an integral role for bone regeneration and the optimal healing of the defect region is heavily reliant upon adequate vascularisation.

1.6 Motivation of Study

Existing solutions do not adequately address the limited neovascularisation in voluminous BTE-grafts for the repair of large bone defects. This results in insufficient nutrient and oxygen supply, high cellular death and consequential graft failure. Hence, there is an urgent unmet need for an effective tissue-engineered solution to treat CSD. To overcome current issues with vascular insufficiencies in these artificial grafts, various vascularisation strategies have been developed (Rouwkema *et al.* 2008). The importance of vascularisation and the vascularisation strategies used in tissue engineering will be discussed in detail in Chapter 2.

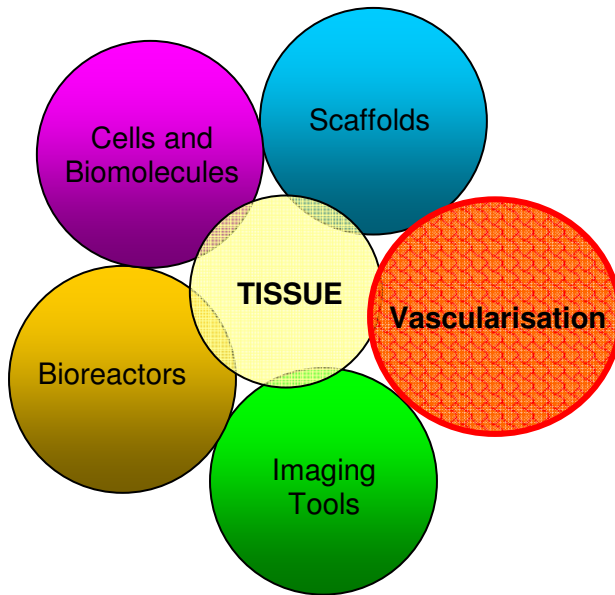


Figure 1-4: Vascularisation as a key component for successful BTE as well as other areas of tissue engineering where vascularisation is needed.

Compared to traditional BTE approaches, vascularisation will be the key component for investigation in this project (**Figure 1-4**). The main aim is to generate a highly vascularised and osteogenic bone graft, with the intention of facilitating fracture healing in a large bone defect and allow for host integration and remodelling over the long term.

1.7 Proposed Approach

1.7.1 Vascularised BTE – A Mimicry of Natural Bone Tissue

In this project, my proposed BTE approach will be designed in close mimicry to the physiological microenvironment of the natural bone tissue. I will leverage on the osteogenic differentiation capacity of human fetal MSC (hfMSC) and the vasculogenic capacity of umbilical cord blood-derived EPC (UCB-EPC). Other specific considerations of the various BTE components includes the type of dynamic bioreactor culture, scaffold material and its architecture, as well as the microenvironment of oxygen tension, biomechanical and biochemical cues. **Table 1-**

2 summarises my proposed BTE approach and the individual BTE components, as well as its relation with the natural bone. Detailed justification of the proposed BTE approach will be discussed in the next chapter.

Table 1-2: Proposed BTE approach and the choice of each individual BTE component, including the choice of cells, scaffolds, bioreactor and microenvironment oxygen tensions.

| | | | | |
|------------------------------|--|--------------------------------|---------------------------------------|--|
| Proposed BTE Approach | | | | |
| BTE Component | Coculture of mesenchymal stem cells (MSC) and endothelial progenitor cells (EPC) | Honeycomb macroporous scaffold | Perfusion biaxial rotating bioreactor | Hypoxia culture (2%) |
| Natural Bone | Presence of both endothelial and osteogenic cells | Trabecular structure | Physiological mechanical forces | Physiological oxygen tension in bone marrow niche (2-8%) |

1.7.2 Aims and Hypotheses

1.7.2.1 Main Aim

This project aims to generate highly vascularised and osteogenic bone grafts using a coculture of stem cells, scaffold and bioreactor technologies through rapid vascularisation and osteogenic strategies for facilitating eventual fracture healing in a large bone defect model.

1.7.2.2 Hypothesis 1

Incorporation of EPC in coculture with hfMSC improves vascularity and consequential cellular survival and osteogenicity, leading to improved bone healing.

1.7.2.3 Hypothesis 2

Bioreactor culture induces early neovasculogenesis of EPC, accelerates vascularisation and enhances osteogenic differentiation of hfMSC, leading to improved bone repair.

1.7.2.4 Hypothesis 3

Exposure of hfMSC and EPC to a hypoxic microenvironment mimicking that of the natural physiology promotes the osteogenic differentiation and vessel-forming ability of the monocultures respectively.

1.7.3 Novelty and Clinical Implications

It is now clear that poor vascularisation of a tissue graft remains a major challenge in inducing effective fracture healing and thus, a major thrust in this project. The interactions of vasculogenic EPC and osteogenic hfMSC will be interrogated for their synergistic effects when in coculture in both *in vitro* and *in vivo* experiments and how it leads to increased vascularisation and bone formation. This work will enhance the understanding of the specific interactions between the two cell types which are involved in the natural repair of skeletal injuries.

In addition, the specific interactions of the coculture with a dynamic bioreactor culture and low oxygen tensions will be investigated in relation to their contributions towards building an efficacious vascularised bone graft. Currently, the use of biomechanical stimulation in current coculture studies is often neglected, likely to be essential for the maturation and long term efficacy of these bone grafts upon clinical translation.

There is also a lack of understanding on the importance of microenvironment oxygen tensions on stem cell fate. Results should identify if there is a need to revolutionise conventional cell culture techniques where stem cells are grown under atmospheric 21% oxygen as compared to the low physiological oxygen tensions in the bone marrow niche. Successful demonstration of effective vascularisation and bone repair of a CSD model in a large animal model should present viable options for more effective treatment of large tissue-engineered bone grafts compared to current BTE strategies.

Chapter 2 – Literature Review

Do not follow where the path may lead.

Go instead where there is no path and leave a trail.

~Ralph W.

Chapter 2 – Literature Review

2.1 The Skeletal System

The adult human skeletal system performs many functions. It provides a structural support to the body and protects vital organs such as the brain, lungs and heart. Bones work in synchrony with muscles to allow for movement and locomotion. The skeleton also acts as a store for minerals such as calcium and phosphorus, maintaining bone homeostasis and ensuring an acid-base balance. In larger bones, it provides an environment for haematopoiesis within the marrow (Clarke 2008).

The skeleton comprises of a total of 213 bones, excluding sesamoid bones which are embedded within a tendon. These bones are generally categorised into four groups – the long bones, short bones, flat bones and irregular bones (Clarke 2008).

2.2 Anatomy of Bone

The human skeletal system consists of 80% cortical bone and 20% spongy bone overall, with varying ratios depending on the skeletal site and type of bone (Eriksen *et al.* 1994). Cortical bone is a dense and solid tissue with only 10% porosity, hence providing the bulk of strength to the skeletal system (Sikavitsas *et al.* 2001). The spongy bone has a honeycomb structure consisting of branching rods and plates of varying sizes, with a porosity of 50-90%, hence keeping bone light (**Figure 2-1**). However, its mechanical properties (modulus and ultimate compressive strength) are 20 times inferior compared to compact bone (Sikavitsas *et al.* 2001).

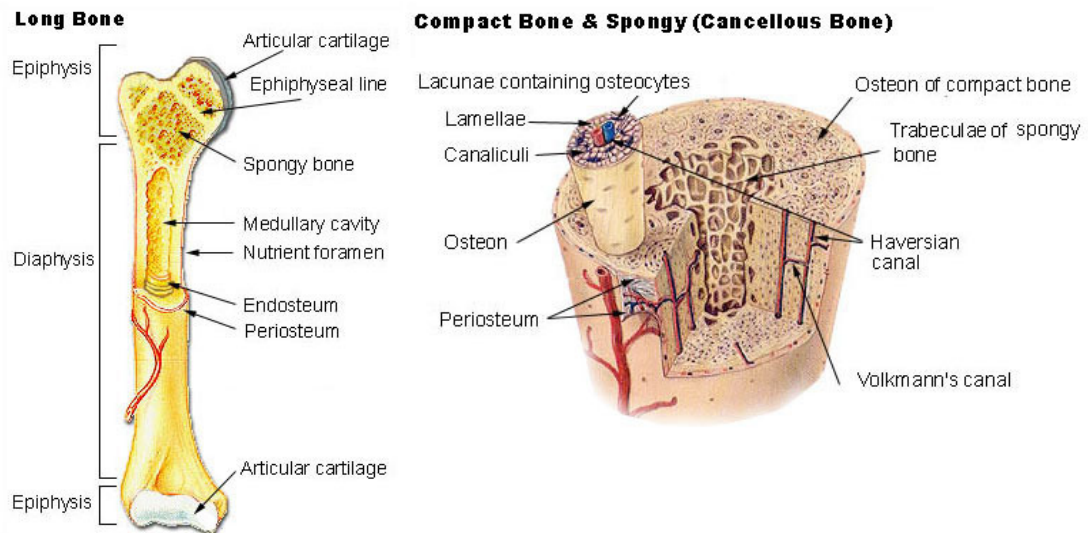


Figure 2-1: Anatomy of the long bone and microstructure of vascularised bone tissue and the comparative porosity of compact bone and spongy bone. *Figures reproduced from U.S. National Cancer Institute's Surveillance, Epidemiology and Eng Results (SEER) Program (U.S. National Cancer Institute's Surveillance 2012; U.S. National Cancer Institute's Surveillance 2012).*

Long bones have a long and hollow diaphysis shaft which is flared slightly at the metaphyses below the growth plates and rounded at its epiphyses ends above the growth plates. Cortical bone surrounds the entire bone and primarily occupies the marrow space at the diaphysis, where Haversian systems (osteons) constitute the basic structural unit of the cortical bone. They are cylindrical in shape with concentric layers of lamellae surrounding a central canal, known as Haversian canals. These Haversian canals, connected to the periosteum and endosteum *via* the Volkmann's canals, contain the bone's nerve and blood supply at a flow rate of 200-400ml/min in adult humans (Gruber 2008). This high level of vascularity in bone is necessary for the maintenance of cellular survival, active remodelling and skeletal integrity. Compared to compact bone, the trabecular bone has a higher surface area and constitutes largely the inner region of the epiphysis and metaphysis (Eriksen *et al.* 1994; Deng and Liu 2005; Gruber 2008). The periosteum surrounds the outside of bone except at areas covered by the articulating cartilage, and the endosteum lines the inner bone surface within the marrow.

Examination of the anatomy of bone also reveals a complex hierarchical structure, starting from the sub-nano level of molecules and minerals, where collagenous proteins are arranged in fibrillar bundles that form lamellae on the sub-micron level. The microstructure of bone comprises of the Haversian systems, osteons and layers of lamellae, forming the macrostructure of cortical and cancellous bone (**Figure 2-2**) (Rho *et al.* 1998).

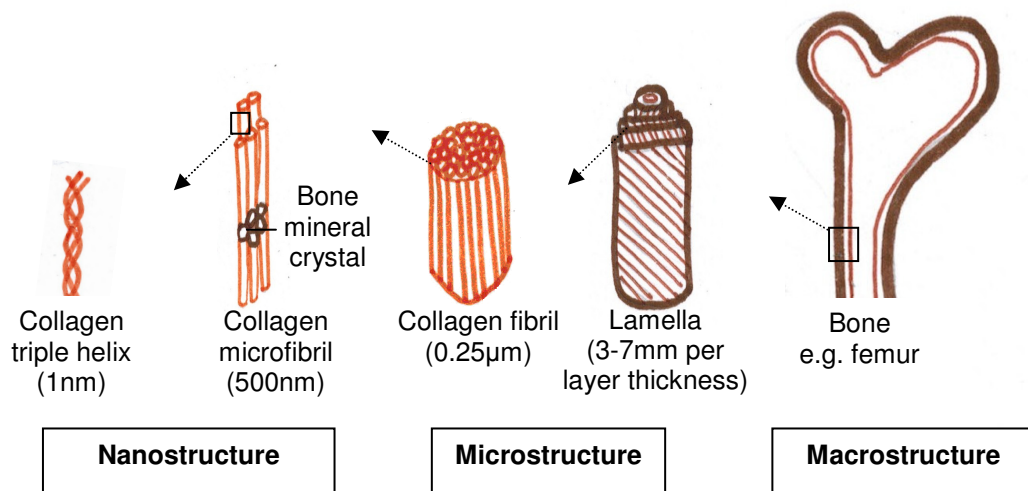


Figure 2-2: A schematic of the hierarchical structure of bone from a sub-nanostructure of collagen molecules to a nanostructure of cylindrically arranged microfibrils to lamellar layers forming the macrostructure of cortical bone. *Figure adapted from Rho et al (Rho et al. 1998).*

2.3 Composition of Bone

2.3.1 Bone Cells

The maintenance of bone as a dynamic living tissue results from the interaction of various cell types, each with a defined function. Bone cells can be classified into five main cell types (Deng and Liu 2005; Clarke 2008; Gruber 2008):

- (1) Osteoblasts are bone-forming cells are located on the surface of mineralised matrix. They are differentiated from mesenchymal stem cells, incapable of mitosis. Osteoblasts secrete an organic bone matrix known as osteoid, which

serves as a template for mineralisation to occur. Upon cessation of matrix formation, osteoblasts can undergo apoptosis, fully differentiate into osteocytes or remain inactive as lining cells on the surface of bone.

- (2) Osteocytes are fully differentiated mature osteoblasts that are unable to divide. They have a stellate morphology and are trapped singly within the tiny lacunae spaces and embedded within the osteoid. They connect and communicate with other bone cells through cytoplasmic protrusions, forming a network of canaliculi. Osteocytes also act as mechanosensors and adapt bone to functional loading during remodelling. They also maintain metabolism by regulating mineral content and play a role in bone turnover.
- (3) Osteoclasts are large multinucleated cells located within bone that are involved in bone resorption. They come from a haematopoietic origin, derived primarily from the fusion of monocytes. They are highly motile and are mostly found at sites of high bone turnover, along the surface of bone.
- (4) Osteogenic cells are immature bone cells found in the inner surface of periosteum, endosteum, within Haversian canals, capable of differentiating into osteoblasts and osteocytes.
- (5) Bone lining cells are quiescent osteoblasts that line the surface of bones. Their role is to regulate mineral content such as calcium and phosphate in the bone.

2.3.2 Bone Matrix

Bone is a composite material made of a mineral phase and an organic phase. It is this matrix composition that gives rise to the unique properties of bone. The mineral

phase comprises largely of hydroxyapatite, providing the bulk of the tensile yield strength and plays an important in the storage of various ions. The mineral salts of bone comprises of largely of calcium and phosphorus (Downey and Siegel 2006). The organic phase is composed of 90% Type 1 collagen as the main structural element with the remaining consisting of non-collagenous proteins, mainly glycoproteins and proteoglycans.

2.4 Natural Bone Forming Process

Bone is a self-reparative tissue, capable of complete regeneration and remodelling without leaving a scar (Sommerfeldt and Rubin 2001). In designing appropriate strategies for accelerating fracture healing, the natural spontaneous bone healing process needs to be understood. In [Section 1.5.2](#), the two main processes of bone formation, namely endochondral and intramembranous ossification were briefly discussed in relation to their need for vessel formation. Here, the processes of endochondral ossification and distraction osteogenesis, which primarily undergoes intramembranous ossification, will be examined in greater detail.

2.4.1 Endochondral Ossification

Endochondral ossification is a process by which bone grows via cartilaginous formation as an intermediate stage. It undergoes four main stages – (1) Inflammation, where a haematoma forms and stabilises the fracture ends; activates a cascade of cellular events which recruits various cell sources to the fracture area, including MSC. (2) Soft callus (cartilage) develops as MSC and other bone forming cells differentiate into chondrocytes and proliferate, synthesising a cartilaginous extracellular matrix. (3) Blood vessels invade and the cartilaginous regions undergo resorption and

mineralise, forming woven bone that (4) ultimately remodels into lamellar structure over time (**Table 2-1**).

Table 2-1: Endochondral ossification involves four main stages, namely the inflammatory phase, soft callus fibrocartilagenous formation, hard callus formation and bone remodelling (Lieberman and Friedlaender 2005).


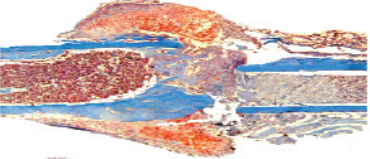
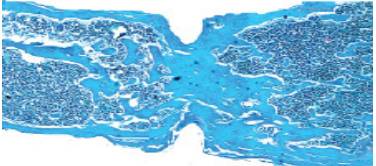
| Stage in bone formation | Process | Duration |
|--------------------------------|---|-------------------------|
| Inflammation | <ul style="list-style-type: none"> • Release of cytokines • Dead cells removed by osteoclasts • Movement of fracture fragments stops osteoblast activity and blood flow • Haematoma formation linking bone fragments • Recruitment of fibroblasts, MSC • Granulation tissue formation | 3 to 5 days |
| Soft callus formation | <ul style="list-style-type: none"> • Cartilage formation and endochondral ossification occurs • Weak to external stresses • Sufficient stability for vessels to form • Vasculogenesis and angiogenesis | 4 days to 3 weeks |
| Hard callus formation | <ul style="list-style-type: none"> • Cartilage resorbs and mineralises • Woven bone formation • Fracture union achieved | 3 weeks to 6 - 12 weeks |
| Bone remodelling | <ul style="list-style-type: none"> • Normal bone shape restored • Continuous resorption and bone formation throughout lifetime • Lamellae bone formation | Up to several years |

2.4.2 Distraction Osteogenesis

Distraction osteogenesis is one surgical method where induction of natural bone formation is observed, and its predominant mechanism is via intramembranous bone formation where an adequate blood supply is present (Delloye *et al.* 1990; White and Kenwright 1990). It is used primarily for reconstruction of skeletal deformities or defects secondary to trauma, infection or bone resection, and for bone lengthening to fix length discrepancies. An osteotomy is first performed to fracture bone into two pieces, and the two vascularised bone surfaces are gradually pulled apart by tensile forces at a fixed rate and timing. The longitudinal mechanical strain exerted on the

callus during the distraction phase initiates biological responses that stimulate the formation of mineralised bone, followed by eventual remodelling (Ai-Aql *et al.* 2008). During this regenerative process, bone is formed at a rate of 200-400µm/day. The histological representation of each stage during distraction osteogenesis is as illustrated in **Table 2-2** below.

Table 2-2: The process of distraction osteogenesis involves three stages, namely latency, distraction and consolidation. *Figures reproduced from Ai-Aql et al (Ai-Aql et al. 2008).*

| Stage | Process |
|--|--|
| <p data-bbox="437 734 539 768">Latency</p>  <p data-bbox="323 898 655 965">Histology taken on Day 7 post-surgery</p> | <ul style="list-style-type: none"> • Osteotomy of bone • Hematoma formation • Inflammatory process occurs as per fracture repair • Recruitment of MSC • Soft callus and cartilage formation |
| <p data-bbox="373 965 603 999">Active distraction</p>  <p data-bbox="316 1173 663 1240">Histology taken on Day 10 post-surgery</p> | <ul style="list-style-type: none"> • Tensile forces applied to callus (rate of 1mm/day) • Cartilage resorps and forms endochondral bone • Fibrous interzone forms (Rich in chondrocyte-like cells, fibroblasts, and oval cells) • Angiogenesis • Osteoblasts recruited and differentiated, forming bone columns (intramembranous bone) • Distraction ceases upon desired bone length |
| <p data-bbox="395 1249 580 1283">Consolidation</p>  <p data-bbox="316 1453 663 1520">Histology taken on Day 31 post-surgery</p> | <ul style="list-style-type: none"> • Bone columns connect • Osteoclast recruited • Bone and osteoid mineralises and remodels |

2.5 Physiological Microenvironment of Bone

Looking at the physiological environment of bone, there are various microenvironment cues involved in facilitating bone formation and repair, of which includes biomechanical, biochemical and oxygen tension cues. It is therefore essential to consider these microenvironmental cues during the process of engineering solutions for bone repair (**Figure 2-3**).

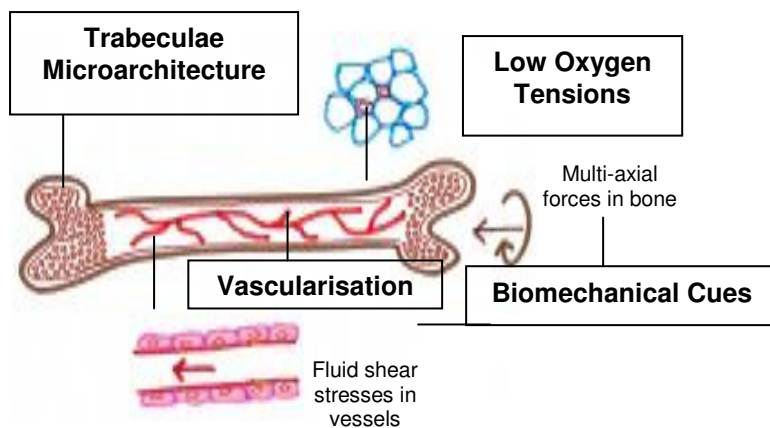


Figure 2-3: Vascularised bone anatomy and microenvironmental influences such as biomechanical, microarchitectural and low oxygen tension cues.

2.5.1 Biomechanical Cues

There are various biomechanical cues involved in this process of bone formation and remodelling. During daily activities, the human skeletal system experiences various biomechanical forces, including compressive, bending and torsional loads (Shelburne *et al.* 2005). On a microscopic level in bone, strain is experienced due to tissue deformation. Fluid shear stresses is also exerted by interstitial fluid flow through the lacunae, driven largely by compression and tension under loading onto the bone (McCoy and O'Brien 2010). Bone, as a dynamic living tissue, undergoes remodelling where it continuously gets resorbed and deposits new bone concurrently during physiological homeostasis in the lifetime of an individual. Early observations showed that this process could be adapted by mechanical stimuli, where Wolff's Law (1892) states that bone adapts its structure and remodels accordingly to mechanical loads (Wolff 1892). Although the influence of the mechanical transduction pathway on bone cells during adaptive remodelling is poorly understood, it has been well-demonstrated that mechanical stress favours the formation of bone as opposed to bone loss which happens under non-weight bearing circumstances such as in space or non-gravitational situations (Leondes 2001). In soft tissue remodelling, a similar

concept has been proposed by Davis (1953) stating that the remodelling efficacy of soft tissues is based on imposed demands (Henenfeld 1953). Putting Davis' Law into perspective during bone formation, the induction of bone formation in distraction osteogenesis relies on mechanical stimulus (tensile forces) as the osteotomised bone ends are gradually distracted, with new bone being deposited within the enlarging gap. The longitudinal mechanical strain exerted on the callus during the distraction phase then initiates biological responses that stimulate the formation of mineralised bone and eventual remodelling (Ai-Aql *et al.* 2008).

Biomechanical cues are also relevant in vascular physiology in the bone, where the endothelial cells in blood vessels are constantly exposed to blood flow tangential to the endothelial monolayer. This is essential in controlling many aspects during the fate of an endothelial cell, including the mediation of transcriptional changes, endothelial sprouting (Song and Munn 2011), proliferation (Lin *et al.* 2000) and vessel homeostasis (Hudlicka *et al.* 2006; Jones *et al.* 2006). The profound effects of biomechanical forces for stimulating vessel and bone formation and remodelling have also been well demonstrated experimentally (Ehrlich and Lanyon 2002; Yamamoto *et al.* 2003; Yamamoto *et al.* 2005; McCloskey *et al.* 2006; Grellier *et al.* 2009; Stolberg and McCloskey 2009; Kimelman-Bleich *et al.* 2011).

2.5.2 Oxygen Tension Cues

During a fracture, the vascular supply gets disrupted, resulting in a hypoxic environment. This acts as a stimulus for the upregulation of various angiogenic factors towards forming a vascular network. The mechanisms of vessel formation occur *via* activation of the hypoxia-inducible factor (HIF) pathways upon ischemia during a fracture. Ischemia at sites of injured tissues would mobilise cells which migrate towards the site for repair. The master control in the trafficking of these cells

is a result of the activation of the HIF-1 pathway, triggering the upregulation of a series of angiogenic factors such as VEGF and the Angiopoietins (**Figure 2-4A**) (Germain *et al.* 2010). The generation of a concentration gradient of growth factor instructs the migration of endothelial cells, with its tip cells acting as oxygen sensors to guide vascular invasion into hypoxic zones, while its stalk cells proliferate, hence forming a vascular network (**Figure 2-4B**) (Coulon *et al.* 2010; Germain *et al.* 2010). It is the molecular mechanisms induced by the hypoxia-activated master switch HIF-1 α , 2 α that are involved in assisting vessel formation and stabilisation respectively (Coulon *et al.* 2010). It has been demonstrated that HIF-1 α stimulates neovascularisation and improves functional recovery in ischemic tissues of various animal models (Vincent *et al.* 2000; Jiang *et al.* 2008; Li *et al.* 2011) as well as promotes the recruitment and homing of bone marrow progenitors to these ischemic sites (Ceradini *et al.* 2004; Du *et al.* 2008).

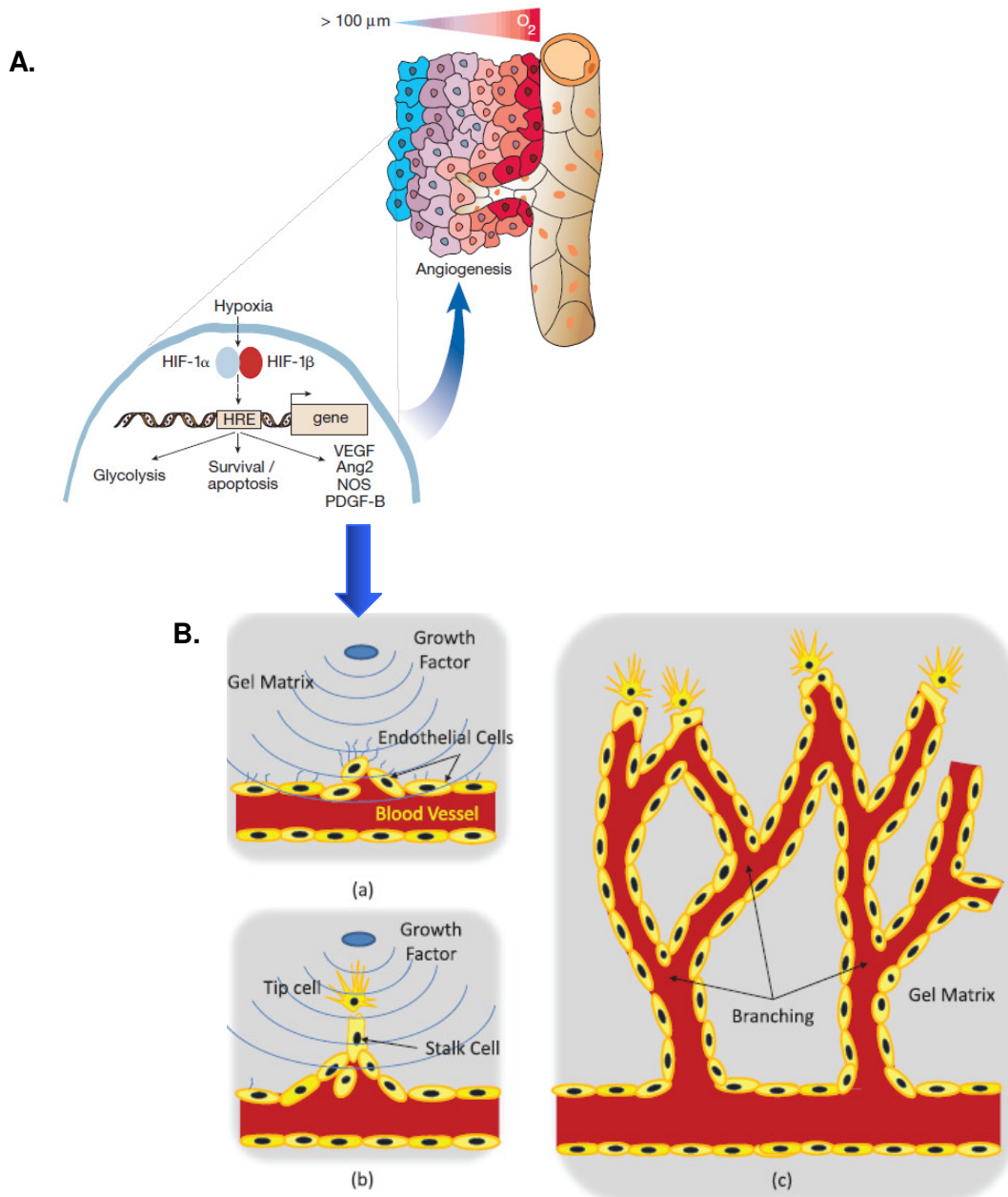


Figure 2-4: (A) Under hypoxic conditions, the HIF-1 α subunit accumulates and is stabilised, allowing it to translocate into the nucleus for dimerisation with the HIF-1 β subunit, forming the HIF-1 complex. This initiates the upregulation of several angiogenic genes and secretion of growth factors. *Figure reproduced from Carmeliet and Jain (Carmeliet and Jain 2000).* (B) Sprouting of the endothelial cells is induced, resulting in tip cells migrating towards the hypoxic stimulus, with stalk cells following behind. New vascular network forms with the emergence of various branch points overtime. *Figure reproduced from Wood et al (Wood 2011).*

2.5.3 Biochemical Cues

The natural fracture healing process is also regulated by a milieu of growth factors that is responsible for the vascularised bone formation. Growth factors such as

BMPs and TGFs belonging under the TGF- β superfamily are known for their important contributions in regulating mineralisation and bone formation (Wozney 1989; Chen *et al.* 2004), while angiogenic factors such as VEGF and angiopoietins are critical for directing angiogenesis (Schott and Morrow 1993; Ribatti *et al.* 2000). Various molecular regulators such as inflammatory, osteogenic and angiogenic factors have been identified at different stages of bone repair and described to be expressed in a sequential and temporal fashion at varying levels (Ai-Aql *et al.* 2008) **(Table 2-3A).**

The vascularised microenvironment of bone and their corresponding biomechanical and biochemical cues involved during natural bone repair is summarised in **Table 2-3B.**

Table 2-3: (A-B) Comparison between the natural fracture healing and distraction osteogenesis processes and their various microenvironmental cues that contribute to vascular and bone formation, including the relative up and down expressions of molecular regulators involved in various stages of bone repair and distraction osteogenesis. *Table 2-3A reproduced from Ai-Aql et al (Ai-Aql et al. 2008).*

A.

| Endochondral Ossification | | | | | Distraction Osteogenesis | | | | | | |
|---------------------------|--------------|---|---|---|---------------------------|---------|------|--------------------|------|---------------|------|
| Signaling Molecules | Inflammation | Cartilage Formation and Periosteal Response | Cartilage Resorption and Primary Bone Formation | Secondary Bone Formation and Remodeling | Signaling Molecules | Latency | | Active Distraction | | Consolidation | |
| | | | | | | Early | Late | Early | Late | Early | Late |
| Cytokines | | | | | Cytokines | | | | | | |
| IL-1 | ↑↑↑ | | | ↑↑ | IL-1 | ↑↑↑ | | ↑↑↑ | ↑↑↑ | | |
| IL-6 | ↑↑↑ | | | | IL-6 | ↑↑↑ | | ↑↑↑ | ↑↑↑ | | |
| TNF-α | ↑↑↑ | | ↑↑ | ↑↑ | TNF-α | | | | | | ↑↑↑ |
| RANKL | ↑↑↑ | | ↑↑↑ | ↑↑ | RANKL | | ↑↑↑ | ↑↑↑ | | | |
| OPG | ↑↑↑ | ↑↑↑ | | | OPG | | ↑↑ | ↑↑↑ | ↑↑↑ | | |
| MCSF | ↑↑↑ | | ↑↑↑ | | | | | | | | |
| TGF-β Superfamily | | | | | TGF-β Superfamily | | | | | | |
| BMP-2 | ↑↑↑ | ↑↑↑ | ↑↑↑ | ↑↑↑ | BMP-2 | ↑↑ | | ↑↑↑ | ↑↑↑ | ↑↑ | ↑ |
| BMP-3 | | ↑ | ↑↑↑ | ↑ | BMP-4 | ↑↑ | | ↑↑↑ | ↑↑↑ | ↑↑ | ↑ |
| BMP-4 | ↑ | ↑↑↑ | ↑↑↑ | ↑ | BMP-6 | | ↑↑↑ | ↑↑↑ | ↑ | | |
| BMP-5 | ↑ | ↑↑↑ | ↑↑↑ | ↑ | TGF-β | | ↑↑↑ | ↑↑↑ | ↑↑↑ | | |
| BMP-6 | ↑ | ↑↑↑ | ↑↑↑ | ↑ | bFGF | | | ↑↑ | ↑↑ | ↑ | ↑ |
| BMP-7 | | | ↑↑↑ | | IGF | | | ↑↑ | ↑↑ | | |
| BMP-8 | | | ↑↑↑ | | | | | | | | |
| TGF- 2 | | ↑↑↑ | | | | | | | | | |
| TGF- 3 | | ↑↑↑ | ↑↑ | | | | | | | | |
| GDF-5 | | ↑↑↑ | | | | | | | | | |
| GDF-8 | ↑↑↑ | | | | | | | | | | |
| GDF-10 | | ↑↑↑ | ↑↑↑ | ↑↑↑ | | | | | | | |
| Angiogenic Factors | | | | | Angiogenic Factors | | | | | | |
| VEGF A | | ↑ | ↑↑ | | VEGF A | | | ↑ | ↑ | ↑ | |
| VEGF B | | | ↑↑ | | VEGF B | | | ↑ | ↑ | ↑ | |
| VEGF C | | | ↑↑ | | VEGF C | ↑↑ | | ↑ | ↑ | ↑ | |
| VEGF D | | ↑↑ | ↑ | | VEGF D | | ↑↑ | ↑ | ↑ | | |
| Angiopoietin 1 | ↑↑ | ↑↑ | ↑ | ↑ | Angiopoietin 1 | | | ↑ | ↑ | | |
| Angiopoietin 2 | ↑ | ↑ | ↑ | ↑ | Angiopoietin 2 | | | ↑ | ↑ | | |

B.

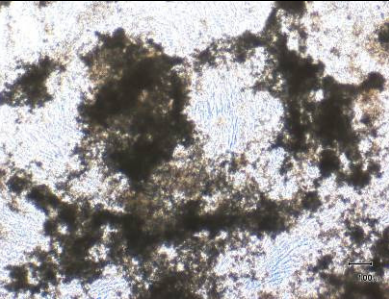
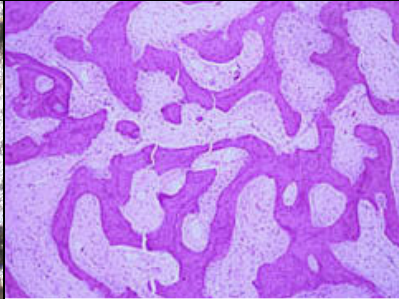
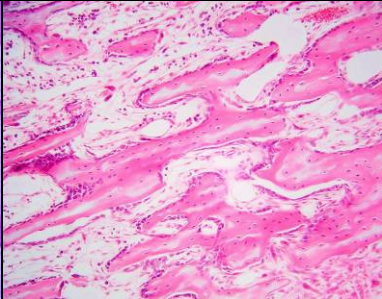
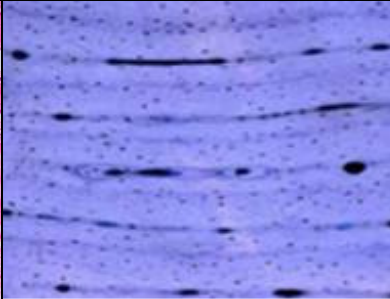
| | Fracture Repair (Endochondral Ossification) | Distraction Osteogenesis | | | | | | | | | | | | | | | | | | | | | | | | | | | | | | | | | | | | | | | | | | | | | | | | | | | | | | | | | | | | | | | | | |
|---|--|--|------------------------|------------------------|------------------------|----------------------|------|---|-----|---|-------|------|---|-----|---|-------|------|-----|-----|---|---------------|------|-----|-----|-----|--|--------|-----------------|----------------|---------------------|--------------------|---|----------------------|-----------------|----------------|---------------------|--------------------|-----------------------|----------------------|------|-------|-----|---|---|---|---|------|-------|---|---|-----|-----|---|----------|---------------|-----|-----|-----|-----|-----|-----|---|---|---|---|---|---|
| Stages | <ul style="list-style-type: none"> • Haematoma formation • Cartilage formation • Vascular infiltration • Primary bone formation • Secondary bone formation and remodelling | <ul style="list-style-type: none"> • Latency • Active distraction • Consolidation | | | | | | | | | | | | | | | | | | | | | | | | | | | | | | | | | | | | | | | | | | | | | | | | | | | | | | | | | | | | | | | | | |
| Bone formation and role of vasculature | <ul style="list-style-type: none"> • Mineralisation of the cartilaginous callus region relies on the extent of vascularisation • Blood vessel invasion required to recruit and differentiate MSC into osteoblasts | <ul style="list-style-type: none"> • Bone is osteotomised into two pieces; periosteum and medullary vessels remain intact • Bone pieces pulled apart while bone forms in gap | | | | | | | | | | | | | | | | | | | | | | | | | | | | | | | | | | | | | | | | | | | | | | | | | | | | | | | | | | | | | | | | | |
| Biomechanical Induction | No induction except for physiological interstitial flow and mechanical loading arising from daily activities | Yes, tensile forces applied to callus under specific loading rates and rhythm | | | | | | | | | | | | | | | | | | | | | | | | | | | | | | | | | | | | | | | | | | | | | | | | | | | | | | | | | | | | | | | | | |
| Biochemical Regulators | <p style="text-align: center;">Osteogenic</p> <p style="text-align: center;">Fracture Repair (TGF-beta Superfamily)</p> <table border="1"> <caption>Relative expression of TGF-beta Superfamily factors in Fracture Repair</caption> <thead> <tr> <th>Factor</th> <th>Inflammation</th> <th>Cartilage formation</th> <th>Primary bone formation</th> <th>Bone remodelling</th> </tr> </thead> <tbody> <tr> <td>BMP2</td> <td>0</td> <td>3</td> <td>3</td> <td>3</td> </tr> <tr> <td>BMP4</td> <td>1</td> <td>3</td> <td>3</td> <td>1</td> </tr> <tr> <td>BMP8</td> <td>0</td> <td>0</td> <td>3</td> <td>0</td> </tr> <tr> <td>TGF2</td> <td>0</td> <td>0</td> <td>0</td> <td>0</td> </tr> <tr> <td>GDF8</td> <td>3</td> <td>0</td> <td>0</td> <td>0</td> </tr> </tbody> </table> | Factor | Inflammation | Cartilage formation | Primary bone formation | Bone remodelling | BMP2 | 0 | 3 | 3 | 3 | BMP4 | 1 | 3 | 3 | 1 | BMP8 | 0 | 0 | 3 | 0 | TGF2 | 0 | 0 | 0 | 0 | GDF8 | 3 | 0 | 0 | 0 | <p style="text-align: center;">Distraction Osteogenesis (TGF-beta Superfamily)</p> <p style="text-align: center;">Distraction Osteogenesis (TGF-beta Superfamily)</p> <table border="1"> <caption>Relative expression of TGF-beta Superfamily factors in Distraction Osteogenesis</caption> <thead> <tr> <th>Factor</th> <th>Latency (early)</th> <th>Latency (late)</th> <th>Distraction (early)</th> <th>Distraction (late)</th> <th>Consolidation (early)</th> <th>Consolidation (late)</th> </tr> </thead> <tbody> <tr> <td>BMP2</td> <td>2</td> <td>0</td> <td>3</td> <td>3</td> <td>2</td> <td>1</td> </tr> <tr> <td>BMP6</td> <td>0</td> <td>0</td> <td>3</td> <td>2</td> <td>1</td> <td>1</td> </tr> <tr> <td>TGF-beta</td> <td>0</td> <td>0</td> <td>3</td> <td>3</td> <td>0</td> <td>0</td> </tr> <tr> <td>IGF</td> <td>0</td> <td>0</td> <td>2</td> <td>2</td> <td>0</td> <td>0</td> </tr> </tbody> </table> | Factor | Latency (early) | Latency (late) | Distraction (early) | Distraction (late) | Consolidation (early) | Consolidation (late) | BMP2 | 2 | 0 | 3 | 3 | 2 | 1 | BMP6 | 0 | 0 | 3 | 2 | 1 | 1 | TGF-beta | 0 | 0 | 3 | 3 | 0 | 0 | IGF | 0 | 0 | 2 | 2 | 0 | 0 |
| | Factor | Inflammation | Cartilage formation | Primary bone formation | Bone remodelling | | | | | | | | | | | | | | | | | | | | | | | | | | | | | | | | | | | | | | | | | | | | | | | | | | | | | | | | | | | | | | |
| BMP2 | 0 | 3 | 3 | 3 | | | | | | | | | | | | | | | | | | | | | | | | | | | | | | | | | | | | | | | | | | | | | | | | | | | | | | | | | | | | | | | |
| BMP4 | 1 | 3 | 3 | 1 | | | | | | | | | | | | | | | | | | | | | | | | | | | | | | | | | | | | | | | | | | | | | | | | | | | | | | | | | | | | | | | |
| BMP8 | 0 | 0 | 3 | 0 | | | | | | | | | | | | | | | | | | | | | | | | | | | | | | | | | | | | | | | | | | | | | | | | | | | | | | | | | | | | | | | |
| TGF2 | 0 | 0 | 0 | 0 | | | | | | | | | | | | | | | | | | | | | | | | | | | | | | | | | | | | | | | | | | | | | | | | | | | | | | | | | | | | | | | |
| GDF8 | 3 | 0 | 0 | 0 | | | | | | | | | | | | | | | | | | | | | | | | | | | | | | | | | | | | | | | | | | | | | | | | | | | | | | | | | | | | | | | |
| Factor | Latency (early) | Latency (late) | Distraction (early) | Distraction (late) | Consolidation (early) | Consolidation (late) | | | | | | | | | | | | | | | | | | | | | | | | | | | | | | | | | | | | | | | | | | | | | | | | | | | | | | | | | | | | | |
| BMP2 | 2 | 0 | 3 | 3 | 2 | 1 | | | | | | | | | | | | | | | | | | | | | | | | | | | | | | | | | | | | | | | | | | | | | | | | | | | | | | | | | | | | | |
| BMP6 | 0 | 0 | 3 | 2 | 1 | 1 | | | | | | | | | | | | | | | | | | | | | | | | | | | | | | | | | | | | | | | | | | | | | | | | | | | | | | | | | | | | | |
| TGF-beta | 0 | 0 | 3 | 3 | 0 | 0 | | | | | | | | | | | | | | | | | | | | | | | | | | | | | | | | | | | | | | | | | | | | | | | | | | | | | | | | | | | | | |
| IGF | 0 | 0 | 2 | 2 | 0 | 0 | | | | | | | | | | | | | | | | | | | | | | | | | | | | | | | | | | | | | | | | | | | | | | | | | | | | | | | | | | | | | |
| <p style="text-align: center;">Angiogenic</p> <p style="text-align: center;">Fracture Repair (Angiogenic Factors)</p> <table border="1"> <caption>Relative expression of Angiogenic Factors in Fracture Repair</caption> <thead> <tr> <th>Factor</th> <th>Inflammation</th> <th>Cartilage formation</th> <th>Primary bone formation</th> <th>Bone remodelling</th> </tr> </thead> <tbody> <tr> <td>VEGFA</td> <td>0</td> <td>0</td> <td>2.0</td> <td>0</td> </tr> <tr> <td>VEGFC</td> <td>0</td> <td>0</td> <td>2.0</td> <td>0</td> </tr> <tr> <td>VEGFD</td> <td>0</td> <td>2.0</td> <td>1.0</td> <td>0</td> </tr> <tr> <td>Angiopoietin2</td> <td>1.0</td> <td>1.0</td> <td>1.0</td> <td>1.0</td> </tr> </tbody> </table> | Factor | Inflammation | Cartilage formation | Primary bone formation | Bone remodelling | VEGFA | 0 | 0 | 2.0 | 0 | VEGFC | 0 | 0 | 2.0 | 0 | VEGFD | 0 | 2.0 | 1.0 | 0 | Angiopoietin2 | 1.0 | 1.0 | 1.0 | 1.0 | <p style="text-align: center;">Distraction Osteogenesis (Angiogenic Factors)</p> <p style="text-align: center;">Distraction Osteogenesis (Angiogenic Factors)</p> <table border="1"> <caption>Relative expression of Angiogenic Factors in Distraction Osteogenesis</caption> <thead> <tr> <th>Factor</th> <th>Latency (early)</th> <th>Latency (late)</th> <th>Distraction (early)</th> <th>Distraction (late)</th> <th>Consolidation (early)</th> <th>Consolidation (late)</th> </tr> </thead> <tbody> <tr> <td>VEGFA</td> <td>0</td> <td>0</td> <td>1.0</td> <td>1.0</td> <td>1.0</td> <td>0</td> </tr> <tr> <td>VEGFC</td> <td>2.0</td> <td>0</td> <td>0</td> <td>0</td> <td>0</td> <td>0</td> </tr> <tr> <td>VEGFD</td> <td>0</td> <td>0</td> <td>2.0</td> <td>1.0</td> <td>0</td> <td>0</td> </tr> <tr> <td>Angiopoietin2</td> <td>1.0</td> <td>1.0</td> <td>1.0</td> <td>1.0</td> <td>1.0</td> <td>1.0</td> </tr> </tbody> </table> | Factor | Latency (early) | Latency (late) | Distraction (early) | Distraction (late) | Consolidation (early) | Consolidation (late) | VEGFA | 0 | 0 | 1.0 | 1.0 | 1.0 | 0 | VEGFC | 2.0 | 0 | 0 | 0 | 0 | 0 | VEGFD | 0 | 0 | 2.0 | 1.0 | 0 | 0 | Angiopoietin2 | 1.0 | 1.0 | 1.0 | 1.0 | 1.0 | 1.0 | | | | | | |
| Factor | Inflammation | Cartilage formation | Primary bone formation | Bone remodelling | | | | | | | | | | | | | | | | | | | | | | | | | | | | | | | | | | | | | | | | | | | | | | | | | | | | | | | | | | | | | | | |
| VEGFA | 0 | 0 | 2.0 | 0 | | | | | | | | | | | | | | | | | | | | | | | | | | | | | | | | | | | | | | | | | | | | | | | | | | | | | | | | | | | | | | | |
| VEGFC | 0 | 0 | 2.0 | 0 | | | | | | | | | | | | | | | | | | | | | | | | | | | | | | | | | | | | | | | | | | | | | | | | | | | | | | | | | | | | | | | |
| VEGFD | 0 | 2.0 | 1.0 | 0 | | | | | | | | | | | | | | | | | | | | | | | | | | | | | | | | | | | | | | | | | | | | | | | | | | | | | | | | | | | | | | | |
| Angiopoietin2 | 1.0 | 1.0 | 1.0 | 1.0 | | | | | | | | | | | | | | | | | | | | | | | | | | | | | | | | | | | | | | | | | | | | | | | | | | | | | | | | | | | | | | | |
| Factor | Latency (early) | Latency (late) | Distraction (early) | Distraction (late) | Consolidation (early) | Consolidation (late) | | | | | | | | | | | | | | | | | | | | | | | | | | | | | | | | | | | | | | | | | | | | | | | | | | | | | | | | | | | | | |
| VEGFA | 0 | 0 | 1.0 | 1.0 | 1.0 | 0 | | | | | | | | | | | | | | | | | | | | | | | | | | | | | | | | | | | | | | | | | | | | | | | | | | | | | | | | | | | | | |
| VEGFC | 2.0 | 0 | 0 | 0 | 0 | 0 | | | | | | | | | | | | | | | | | | | | | | | | | | | | | | | | | | | | | | | | | | | | | | | | | | | | | | | | | | | | | |
| VEGFD | 0 | 0 | 2.0 | 1.0 | 0 | 0 | | | | | | | | | | | | | | | | | | | | | | | | | | | | | | | | | | | | | | | | | | | | | | | | | | | | | | | | | | | | | |
| Angiopoietin2 | 1.0 | 1.0 | 1.0 | 1.0 | 1.0 | 1.0 | | | | | | | | | | | | | | | | | | | | | | | | | | | | | | | | | | | | | | | | | | | | | | | | | | | | | | | | | | | | | |

2.6 Bone Tissue Engineering

2.6.1 Four-Stage Bone Formation in Bone Tissue Engineering

In Section 1.4, the four key technologies such as cells, scaffolds, bioreactors and imaging tools that are used in BTE has been discussed. In addition to designing successful BTE constructs, strategies should be directed towards achieving mature bone with a more oriented bony structure associated with at least moderate mechanical properties. Current BTE strategies often report success in the formation of early-stage bone, with few demonstrating late-stage bone. To track the stage of maturity of bone formation during BTE, the progression of bone formation has been categorised into four distinct stages, starting from the precipitation of mineralised nodules to eventual lamellar bone formation (**Table 2-4**).

Table 2-4: Four-staged bone forming process relating to the structural bone, its mechanical properties and vessel formation over time of healing; + indicates the relative intensity.

| Stage of Bone Formation | Stage 1 | Stage 2 | Stage 3 | Stage 4 |
|----------------------------|---|---|---|---|
| Mineralisation | Mineralisation | Woven bone | Trabecular bone | Lamellae bone |
| Mechanical Strength | + | ++ | +++ | ++++ |
| Bone Structure | Random distribution Nucleation and rapid growth of mineral nodules occurs under a thermodynamic driving force when in a 3D space | Disjointed fine plate-like networks of two or more connecting fibres randomly oriented Low density with large porosity | Bone plates are joined and highly oriented, conforming to the applied stresses | Dense and compact Multilayered bone plates arranged in a concentric manner conforming to applied stresses |
| |  |  (Barbashina <i>et al.</i> 2004) |  (Ribó 2011) |  (Meijer <i>et al.</i> 2007) |
| Time from injury | 1-2 weeks | 3-6 weeks | ~3-6 months | Months-Years |
| Vascularisation | | | | |
| (a) Extrasosseous | + | +++ | +++ | +++ |
| (b) Medullary | - | + | ++ | +++ |
| Cytokines | Discontinuous and temporally regulated at high levels | | Moderate regulation for homeostasis and remodelling | |

2.6.2 Strategies in Bone Tissue Engineering

BTE strategies can be broadly categorised into two main approaches, namely the growth factor and cell-based approach. The growth factor approach is simple and relies on the mobilisation of the patient's own stem cells for self-reparative bone healing mechanisms, hence avoiding all issues pertaining to cell culture and expansion. However, this technique might not be beneficial to the aged or patients suffering from severe trauma, poorly controlled diabetes, and osteoporosis due to their diminishing pool of endogenous osteogenic cells (Bruder and Fox 1999; Service 2000). On the other hand, a cell-based approach utilises an exogenous supply of osteogenic cells in sufficient numbers for direct bone repair.

2.6.2.1 Growth Factors Approach

One strategy utilises growth factors which are commonly used as signalling molecules for the stimulation of cellular growth, proliferation and differentiation. The use of growth factors for bone regeneration has been reported with some success in various animal and clinical models (Luginbuehl *et al.* 2004; Lee *et al.* 2011). However, the intrinsic instability of growth factors and short half-life leads to rapid loss in bioactivity upon release *in vivo* (Tabata 2003). To attain a therapeutic effect, a high supraphysiological dosage is often used, raising concerns of possible risks of overriding the normal regulation of osteoinduction. To overcome this problem, delivery systems are used in conjunction with growth factors for controlled sustained delivery through non-covalent or covalent entrapment methodologies (**Figure 2-5**) (Luginbuehl *et al.* 2004).

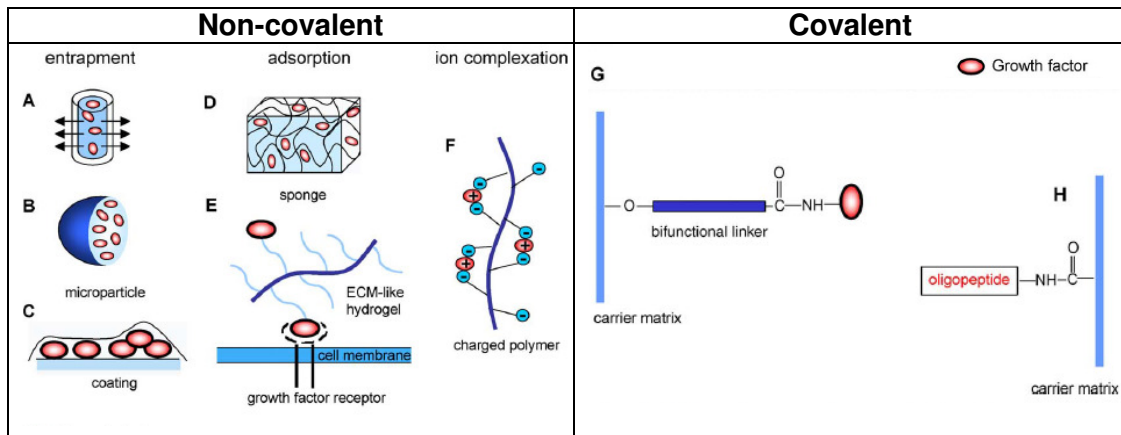


Figure 2-5: Growth factor delivery systems and their various entrapment methodologies. Non-covalent strategies include (A-C) physical entrapment released by diffusion with or without degradation of delivery system (D-E) adsorption through physiochemical interactions with material or receptor-proteins (F) ion complexation of growth factors with oppositely charged molecules or *via* (G) covalent means through direct coupling or *via* a bifunctional linker. *Figures reproduced from Luginbuehl et al (Luginbuehl et al. 2004).*

To note, these growth factor delivery systems release growth factors on a continuous burst release profile. Hence, it is difficult to control the temporal and spatial release profile of growth factors in a way that mimics the physiological up and down-expression of cytokine response during different stages in bone repair as discussed in the earlier section (Ai-Aqi *et al.* 2008). Furthermore, the lack of information on the optimal concentrations and controlled time of release makes delivery of multiple growth factors difficult. Apart from the high costs, recent issues relating to the safety and long term efficacy of growth factors have also been highlighted (Poynton and Lane 2002). For example, bone morphogenetic proteins (BMPs) are potent bone-stimulating growth factors, of which BMP-2 and BMP-7 are FDA-approved for the treatment of long bone non-union fractures and spinal fusions. However, recent off-label use of bone morphogenetic protein (BMP) for lumbar interbody fusions have resulted in ectopic bone formation associated with severe neurological impairment (Wong *et al.* 2008); other adverse complications arising from BMP use include excessive swelling at neck and throat, breathing and swallowing difficulties (Shields *et al.* 2006; Boraiah *et al.* 2009). Thus, the use of the growth factor requires much

caution and is deemed less ideal as a therapeutic modality for BTE applications. Better understanding of growth factors including the appropriate dosage, mode of administration as well as other clinical trial design-related issues is required (Lee *et al.* 2011).

2.6.2.2 Cell-Based Approach

The first cell-based approach using unfractionated fresh bone marrow was implemented in 1989 (Connolly 1989), with other cell sources such as undifferentiated stem cells and differentiated osteoblasts also being used and reported with some success in various experimental animal models (Tseng *et al.* 2008) and in the clinical realm (Salter *et al.* 2011). Compared to the growth factor strategy, a cell-based strategy has the inherent ability to secrete a milieu of growth factors at its physiological doses and timings that is likely to be more conducive for tissue regeneration compared to the growth factor approach (Rouwkema *et al.* 2008). However, stringent regulatory approvals of cellular therapy also warrant greater caution when used in the clinics.

This PhD project will focus on a cell-based strategy for vascularised BTE due to the reported clinical efficacy in various cell-based therapies (Zhang *et al.* 2012).

2.7 Vascularisation Strategies in Bone Tissue Engineering

Keeping in mind the extensive vasculature within the natural bone tissue, bone is heavily reliant on this supply of blood vessels for maintenance of cell survival and skeletal integrity. Generally, tissues rely on blood vessels within close proximity of 100-200 μ m to supply sufficient nutrients and oxygen (Carmeliet and Jain 2000). Successful advances of tissue engineering into clinically viable products have so far

been limited to thin or avascular tissues such as skin and cartilage respectively, while vascular insufficiency exists in other thick tissues and voluminous tissue-engineered grafts. In times of a bone fracture, the vascular supply in the defect zone is disrupted. Slow spontaneous vascular ingrowth is inadequate (Rouwkema *et al.* 2008). Hence, large BTE-grafts often suffer from poor cellular survival particularly in the core due to inadequate exchange of nutrient and oxygen (**Figure 2-6**) (Rouwkema *et al.* 2008). This results in non-uniform cell integration, cellular necrosis and eventual failure of the BTE-graft (Ko *et al.* 2007; Kanczler and Oreffo 2008; Rouwkema *et al.* 2008), limiting the clinical translation of tissue engineering research. Muschler's theoretical model illustrates the oxygen concentration gradient within a cellular-scaffold graft, where cell survivability is based on a balance between cellular density, their oxygen consumption as well as diffusion distance within the scaffold (Muschler *et al.* 2004). To approach this issue, several strategies have been undertaken to introduce vasculature into tissue-engineered constructs (Rouwkema *et al.* 2008; Lovett *et al.* 2009).

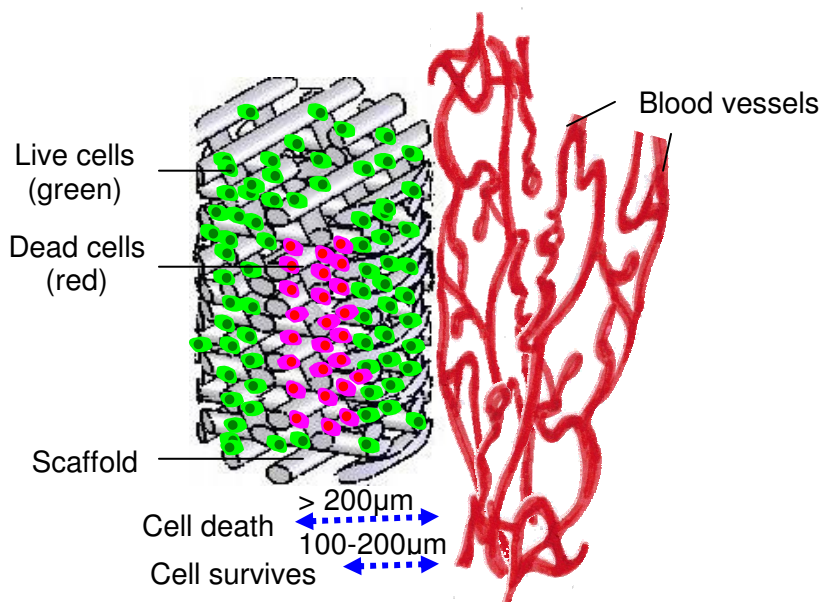


Figure 2-6: Conceptual illustration of cell viability and cell death within the thick scaffold graft towards its core where cells are found more than 200 μ m away from the blood vessel supply.

2.7.1 'Smart'-scaffolds and Growth Factors

One strategy involves the use of 'smart'-scaffold technology by functionalising scaffolds surfaces through physical adsorption *via* intermediate proteins or biological molecules or by direct covalent immobilisation of bioactive molecules such as growth factors. Growth factors can also be physically encapsulated within the scaffolds, acting as delivery systems for controlled release (Lee *et al.* 2011) (**Figure 2-7**). For example, VEGF covalent linked-collagen scaffolds resulted in rapid vascularisation *in vivo*, leading to improved myocardial repair compared to its untreated control. In another study, Kaigler showed increased blood vessel formation invading the VEGF-encapsulated poly(lactic-co-glycolic acid) scaffolds, accompanied by earlier and greater bone formation in an irradiated rat calvarial defect model compared to scaffolds alone (Kaigler *et al.* 2006). In gene therapy, stem cells such as MSC are used as vehicles for the delivery of angiogenic growth factors, where cells are transduced *ex vivo*, encoding the growth factor/s of interest. For example, the use of VEGF-transduced MSC showed increased vascularity upon VEGF expression alone, which in synergy with VEGF/bone morphogenetic protein-2 (BMP-2) transduced MSC enhanced bone formation in a segmental tibia defect mice model (Kumar *et al.* 2010). Numerous other studies have also demonstrated significant benefits of angiogenic growth factor delivery (Street *et al.* 2002; Kempen *et al.* 2009) or gene therapy (Peng *et al.* 2002; Ito *et al.* 2005) in aiding bone regeneration for use in BTE applications.

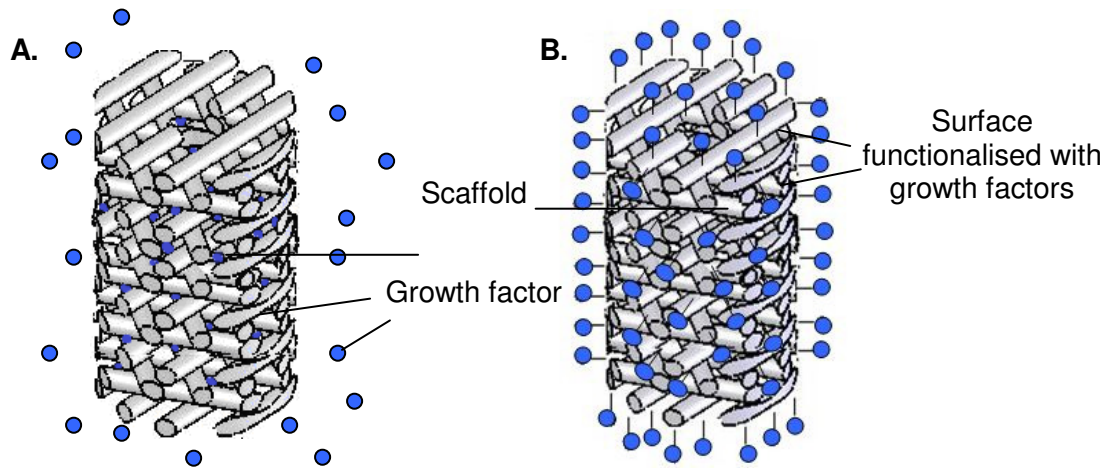


Figure 2-7: Diagrammatic representation of porous scaffold constructs (A) encapsulated with growth factors and its time-dependent control release (B) surface functionalised with growth factors either *via* physical adsorption or covalent immobilisation methods.

This method avoids all issues pertaining to cell culture and expansion by allowing mobilisation of the patient's own stem cells for self-reparative bone healing mechanisms. However, such a method relies on the ingrowth of host vasculature which often takes time. Other issues relating to the use of growth factors have been discussed earlier in [Section 2.6.2](#).

2.7.2 Prevascularisation Techniques

To facilitate full vascularisation of the tissue-engineered graft, *in vitro* and *in vivo* prevascularisation methodologies have been introduced. This is done by first incorporating vessel structures within the graft prior to implantation at the defect site, with the aim of facilitating rapid anastomosis with the host vasculature and re-establishing blood perfusion at the defect site.

2.7.2.1 *In Vivo* Prevascularisation

In vivo prevascularisation involves initial implantation of the tissue-engineered graft within well-vascularised sites, such as the muscle, for complete vascularisation prior to subsequent implantation at the defect site. **Figure 2-8** shows a mandibular replacement transplantation using a bone-muscle-flap prefabrication technique for the repair of a patient's mandibular discontinuity defect. The titanium loaded with BMP was grown inside the latissimus muscle until adequate with a vessel pedicle prior to subsequent transplantation into the defected mandibular region. This approach allows for instantaneous reperfusion *via* surgical anastomosis, hence ensuring its therapeutic efficacy. However, it requires multiple surgeries, accompanied by significant morbidity at the secondary site, thus limiting its clinical appeal.

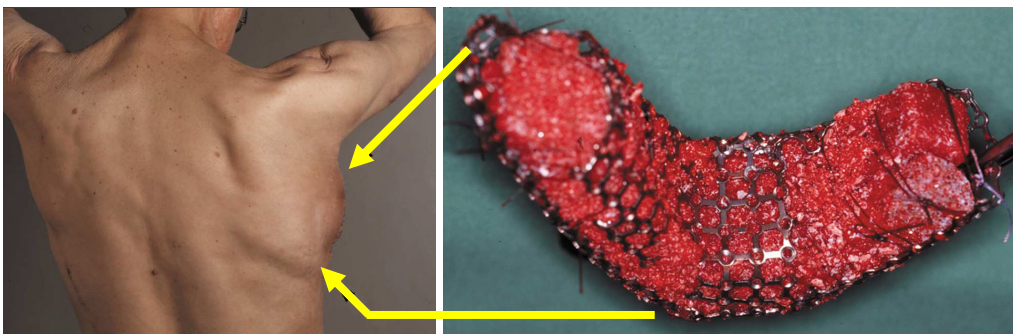


Figure 2-8: An example of an *in vivo* prevascularisation technique. The implant is grown inside the latissimus dorsi muscle, followed by subsequent transplantation in the mandible. *Figures reproduced from Warnke et al (Warnke et al. 2004).*

2.7.2.2 *In Vitro* Prevascularisation

Another prevascularisation method commonly referred to as the *in vitro* prevascularisation technique is one that avoids the need for an initial *in vivo* implantation. This strategy relies on the utility of endothelial cells in coculture with the other cell type, to generate an *in vitro* vascular network. It has been shown to augment vascularisation within the scaffold constructs which was accompanied by

functional anastomosis (Fuchs *et al.* 2007; Melero-Martin *et al.* 2008; Fuchs *et al.* 2009; Tsigkou *et al.* 2010). With the preformed vessels, host vessels would only need to grow to the outer regions of the graft until it reaches the prevascularised vessels, hence, drastically shortening the time required to completely vascularise the tissue-engineered graft. Although this method involves the complexity of forming stable *in vitro* vasculature in the constructs and has a slower rate of anastomosis efficacy compared to *in vivo* prevascularisation, this approach avoids the need for multiple surgeries (Rouwkema *et al.* 2008).

A summary comparing the advantages and disadvantages of both *in vitro* and *in vivo* prevascularisation approaches can be found in **Table 2-5** below.

Table 2-5: A summary of the advantages and disadvantages of *in vitro* and *in vivo* prevascularisation strategies. *Adapted from Rouwkema et al (Rouwkema et al. 2008).*

| <i>In vitro</i> Prevascularisation | <i>In Vivo</i> Prevascularisation |
|---|---|
| <ul style="list-style-type: none"> + Does not rely on ingrowth of host vasculature into entire construct + No extra surgery necessary | <ul style="list-style-type: none"> + Direct perfusion after microsurgery + Mature, organised vasculature |
| <ul style="list-style-type: none"> - Complex strategy, varying from tissue to tissue - Vessel maturation <i>in vitro</i> needs attention - Anastomosis not as fast as with <i>in vivo</i> prevascularisation | <ul style="list-style-type: none"> - Extra implantation/surgery necessary - Need of finding a proper location with vascular axis for prevascularisation - Scaffold might be filled with fibrous tissue during initial implantation |

Considering these vascularisation strategies, the use of a safe and efficacious off-the-shelf vascularised BTE product that requires only one implantation surgery is favoured. In this project, an *in vitro* prevascularisation approach using a cell-based coculture system will be investigated.

2.8 Components of Bone Tissue Engineering

In devising a vascularised BTE graft, there are various components that need to be carefully considered to ensure success when combined together. These include the

converging use of osteoconductive scaffolds, osteogenic and vasculogenic cells that secrete potent biomolecules, in an appropriate culture system under an optimal microenvironment.

2.8.1 Scaffolds

Three-dimensional (3D) scaffolds have been used in BTE to provide a local environment for cells, serving as temporary matrix to support/direct cellular growth/differentiation (Langer and Vacanti 1993) and provide mechano-induction for expression of growth factors and ultimately bone remodeling. Particularly for bone, the ideal scaffold has to be mechanically stable to temporarily support the defect zone while resorbing at a rate in tandem with new bone formation in the defect region as illustrated in **Figure 2-9** (Hutmacher 2000).

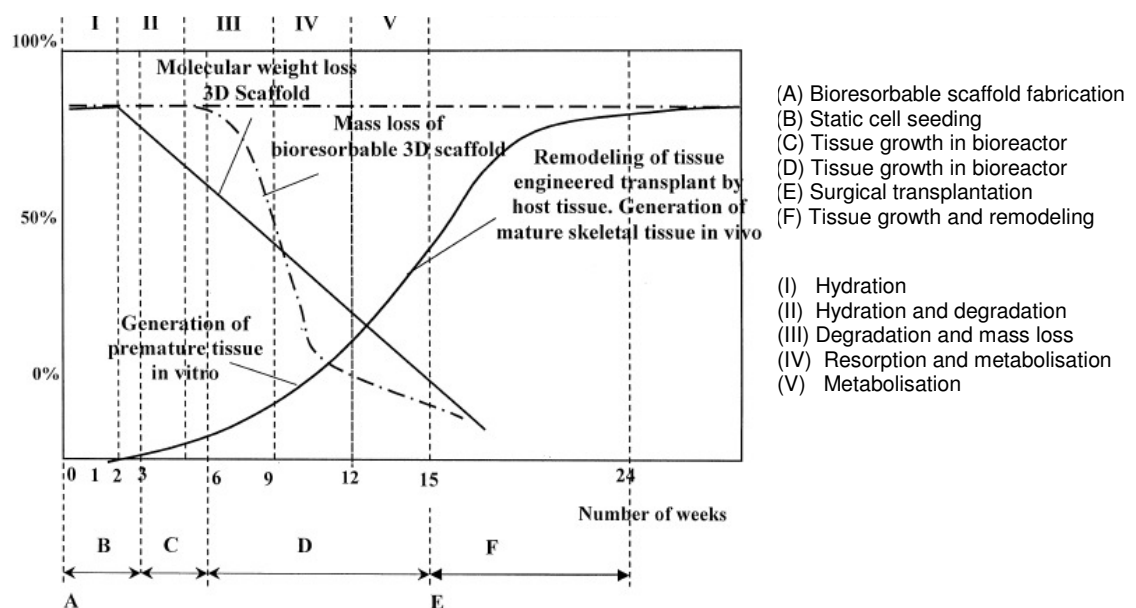


Figure 2-9: Graphical representation of the molecular weight loss of the 3D scaffold with respect to the growth and remodelling of the tissue-engineered constructs over time. *Figure reproduced from Hutmacher et al (Hutmacher 2000).*

In tissue remodelling, cells can recognise the architectural feature of microenvironment and differentiate accordingly. Therefore, it follows that the structural characteristics of the scaffold are important in guiding cellular distribution and organisation, and should be designed to mimic the trabecular bone structure closely. The emphasis on sufficient scaffold porosity to accommodate vascular infiltration, tissue ingrowth and mass transport for maintaining cell survival in thick grafts has also been highlighted (**Figure 2-10**) (Muschler *et al.* 2004). Most importantly, the biomaterial should interact with the host tissue to exert a desirable cellular response that aids tissue repair (Lanza *et al.* 2007).

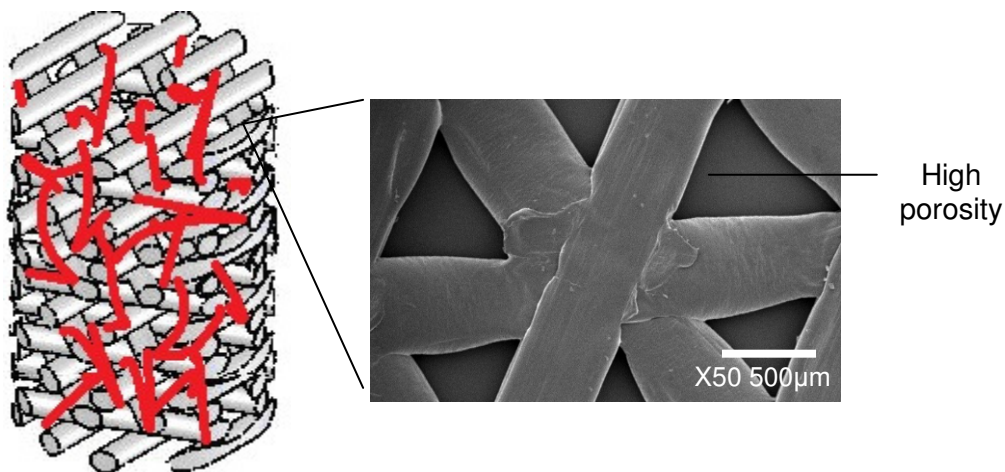


Figure 2-10: Illustration of a scaffold with a trabecular-like honeycomb structure and high porosity that allows for vascular infiltration, mass transport and new tissue formation. (Right-hand image) Scanning electron microscopy shows a honeycomb polycaprolactone/tri-calcium phosphate scaffold, with an average pore size within the range of 500µm.

Fundamental scaffold design factors for consideration include type of material, its architecture and porosity, surface chemistry and osteoinductivity, mechanical strength, ease of manufacturability and clinical handling. **Table 2-6** summarises the importance of each criteria in order for the scaffold to perform its function in BTE.

Table 2-6: Basic criteria and considerations when designing a scaffold for use in BTE applications (Hutmacher 2000; Salgado *et al.* 2004).

| Criteria | Feature | Function |
|-----------------------|--|---|
| Biocompatibility | Good integration with host tissue | Do not elicit immune response |
| Microarchitecture | Interconnected scaffold struts that complies to applied stresses | To uniformly distribute stresses throughout scaffold |
| Porosity | Large surface area: volume, ideally with pore size ranging between 200-900 μ m | Allow for cell in-growth, neovascularisation, sufficient mass transport and osteogenesis |
| Surface properties | Appropriate chemical and topographical properties | Affects cellular adhesion, proliferation, protein interactions and osteoconduction |
| Osteoinductivity | Osteoinductive properties | To recruit and differentiate osteoprogenitors to the defect region |
| Mechanical properties | Sufficient mechanical strength, appropriately tuned with porosity | To withstand loading forces <i>in vivo</i> ; withstand hydrostatic pressure; allow for cellular in-growth and matrix production |
| Biodegradability | Biodegradable at an appropriate rate to match growth of neotissue | To temporarily support the defect zone as scaffold gets replaced by new bone |

2.8.1.1 Biomaterial Selection

The choice of an appropriate material is key in determining the properties of the scaffold for BTE. Current biomaterials used in BTE are limited a small selection of ceramics and biodegradable polymers. Ceramics have good osteoinductivity which makes it ideal for osteogenic cells to adhere, growth and differentiate towards an osteolineage (Roether *et al.* 2002; Lu *et al.* 2005). The bioactive properties of ceramics also allow for good bonding to native bone by forming an interfacial layer with surrounding tissues to prevent eventual implant expulsion. However, their main limitation is due to the poor processability due to their brittleness, hence making it difficult to process to achieve the desired porosity (Cooke 1992). Examples include natural origin such as coralline and synthetic hydroxyapatite (HA) or ceramics like β -tri-calcium phosphate (β -TCP) (LeGeros 2002).

Biodegradable polymers are believed to be an ideal alternative. Natural polymers such as collagen, chitosan, hyaluronic acid have a low immunogenic potential, with a bioactive potential that is capable of interacting with the host tissue (Salgado *et al.* 2004). Synthetic polymers are more widely used in biomedical applications as their biodegradation rates can be controlled as desired and they could be easily fabricated and shaped accordingly. Furthermore, polymers can be surface modified to attach appropriate chemical functional groups to achieve specific responses that help in directing cell growth (Gunatillake and Adhikari 2003). However, they have limited capabilities in achieving strong bonding and integration with bone, have weak mechanical properties [Elastic Modulus_{polymer} 3GPa versus Elastic Modulus_{bone} 21GPa (Teoh 2004)] and some also release acidic degradation by-products *in vivo*, resulting in inflammatory responses (Bostman *et al.* 1990; Bergsma *et al.* 1995; Gunatillake and Adhikari 2003). Regulatory approved biodegradable and bioresorbable polymers include collagen, polyglycolide (PGA), polylactides (PLLA, PDLA) and polycaprolactone (PCL).

2.8.1.2 Polycaprolactone

PCL is a semicrystalline biodegradable polymer from the family of aliphatic polyesters. It has a low glass transition temperature of -60°C and low melting point (59-64°C). It is non-toxic and biocompatible, degrading into non-harmful by-products such as CO₂ and water, which will not induce a deleterious inflammatory response unlike other polyesters. Compared to other polymers, PCL is one of the slowest in its degradation (>24 months) (Gunatillake and Adhikari 2003). This makes it suitable for long term bone implantations to provide temporary mechanical support and structural integrity at the defect site, while matching the rate of new bone formation and remodeling. However, it has poor mechanical properties with an elastic modulus of 0.4GPa (Hutmacher 2000) as compared to 21GPa in bone (Teoh 2004).

2.8.1.3 Tri-calcium Phosphate

Due to the inherent stiffness of inorganic ceramics, the incorporation of TCP [Elastic modulus_{TCP} 7GPa versus Elastic modulus_{polymer} 3GPa (Teoh 2004)] would act as a reinforcing material to improve the weak mechanical properties of PCL. Its osteoinductivity would also permit better cell growth and interaction with surrounding host bone (Rezwan *et al.* 2006; Guarino *et al.* 2007). The incorporation of the bioactive phases will increase water ingress into the polymer/ceramic interfaces, allowing the degradation kinetics of the polymeric scaffold to be tailored as desired (Hutmacher 2000; Kim *et al.* 2005).

2.8.1.4 Proposed Scaffold – Polycaprolactone/Tri-calcium Phosphate Composite

Due to the individual material limitations, the use of composite materials has been of increased popularity in tissue engineering approaches as it combines the desired properties of both materials. In this project, the use of a polymer composite scaffold with ceramic inclusions of TCP granules will be embedded within a polymeric matrix as seen in the micro-computed tomography (Micro-CT) image in **Figure 2-11**.

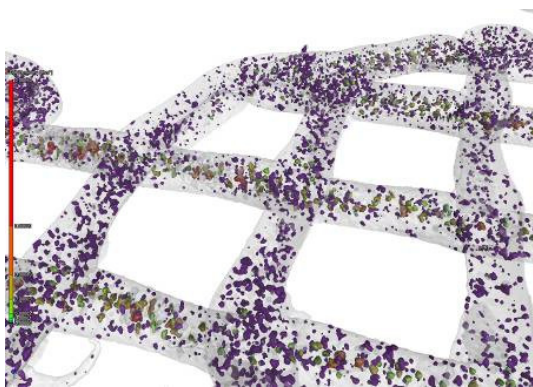


Figure 2-11: Micro-computed tomography imaging of PCL/TCP composite scaffold showing fine TCP granules interspersed randomly within the polymer matrix (Courtesy of GE Sensing & Inspection Technologies).

2.8.3.1 Scaffold Design and Characteristics

These PCL/TCP scaffolds have been used extensively in many *in vitro* and *in vivo* experiments since the past decade. It has a unique honeycomb microarchitecture with a lay-down pattern of 0/60/120° and interconnected pores for promoting cellular bridging and ingrowth of bone tissue. At the same time, its large pores support mass transport and vascular infiltration into the scaffold (**Figure 2-10**).

The efficacy of these PCL/TCP scaffolds has been demonstrated in several BTE investigations, exhibiting good biocompatibility and the ability to induce robust osteogenic differentiation and bone repair in various critical-sized defect animal models (Rai *et al.* 2007; Zhang *et al.* 2009; Zhang *et al.* 2010; Bae *et al.* 2011; Lim *et al.* 2011). Its unique scaffold microarchitecture also plays an important role in aiding *in vivo* vascularisation. Zhang *et al.* (Zhang *et al.* 2010) and Rai *et al.* (Rai *et al.* 2007) demonstrated the formation of extensive vasculature within the MSC or platelet-rich plasma-loaded PCL/TCP scaffold respectively 12 weeks post-implantation in a critical-sized rat femoral model. These studies demonstrate their ability of the scaffold construct in supporting cell adhesion, proliferation, bone formation as well as vessel network formation. In addition, Rai *et al.* showed a discontinuous growth factor release profile from BMP-2-loaded PCL-based scaffolds *in vitro* (Rai *et al.* 2005), similar in fashion to the up and down regulation of various cytokines during natural bone repair (Ai-Aql *et al.* 2008), suggesting its feasibility as a drug delivery system. Fabricated by fused deposition modelling technique, the shape of the scaffold can be customised accordingly to fit the bone defect. The main features of this composite PCL/TCP scaffold are summarised in **Table 2-7** below.

Table 2-7: PCL/TCP scaffold design and its characteristics as reported in literature data.

| Proposed PCL/TCP scaffold | Evidence | Reference |
|---|---|--|
| Excellent biocompatibility Osteoconductive | <ul style="list-style-type: none"> • Implanted in many small and large animal models over long term without provoking a foreign host response • Showed evidence of good bony regeneration | (Rai <i>et al.</i> 2007; Zhang <i>et al.</i> 2009; Zhang <i>et al.</i> 2010; Bae <i>et al.</i> 2011; Lim <i>et al.</i> 2011; Yeo <i>et al.</i> 2011) |
| Interconnected honeycomb structure and mechanical stiffness | <ul style="list-style-type: none"> • Simulated and shown to uniformly distribute shear stresses along its filaments • Similar to cancellous bone | (Singh <i>et al.</i> 2005) (Hutmacher <i>et al.</i> 2001; Yeo <i>et al.</i> 2008) |
| Macro-porosity; 75% porous with ~ 500um pore size | <ul style="list-style-type: none"> • Allowed for vascular infiltration and tissue formation | (Rai <i>et al.</i> 2007; Zhang <i>et al.</i> 2010) |
| Slow degradation | <ul style="list-style-type: none"> • Slow degradation <i>in vitro</i> and <i>in vivo</i>, providing temporary support at defect region | (Lam <i>et al.</i> 2008; Yeo <i>et al.</i> 2008) |

Having obtained a suitable scaffold, the next step is to select reliable cells sources that could give rise to *in vitro* vessels and osteogenesis within the 3D scaffold construct.

2.8.2 Cellular Sources

The selection of an appropriate cell source for BTE applications is important in ensuring a successful outcome. Two main cell sources are considered here; one cell type will be selected for its osteogenic potential, and another cell type for its vessel forming ability.

2.8.2.1 Osteogenic Cells

The use of autologous fresh bone marrow aspirates is widely practiced in the clinical setting (Connolly 1989; Quarto *et al.* 2001; Hernigou *et al.* 2006) due to its ease of harvest and bone regenerative efficacy. However, its use is constrained by patient-dependent factors that determine the quantity of osteoprogenitors in the bone marrow. While osteoblast remains to be the best performing osteogenic cell type,

they have a limited expansion *in vitro* with only a few cells available upon dissociation of tissue, hence making it challenging for applications that require large cell numbers (Heath 2000).

The use of stem cells has presented themselves as a favourable alternative due to their high proliferative capability, ability to self-renew and differentiate into multiple tissue types upon directed induction. Their utility for bone repair has been demonstrated in various small and large animal models (Tseng *et al.* 2008). Embryonic Stem Cells (ESC) and induced Pluripotent Stem Cells (iPSC) are pluripotent stem cells that can differentiate into all cell types of the three germ layers and can be expanded to large numbers. However, their utility *in vivo* are fraught with concerns such as teratoma formation (Fong *et al.* 2010), potential immunogenic rejection (Drukker and Benvenisty 2004; Grinnemo *et al.* 2008; Zhao *et al.* 2011). Compared to other cellular sources, MSC has emerged as the most ideal cell source for use in BTE applications (**Table 2-8**) (Zhang *et al.* 2012).

Table 2-8: Comparison of different cellular sources, including MSC for their potential in BTE applications. *Table reproduced from Zhang et al (Zhang et al. 2012).*

| | Fresh BM | Osteoblast | Stem cells | | |
|----------------------------|-------------------|-------------------|--------------------|-----|-------|
| | | | IPS and ESC | MSC | hfMSC |
| Harvesting efficiency | +++ | + | + | ++ | ++ |
| Expansion capacity | N.A. | + | +++ | ++ | +++ |
| Cryopreservation | N.A. | + | +++ | +++ | +++ |
| Off-the-shelf availability | N.A. ^a | N.A. ^a | ++ | ++ | +++ |
| Immunogenicity | +++ | ++ | -/+++ ^b | - | - |
| Osteogenic potential | + | +++ | ++ | ++ | +++ |
| Tumorigenicity | - | - | + | - | - |

^a Allogeneic applications can be achieved by proper HLA matching.

^b IPS and ESC are generally non-immunogenic when undifferentiated, but may become immunogenic on differentiation.

2.8.2.2 Mesenchymal Stem Cells

MSC are multipotent cell sources that have the capacity to differentiate into various cell types such as bone, cartilage, muscle, fat and other tissue types (**Figure 2-12**) (Caplan 2006). They can be readily isolated by plastic adherence from various sources such as the umbilical cord blood, adipose tissues, liver, amniotic fluid, with the bone marrow being the most well-studied source (Prockop 1997; Pittenger *et al.* 1999). The ease of isolation, extensive expansion without undergoing differentiation (Haynesworth *et al.* 1992; Bruder *et al.* 1997) and stable phenotype in culture (Bruder *et al.* 1997; Pittenger *et al.* 1999) makes MSC an attractive therapeutic cell source for BTE. Furthermore, its low immunogenicity also suggests the potential of allogeneic use in therapeutic applications (Le Blanc 2003; Zhang *et al.* 2012). Their use for the treatment of various non-orthopaedic and orthopaedic diseases and defects in BTE have shown promising clinical results (Zhang *et al.* 2012).

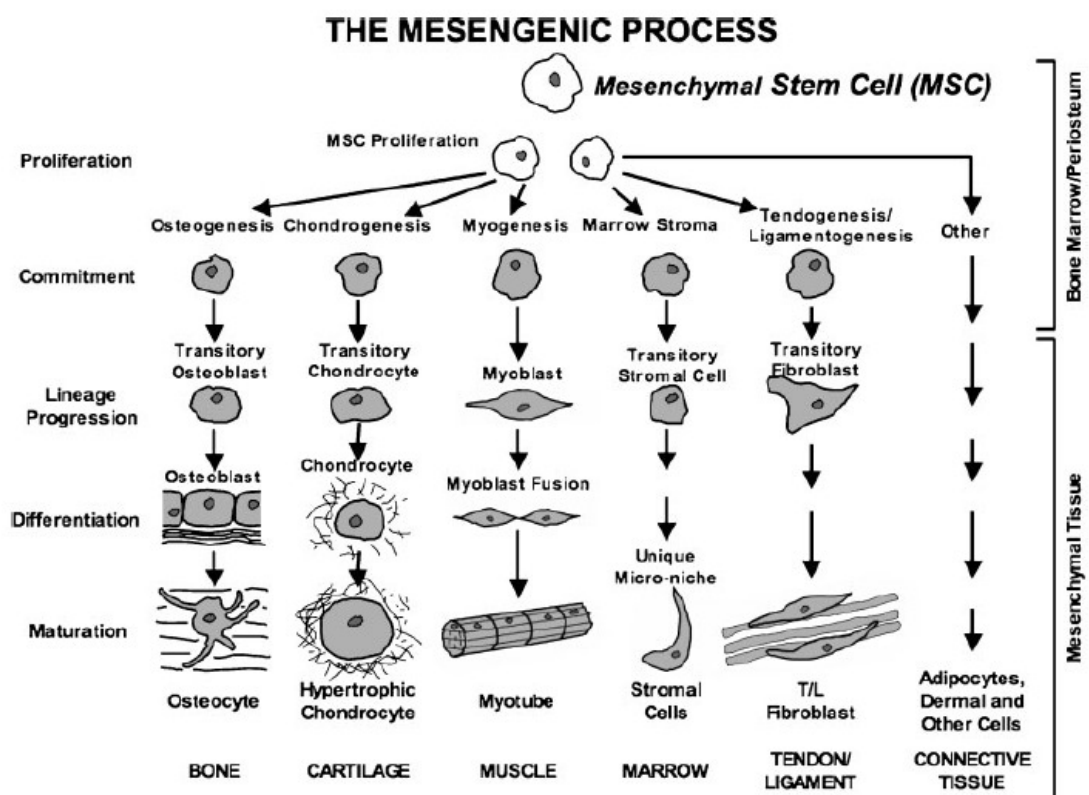


Figure 2-12: The process of mesengensis illustrates the ability of MSC to undergo defined differentiate into various cellular lineages, including bone. *Figure reproduced from Caplan et al (Caplan 2006).*

2.8.2.3 Mesenchymal Stem Cells in Bone Tissue Engineering

The efficacy of MSC for fracture healing has been demonstrated in various preclinical animal models such as rodents (Bruder *et al.* 1998; Meinel *et al.* 2006), dogs (Bruder *et al.* 1998), goats (Kruyt *et al.* 2004) and sheep (Bensaid *et al.* 2005). The first proof-of-principle of MSC ability in aiding bone repair and regeneration was demonstrated in an 8mm segmental rat femur defect. New bone formation was observed throughout the pores of the macroporous osteoconductive scaffold by eight weeks with good bony integration between the host and implant interface upon autologous MSC implantation (Kadiyala *et al.* 1997). Other studies showed the efficacy of autologous bone marrow stromal cells for healing of CSD in large animal models (Bruder *et al.* 1998; Kon *et al.* 2000; Zhu *et al.* 2006), showing significant improvement in fracture healing and osseous integration. For example, Bruder *et al.* demonstrated significant healing and defect union at a 21mm femoral defect region of a canine model upon implantation with MSC-loaded scaffolds, with eventual integration and remodelling at 16 weeks (Bruder *et al.* 1998). Clinically, Quarto *et al.* was the first to report success in the repair of large bone defects with the use of autologous bone marrow stromal cells seeded onto macroporous hydroxyapatite scaffolds, with all three patients attaining recovery of limb function without any reported complications over long term monitoring (Quarto *et al.* 2001; Marcacci *et al.* 2007).

Compared to other sources of MSC, bone-marrow derived MSC (BM-MSC) are currently benchmarked as the next most appropriate cell source, reported to undergo a well-defined osteogenic differentiation pathway (Frank *et al.* 2002; Qi *et al.* 2003). Other cell types such as adipose, muscle, dental pulp-derived MSC are less well understood for their skeletal therapeutic potential (Robey 2011) as they exhibit weak

osteogenic differentiation *in vivo* (Colnot 2011) and do not support formation hematopoietic marrow (Robey 2011).

2.8.2.4 Proposed Cell Type – Human Fetal Mesenchymal Stem Cells

hfMSC was identified by Campagnoli *et al* in 2001 from first trimester fetal blood, liver, and bone marrow (Campagnoli *et al.* 2001) and found to exhibit typical MSC characteristics in terms of its morphology and immunophenotype and tri-lineage differentiation like its adult MSC (Campagnoli *et al.* 2001; Zhang *et al.* 2009). hfMSC was compared head-to-head to its adult counterparts, found to exhibit higher proliferation and osteogenic capacity, with lowered immunogenicity (O'Donoghue and Fisk 2004; Gotherstrom *et al.* 2005; Zhang *et al.* 2009). In terms of its osteogenic capacity, Guillot *et al* demonstrated significant reduction of fracture rates in osteogenesis imperfecta mice upon intrauterine transplantation of hfMSC (Guillot *et al.* 2008); Clinically, Le Blanc *et al* also showed engraftment and differentiation of hfMSC into bone after in utero transplantation in a patient with severe osteogenesis imperfecta, followed by consequential normal growth rates at two years of age (Le Blanc *et al.* 2005). More recently, the implantation of hfMSC-graft into a critical-sized rat femoral defect led to formation of an extensive vasculature network with functional union repair as compared to little vessel infiltration in the control group after 12 weeks (**Figure 2-13**) (Zhang *et al.* 2010). These studies suggest the potential of hfMSC as a cell source for bone regeneration.

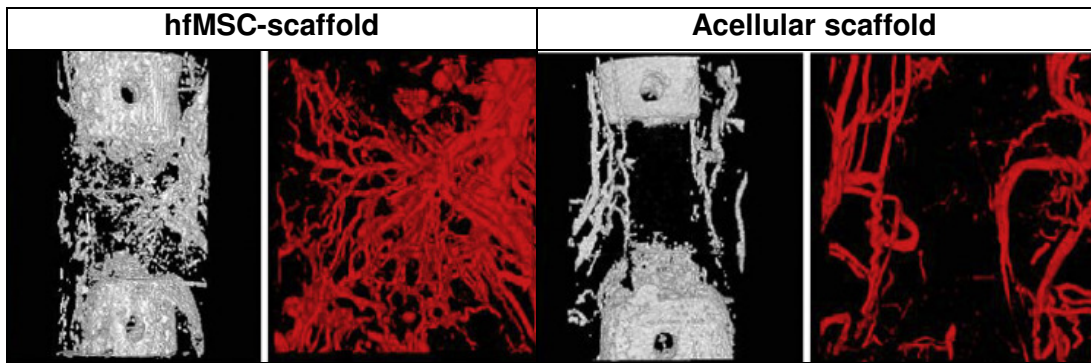


Figure 2-13: hfMSC constructs showed formation of an extensive vasculature network with functional union repair after 12 weeks as compared to little vasculature in the defect region of acellular constructs. *Figures reproduced from Zhang et al (Zhang et al. 2010).*

2.8.2.5 Endothelial Cell Types

In vascularised tissue engineering, the choice of endothelial cell (EC) type used for prevascularisation of graft is crucial. Adult vascularisation is traditionally believed to occur *via* the process of angiogenesis rather than vasculogenesis. Angiogenesis is the process whereby new blood vessels are formed as mature EC sprout from pre-existing vessel structures (D'Amore and Thompson 1987; Risau 1997), while vasculogenesis is the formation of new blood vessels from the differentiation of progenitor cells, thought to occur only in embryogenesis (**Figure 2-14**) (Krenning *et al.* 2009). However, recent identification of EPC have challenged this theory, suggesting its role in postnatal vasculogenesis for neovascularisation and remodelling (Mund *et al.* 2009).

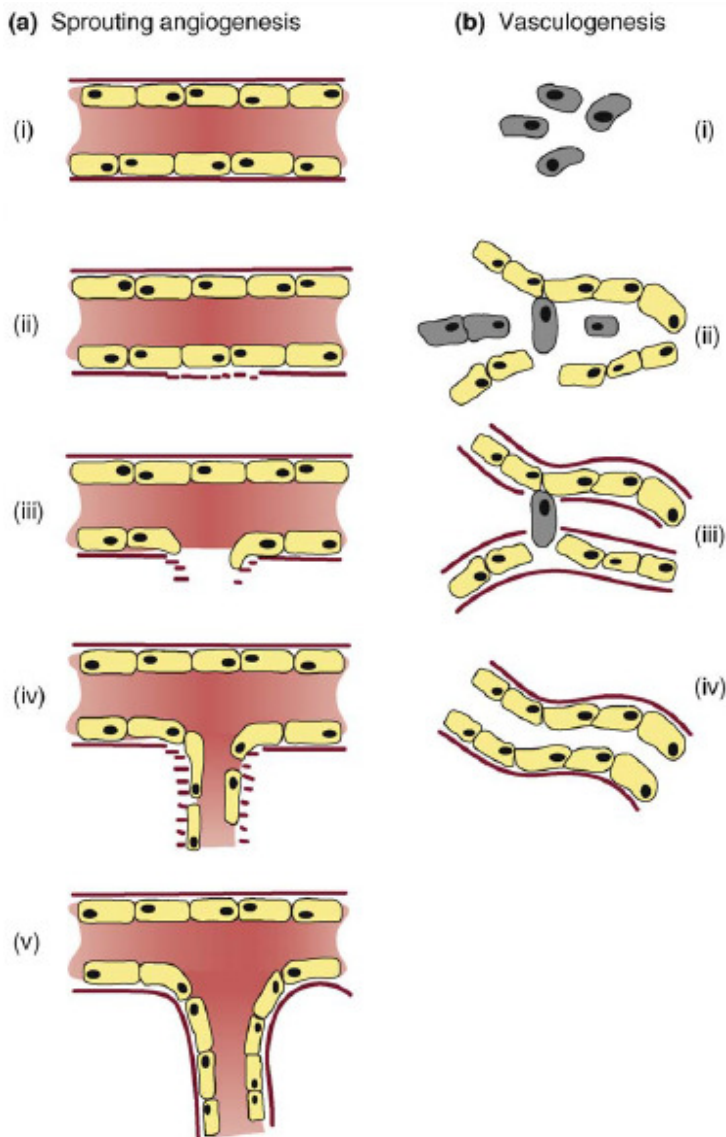


Figure 2-14: Mechanisms of angiogenesis and vasculogenesis. (a) Sprouting angiogenesis from a pre-existing vessel through the secretion of matrix metalloproteases that degrade the vascular basement membrane, allowing endothelial cells to migrate and form a new vessel branch. (b) EPC forms a vascular plexus, deposits matrix and forms a lumen resulting in the formation of immature capillaries. *Figure reproduced from Krenning et al (Krenning et al. 2009).*

2.8.2.6 Endothelial Progenitor Cells

EPC are endothelial precursor cell types, first identified from adult peripheral blood (PB) by Asahara in 1997 (Asahara *et al.* 1997) and subsequently isolated from other sources such as cord blood (Murohara 2001), monocytes (Moldovan *et al.* 2000) and bone marrow (Gehling *et al.* 2000). EPC arise from the hemangioblasts of the mesodermal layer of the embryonic stem cell. Blood islands in the yolk sac of the

embryo grow and fuse, forming a yolk sac capillary network which differentiates into an arteriovenous vascular system upon the onset of blood circulation. Cells destined to form EPC are located at the periphery of the blood islands (Asahara and Kawamoto 2004; Murasawa and Asahara 2005).

As a circulating cell type, EPC are immobilised from the bone marrow into the systemic circulation of the adult peripheral blood in response to cytokines and the ischemia environment during an injury. They then invade and home into sites of neovascularisation and then differentiate into mature EC (Murasawa and Asahara 2005).

Despite being a relatively newly identified cell type, numerous studies have since confirmed its vasculogenic potential. For example, exogenously administered EPC have been shown to augment vascularisation in diseases such as hindlimb ischemia (Tateishi-Yuyama *et al.* 2002), myocardial infarction (Dimmeler and Zeiher 2009) and contributing to fracture healing *via* neovasculogenesis (Rozen *et al.* 2009; Atesok *et al.* 2010). Their success in augmenting angiogenesis and functional recovery has been reported in various clinical trials and animal models as reviewed by Krenning *et al* (Krenning *et al.* 2009).

2.8.2.7 Endothelial Progenitor Cells in Fracture Healing

Apart from promoting therapeutic neovascularisation, the contributions of EPC in BTE applications have also been demonstrated by several groups over the recent years. In a rodent tibia fracture and distraction osteogenesis model, it was suggested that EPC participated in neovascularisation and subsequent bone repair due to temporal coincidences of increased EPC mobilisation from the bone marrow, followed by homing at the site of injury with the fracture healing and

distraction/consolidation models respectively (Lee *et al.* 2008). Matsumoto's group also demonstrated functional fracture healing *via* peripheral blood EPC-derived vasculogenesis (Matsumoto *et al.* 2006; Matsumoto *et al.* 2008; Mifune *et al.* 2008). More recently, Rozen *et al* demonstrated the formation of dense woven bone within a critical-sized defect zone in sheep tibiae 12 weeks after autologous EPC implantation (Rozen *et al.* 2009), while Atesok *et al* showed complete union of a rat femoral defect within 10 weeks (Atesok *et al.* 2010). These studies demonstrated the therapeutic efficacy of EPC in fracture repair through neovasculogenesis.

2.8.2.8 Proposed Endothelial Cell Type – Umbilical Cord Blood-Endothelial Progenitor Cells

Compared to their mature EC, EPC were found to be 10 fold more proliferative than human umbilical vein endothelial cells (HUVEC) (Murohara 2010). Furthermore, it was reported that transplantation of EPC demonstrated successful rescue and improved blood flow in hindlimb of ischaemic mice, not seen when differentiated microvascular EC which failed to establish limb-saving neovascularisation (Kalka *et al.* 2000). Transplantation of EPC-grafts into immunodeficient mice showed the formation of chimeric blood vessels interspersed with red blood cells compared to none observed in EC-grafts (Yoder *et al.* 2007). As compared to a well-defined circulating population of EPC (Masuda *et al.* 2011), mature EC have also been reviewed as a phenotypically and functionally heterogeneous cell type depending on the origin of isolation along the endothelium, which results in difficulty in experimental comparisons (Aird 2007), as compared to a more well-defined circulating population of EPC (Masuda *et al.* 2011). **Table 2-9** compares the main characteristics of the mature endothelial lineages with its progenitors, with the latter exhibiting superiority in terms of its proliferation and vessel forming ability.

Table 2-9: Summary of the main characteristics of mature endothelial cells and its progenitor cells.

| | EPC | EC |
|----------------------------|--|--|
| Cell type | Progenitor; endothelial lineage-directed | Mature |
| Examples of sources | <ul style="list-style-type: none"> • Peripheral blood • Cord blood • Monocytes • Bone marrow | <ul style="list-style-type: none"> • Umbilical vein • Skin • Adipose tissue |
| Existence | Circulating in blood | Lining interior surface of blood vessels and lymphatics |
| Homogeneity | <ul style="list-style-type: none"> • Circulating population • More well-defined | <ul style="list-style-type: none"> • Origin-dependent (Aird 2007; Aird 2007) • Phenotypically and functionally heterogeneous |
| Proliferation | 10 fold higher | - (Moldovan <i>et al.</i> 2000) |
| Vessel formation | Vessel formation, perfused with red blood cells <i>in vivo</i> | None observed (Yoder <i>et al.</i> 2007) |

The two most commonly explored sources of EPC are from adult PB and UCB, with the perinatal UCB-EPC more primitive and superior in terms of its expansion and differentiation capacity over its adult counterpart (Murohara 2010). Ingram *et al* reported greater proliferative capacity with at least 100 population doublings from UCB-EPC, maintaining high levels of telomerase activity as compared to 20-30 population doublings in PB-EPC. UCB-EPC formed larger colonies that emerged at an earlier time point upon its isolation (Ingram *et al.* 2004). They also underwent faster differentiation (Kalka *et al.* 2000) and formed capillary-like structures faster on Matrigel substrate compared to PB-EPC (Ingram *et al.* 2004) (**Table 2-10**).

Table 2-10: Comparison between UCB and adult PB-EPC in terms of its colony emergence, growth and vessel forming ability (Ingram *et al.* 2004).

| | Cord Blood-EPC | Adult Peripheral Blood-EPC |
|-----------------------------|---|---|
| Colony formation | <ul style="list-style-type: none"> • Earlier emergence • Larger in size and in greater numbers | - |
| Population doublings | <ul style="list-style-type: none"> • At least 100 | <ul style="list-style-type: none"> • 20-30 |
| Vessel formation | <ul style="list-style-type: none"> • Faster and more stable capillary-like network formation <i>in vitro</i> | - |

As UCB-EPC have been identified superior in its proliferative activity and vasculogenic capacity compared to their adult PB and mature EC sources, they are thus selected for use as a vasculogenic cell source in coculture with hfMSC in this project.

2.8.3 Bioreactor

Bioreactors are primarily used to increase mass transport within tissue-engineered constructs to overcome the limits of oxygen diffusion distance of 100-200 μ m in static culture (Goldstein *et al.* 2001; Cartmell *et al.* 2003). Dynamic cultures add convection forces which help to improve nutrient and oxygen supply to the cells, as well as assist in the removal of waste materials. They were also found to improve cell viability and cellularity within the tissue-engineered grafts (Wendt *et al.* 2003). For example, Zhang *et al.* demonstrated improved cellular viability in dynamically-cultured hfMSC-grafts as compared to massive necrosis within the core of the static-grafts (Zhang *et al.* 2009). Bioreactor cultures also ensure homogenous cellular distribution (Wendt *et al.* 2003; Wendt *et al.* 2005) and enhanced osteogenic differentiation (Bancroft *et al.* 2002; Datta *et al.* 2006). The mechanical cues involved trigger onset of several signalling pathways which has been shown to positively influence the osteogenic properties of the graft (McCoy and O'Brien 2010) as well as fundamental to endothelial differentiation and vascular development (Tzima *et al.* 2005).

For example, fluid shear stress has been shown to promote osteogenic differentiation of MSC (Sikavitsas *et al.* 2003; Datta *et al.* 2006; Holtorf *et al.* 2006; Zhang *et al.* 2009). Sikavitsas *et al.* showed increased mineral deposition in the scaffold meshes with a more homogenous ECM as compared to a thin mineralised ECM obtained in static culture (Sikavitsas *et al.* 2003). Meinel *et al.* also demonstrated more robust bone formation with accelerated repair of calvarial critical-

sized mice defect upon implantation of human MSC-scaffolds cultured in 5 weeks of bioreactor culture in bone inductive media compared to its non-treated hfMSC-scaffolds and empty scaffolds (Meinel *et al.* 2005).

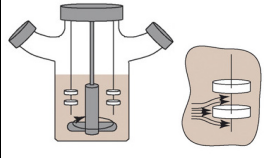
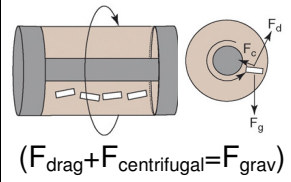
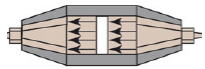
In terms of endothelial differentiation, EPC cultured under dynamic culture showed enhanced vasculogenic potential after Matrigel-induced differentiation (Yamamoto *et al.* 2003). A similar phenomenon has been described in murine embryonic stem cell-derived endothelial cells, which displays heightened endothelial cell characteristics and maturation under dynamic culture conditions but not in static culture (McCloskey *et al.* 2006).

As osteoprogenitors and endothelial cells are mechano-sensitive cell types, it is hypothesised that the exertion of biomechanical stimulation on the coculture system is likely to contribute towards the maturation of vessel and bone formation within the graft construct.

2.8.3.1 Proposed Bioreactor – Perfusion Biaxial Bioreactor

Some commonly used commercial bioreactors for BTE applications include spinner flasks, rotating wall vessels and perfusion bioreactors with their associated advantages and disadvantages as described in **Table 2-11** (Rauh *et al.* 2011). Notably, these bioreactors are mostly uniaxial in rotation, possibly resulting in a non-homogenous media flow and nutrient exchange especially within the internal zones of the scaffolds.

Table 2-11: Comparison of the advantages and disadvantages of the various modes of commonly used bioreactors. *Figures reproduced from Hutmacher and Singh (Hutmacher and Singh 2008).*

| | Bioreactor | Advantages | Disadvantages |
|----------------------|---|---|---|
| Spinner flask |  | <ul style="list-style-type: none"> • Media stirring \uparrow mass transfer <i>via</i> convective transport • \uparrow osteogenicity | <ul style="list-style-type: none"> • Generates turbulent eddies detrimental to cell development • No direct perfusion of media into scaffold |
| Rotating-wall vessel |  ($F_{\text{drag}} + F_{\text{centrifugal}} = F_{\text{grav}}$) | <ul style="list-style-type: none"> • Rotating environment creates low shear stresses with high mass transfer | <ul style="list-style-type: none"> • Constructs in a state of free-fall in media; frequent collision with bioreactor wall • No direct perfusion of media into scaffold • Little improvement in osteogenicity |
| Perfusion bioreactor |  | <ul style="list-style-type: none"> • Media flows directly through pores of constructs, enhancing mass transfer internally • \uparrow osteogenicity | <ul style="list-style-type: none"> • Customised cartridge to fit constructs • Cell “wash-out” due to continuous perfusion |

In mimicking the multi-axial forces experienced by the bone during daily activities, a biaxial bioreactor was designed (US Patent 7,604,987 B2). Briefly, the biaxial bioreactor consists of a culture vessel capable of rotating in two perpendicular axes simultaneously. Media is perfused continuously throughout the chamber from the media reservoir, where cellular-scaffold constructs are secured to the pins during rotation (**Figure 2-15**) (Hutmacher and Singh 2008).

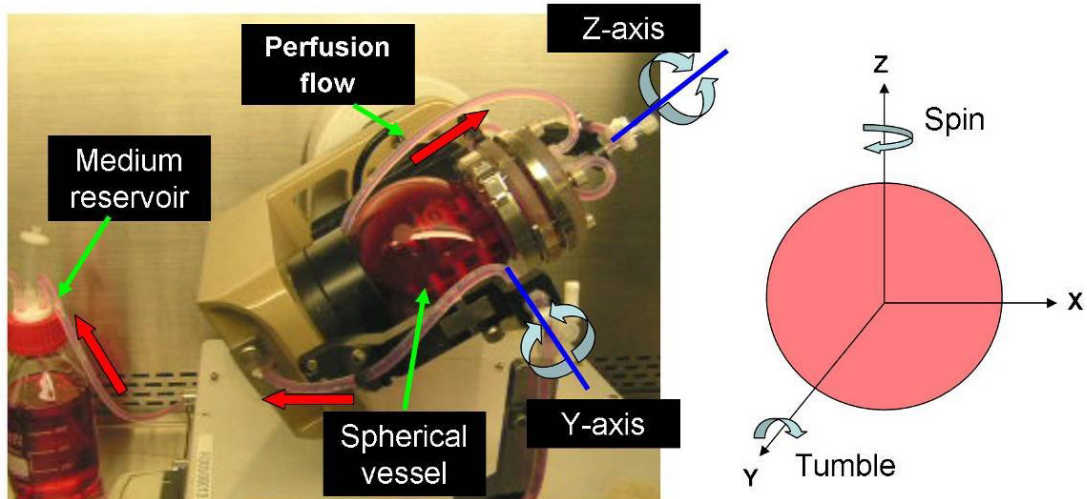


Figure 2-15: The perfusion biaxial bioreactor has two rotational axes (indicated by blue block arrows), with scaffolds pinned and fixed in place while the bioreactor rotates. *Figures reproduced from Zhang et al (Zhang et al. 2009).*

Computational modelling analysis of fluid velocities and shear stresses demonstrated increased fluid velocity and fluid transport within scaffold constructs when rotated in a biaxial manner (Singh *et al.* 2005). This was then experimentally verified and found to significantly enhance cellular viability within hfMSC-grafts upon dynamic culture, as compared to massive necrosis observed in a static-cultured one after 28 days (Zhang *et al.* 2009). Furthermore, when used in conjunction with the proposed macroporous PCL/TCP scaffold, shear stresses were found exerted uniformly along the scaffold filaments upon the biaxial rotational action of the bioreactor (Singh *et al.* 2005).

More recently, a head-to-head comparison of commercially available bioreactors operated at their optimal settings (spinner flasks, perfusion and rotating wall vessel bioreactors) revealed the superiority of the biaxial bioreactor in ensuring an even distribution of seeded hfMSC with the scaffolds, higher proliferation rates, and earlier and more robust osteogenic differentiation (Zhang *et al.* 2009). This suggests improved performance of the biaxial bioreactor over other bioreactor systems for the generation of bone grafts in BTE.

In this project, the biaxial bioreactor will be used in conjunction with the coculture of stem cells and scaffolds. The aim is to generate highly vascularised and osteogenic bone grafts that are highly confluent and viable, with an even distribution of cells throughout the graft prior to implantation.

2.8.4 Hypoxia in the Natural Physiology

Adult tissues experience low oxygen tensions upon inhalation of atmospheric air, which progressively decreases in partial pressure as oxygen travels through the nasal pathway first into the lungs, *via* the blood, then to the various tissues (Mohyeldin *et al.* 2010). Early experiments measured low oxygen levels in tissues of developing embryos (Mitchell and Yochim 1968), and hypoxia was found to influence both embryonic and adult stem biology in recent *in vitro* studies (Panchision 2009; Silvan *et al.* 2009; Eliasson and Jonsson 2010). Low oxygen tensions have also been identified in the various stem cell niches (MSC, neural and hematopoietic niches) in the human body (Mohyeldin *et al.* 2010). In the bone marrow, progenitor cells such as MSC and EPC reside at a low oxygen tension of approximately 2-8%. Hence, the study of oxygen tension for cell culture is physiologically relevant and is believed to be a critical parameter for the maintenance of stem cell phenotype and stem cell fate.

2.8.4.1 Hypoxia and Mesenchymal Stem Cells

There has been an increase in interest investigating the effects of hypoxic culture on MSC growth, proliferation and differentiation in the realm of tissue engineering. Most studies demonstrated increased proliferative rates on monolayer and 3D substrates under hypoxic culture. In terms of its osteogenic capacity, there have been contradictory reports on the effects of hypoxia on the osteogenic differentiation of

MSC (Das *et al.* 2010), although likely attributed to the lack of standardisation of various parameters (cell source, duration of exposure, exact O₂) between studies. More experiments need to be performed to understand the effects of hypoxia preconditioning on MSC differentiation for enhancing fracture repair response upon cell transplantation.

2.8.4.2 Hypoxia and Bone Repair

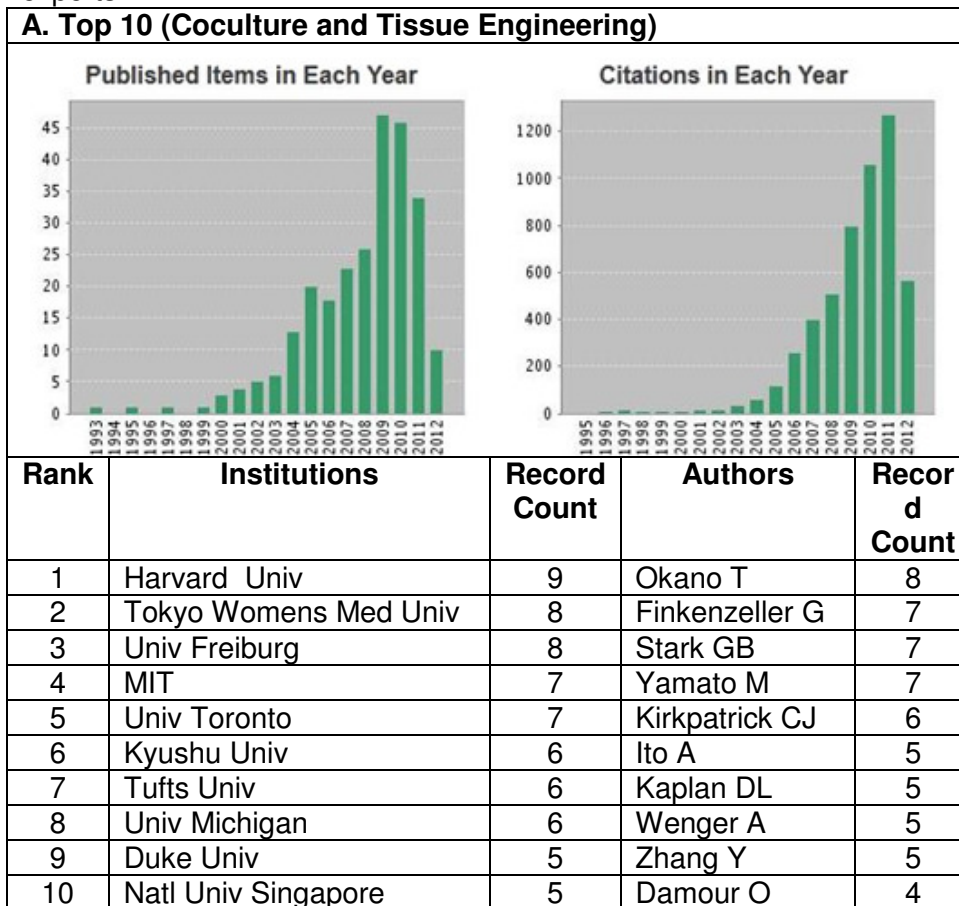
The role of hypoxia in triggering angiogenesis has been described earlier in [Section 2.5.2](#). In terms of its contributions towards bone formation, hypoxia has also been found to exert profound effects in accelerating bone repair. HIF-1 α and its activated pathway has been demonstrated to aid in skeletal development, stimulating osteoprogenitor differentiation and promoting robust bone formation and remodelling, which was coupled by the action of angiogenic mechanisms (Wan *et al.* 2010). Experimentally, Wang *et al* showed robust bone formation accompanied by VEGF upregulation upon constitutive activation of HIF-1 α pathway in osteoblasts, while the inhibition of HIF-1 α led to the formation of narrow and less vascularised bones (Wang *et al.* 2007). A similar improvement in vascularity and bone formation finding was noted in distraction osteogenesis mice upon Von Hippel-Lindau deletion with constitutive HIF-1 α activation compared to mice lacking HIF-1 α (Komatsu and Hadjiargyrou 2004; Wan *et al.* 2008). Also, Zou *et al* induced the overexpression of HIF-1 α through lentiviral mediated gene delivery in bone marrow-derived MSC, leading to significantly improve the vessel forming and osteogenic potential for the repair of a CSD calvarial rat defect as compared to its LacZ control (Zou *et al.* 2011). These studies reiterate the interdependent relationship between vascularisation and its ability to aid in bone formation as discussed earlier ([Section 1.5.1](#)).

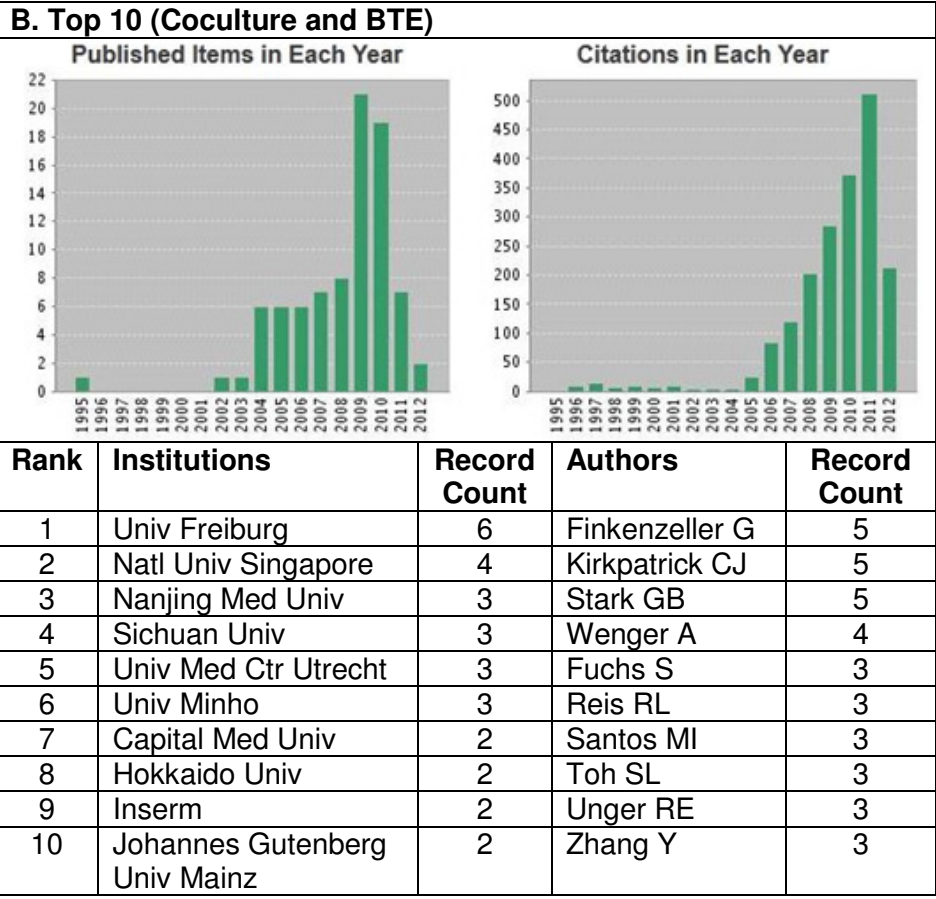
2.9 Coculture Systems

2.9.1 Trends in Coculture Systems

In the area of coculture systems in tissue engineering, there has been a steep increase in the number of publications since the past two decades (259 publications), with a significant proportion dedicated to BTE (85 publications). The top 10 institutions and leading experts in this area are as listed in **Table 2-12** below (Web of Science, 2012).

Table 2-12: (A-B) Citation analysis on the utility of cocultures in tissue engineering and bone tissue engineering respectively, as well as the leading institutions and experts.





2.9.2 Cocultures in Vascularised Bone Tissue Engineering

Leveraging on the osteogenic and vasculogenic properties of osteoblast-like and endothelial monocultures respectively, many groups have utilised a coculture system on the premise that this strategy will generate prevascular networks within BTE grafts towards aiding bone repair (Fuchs *et al.* 2007; Melero-Martin *et al.* 2008; Fuchs *et al.* 2009; Usami *et al.* 2009; Seebach *et al.* 2010; Tsigkou *et al.* 2010). Most reported studies have showed phenomenal observations of increased vascularisation upon the addition of endothelial lineages in coculture, with some showing evidence of integration and chimeric vessel formation *in vivo* (Table 2-13). Fuchs *et al* demonstrated greater potential for vascular network formation, with highly organised microvessel-like structure formation when osteoblastic cells were cocultured with PB-EPC (Fuchs *et al.* 2007). Tsigkou *et al* demonstrated endothelial

tubular networks within the first week, followed by a stabilised mature vascular network within a mineralising bone graft by Week 4 upon coimplantation of undifferentiated MSC and HUVEC subcutaneously in mice (Tsigkou *et al.* 2010).

Although many groups have also shown an increase in osteogenic differentiation upon coculture, few have demonstrated strong evidence for bone healing and regeneration *in vivo*. Usami *et al* showed a 1.6 fold increase in capillary density and 1.3 fold increase in bone formation compared to the use of MSC alone, suggesting the necessity of vasculature formation in aiding bone regeneration (Usami *et al.* 2009). Orthotopic implantation of the EPC/MSC construct led to earlier vascularisation and significantly more bone formation in a rat femoral CSD model, with higher ultimate loading than the MSC alone group (Henrich *et al.* 2009; Seebach *et al.* 2010). The coculture systems and their *in vivo* performance in promoting vascularisation and/or bone formation in various animal models are summarised in **Table 2-13**.

Table 2-13: Summary of various animal models used for implantation of coculture systems in vascularised BTE. * Denotes an orthotopic implantation in the animal model

| Endothelial cell type | Osteoblast-like cell type | Cell origin | Animal model | Implantation result | Reference |
|-----------------------|---------------------------|-------------|---|--|-------------------------------|
| HUVEC | BM-MSC | Human | 4.3mm calvarial critical sized defect in mice * | Coimplantation led to higher human CD31+ neovessels formation but without increase in bone formation compared to MSC-alone | (Koob <i>et al.</i> 2011) |
| | BM-MSC | Human | Subcutaneous in mice | HUVEC-vascular networks infiltrated the scaffold after 4-7 days after implantation, with anastomosis after 11 days; Networks were mature at 4 weeks, with initial mineralisation. Human-derived vessels persisted at 5 months but majority remodeled with host vasculature | (Tsigkou <i>et al.</i> 2010) |
| | BM-MSC | Human | 0.9mm diameter femoral defect in mice * | <i>In vivo</i> mineralisation was observed inside and around cellular-microspheres, but significantly increased when in coculture | (Grellier <i>et al.</i> 2009) |
| | BM-MSC | Human | Subcutaneous in mice | Vessel networks with lumens were formed but with limited anastomosis confined to implant periphery | (Rouwkema <i>et al.</i> 2006) |
| HDMEC | Primary OB | Human | Subcutaneous in mice | Coimplantation led to formation of human HDMEC-vessels that integrated with host vasculature and were perfused, inducing murine vasculature into the implants as compared to none in HDMEC-alone | (Unger <i>et al.</i> 2010) |
| | BM-MSC | Human | Subcutaneous in mice | Coimplantation showed greater human-derived vessels on Week 8, with more bone tissue formation compared to MSC-alone, found to be mediated by BMP-2 secretions from HUVEC | (Kaigler <i>et al.</i> 2005) |
| PB-EPC | BM-MSC | Human | 5mm femoral defect in rat * | EPC-implanted groups showed early vascularisation, but coculture group showed significantly more bony bridging with increased ultimate load compared to other groups | (Seebach <i>et al.</i> 2010) |
| | Primary OB | Human | Subcutaneous in mice | Coimplantation increased neovascularisation, with the formation of perfused human EPC-vessels that anastomosed with host vasculature compared to EPC alone | (Fuchs <i>et al.</i> 2009) |
| | BM-MSC | Human | 5mm femoral defect in rat * | EPC-loaded implants improved neovascularisation; a trend towards increased bone formation was observed upon coculture compared to MSC-alone | (Henrich <i>et al.</i> 2009) |
| | BM-MSC | Canine | Subcutaneous in mice | Coimplantation increased neovascularisation and bone formation compared to MSC-alone | (Usami <i>et al.</i> 2009) |
| UCB-EPC | BM-MSC | Human | Subcutaneous in | Prevascular structures were formed upon addition of EPC to coculture but the | (Rouwkema |

| | | | | | |
|----------------|--------|-------|----------------------|---|-----------------------------|
| HUVEC HDMEC | | | mice | number of vessels were found decreasing in descending order when cocultured with EPC, HUVEC, MVEC respectively, however with greater degree of organisation | <i>et al. 2009)</i> |
| BM-EPC | BM-MSc | Goat | Subcutaneous in goat | Cellular-implants led to higher bone lining scaffold compared to acellular-implants, but no differences were noted between coculture and MSC-alone implants | (Geuze <i>et al. 2009)</i> |
| HSC (CD34+) | BM-MSc | Human | Subcutaneous in mice | Coimplantation led to greater number of vascular structures with engraftment into host vascular endothelium and increased ectopic mineralisation as compared to MSC-alone; Angiogenesis was further increased upon VEGF stimulation | (Moioli <i>et al. 2008)</i> |

Legend: BM-EPC – Bone marrow derived EPC; OB – osteoblast; HDMEC – human dermal microvascular EC; HSC- Haematopoietic stem cell

2.9.3 Considerations for Coculture Systems

Keeping in mind an appropriate choice of BTE components including cell types, scaffolds, bioreactor and microenvironmental oxygen tensions ([Section 2.9](#)), there are other culture parameters for consideration in ensuring a successful outcome of the coculture system.

2.9.3.1 Choice of Media

One consideration factor involves the choice of culture media for the maintenance of cellular viability of both cell types as well as for tissue development. Suitable optimal conditions for inducing both vessel network and bone formation, without adverse influence on cellular differentiation of the other cell type needs to be identified. In addition, the state of cellular differentiation of the graft prior to implantation is crucial in determining its *in vivo* performance. It was reported that pre-differentiation of osteoblast-like cells in bone inductive media prior to implantation accelerates the rate of bone formation *in vivo* compared to undifferentiated MSC (Breitbart *et al.* 1998; Bruder and Fox 1999). In addition, a recent investigation by Schantz and coworkers compared the efficacy of tissue formation of undifferentiated MSC and osteoblasts-loaded scaffolds in a rabbit calvarial defect. Results revealed the importance of directing MSC towards a specific lineage prior to implantation which its cell fate will otherwise be likely determined by its immediate host environment (Schantz *et al.* 2012). However, it is imperative to keep in mind that the differentiated state of MSC might interfere with its role as a pericyte for enwrapping and stabilising the pre-forming vascular network.

Most groups have investigated their coculture systems in one media type often without justification for the choice of media used, while some have utilised a

combination of cell culture media optimal for the different cell types. **Table 2-14** shows a compilation of the various media types used in current coculture systems for BTE. However, the heterogeneity of the experimental parameters in these studies makes comparison between coculture systems challenging. In a recent head-to-head study of various media types (bone media with/without endothelial supplements, endothelial-based media with/without osteoinductive supplements) for MSC/EPC coculture, a general trend towards enhanced vessel formation or more robust mineralisation was noted when endothelial growth media (EGM) and bone media (BM) were used respectively. Kolbe *et al* showed increased microvessel formation efficiency when cultured in EGM as compared to BM with or without growth factor supplements; while the use of BM was found to demonstrate higher osteogenic differentiation capacity of MSC as compared to the other media types (Kolbe *et al.* 2011). Few groups have utilised bone inductive media for the cocultures, lest poor endothelial survival. It was also verified that bone inductive media was the most effective towards inducing osteogenic differentiation of MSC, while there was a lack of osteogenic modulation in EGM-variants (Liu *et al.* 2012). While growth factors supplemented in EGM may effectively promote endothelial differentiation, care must be taken into consideration in ensuring no inhibition of osteogenic differentiation.

Hence, the choice of media and its various soluble components such as angiogenic growth factors and bone inductive components plays an important role in determining cellular fate and differentiation, and needs to be carefully considered in this project.

Table 2-14: Maintenance of coculture systems in BTE, including media used, coculture ratios and the seeding methodology, with coculture in direct contact unless otherwise stated.

| Coculture Media | Cell types | Reference |
|---------------------------------------|---|-------------------------------|
| IMDM-based media | MSC, EC | (Villars <i>et al.</i> 2000) |
| | MSC, HUVEC | (Villars <i>et al.</i> 2002) |
| | OB, HUVEC | (Guillot <i>et al.</i> 2008) |
| | OB, HUVEC | (Hofmann <i>et al.</i> 2008) |
| | MSC, HUVEC | (Grellier <i>et al.</i> 2009) |
| | MSC, EPC | (Aguirre <i>et al.</i> 2010) |
| MesenCult-based media | MSC, EPC | (Henrich <i>et al.</i> 2009) |
| | MSC, EPC | (Seebach <i>et al.</i> 2010) |
| EGM-based media | MG-63 or OB, HDMEC | (Unger <i>et al.</i> 2007) |
| | MSC, EPC | (Fuchs <i>et al.</i> 2009) |
| | OB, EPC | (Fuchs <i>et al.</i> 2009) |
| | MSC, EC | (Xue <i>et al.</i> 2009) |
| | OB, EPC | (Dohle <i>et al.</i> 2010) |
| Bone media | MSC, EPC in BM | (Liu <i>et al.</i> 2012) |
| Separately cultured or in mixed media | MSC, EC in EGM2: DMEM10 (1:1) | (Kaigler <i>et al.</i> 2005) |
| | MSC, HUVEC in EBM2, BM, EBM2:BM (1:1) | (Rouwkema <i>et al.</i> 2006) |
| | MG-63 or OB, EPC in EGM-2 with or without osteogenic supplements | (Fuchs <i>et al.</i> 2007) |
| | MSC predifferentiated in BM, EPC in EGM2 individually cultured and implanted | (Usami <i>et al.</i> 2009) |
| | MSC, EPC in α MEM15:EGM20 (1:1) | (Geuze <i>et al.</i> 2009) |
| | MSC predifferentiated in BM, then in coculture with EC in EGM2 | (Tsigkou <i>et al.</i> 2010) |
| | MSC, HUVEC in IMDM, Medium 199 (M199), DMEM and M199:DMEM (1:1) | (Bidarra <i>et al.</i> 2011) |
| | MSCs predifferentiated in BM, then cocultured with HUVEC grown in EBM with VEGF-A and bFGF | (Koob <i>et al.</i> 2011) |
| | MSC, EPC in EBM2, EGM2 with or without osteogenic supplements, BM with or without endothelial supplements | (Kolbe <i>et al.</i> 2011) |

Legend: OB – osteoblast; MG-63 – osteosarcoma cell line; HDMEC – human dermal microvascular EC; IMDM - Iscove's Modified Dulbecco's Media; DMEM - Dulbecco's Modified Eagle's Medium; α MEM - Alpha Minimum Essential Medium; Figure following media type denotes % fetal bovine serum.

2.9.3.2 Seeding Methodology

There are several methodologies used for seeding cells onto 3D scaffold constructs, although the optimal methodology has yet to be defined. Some consideration factors include the manner in which cells are cultured prior to implantation, whether cells should be combined or cultured separately in their optimal culture media, the need for a dynamic culture system and the duration of biomechanical stimulation before implantation. Other considerations relate to cellular distribution of the coculture in the graft, and the seeding ratios that should be used to allow for efficient cellular interactions and cross-talk. **Table 2-15** summarises the possible advantages and disadvantages associated with the various seeding methodologies which could significantly impact on the outcome of this coculture strategy.

Table 2-15: Advantages and disadvantages of various seeding methodologies of cocultures in vascularised BTE.

| Seeding methodology | Advantages | Disadvantages | Reference |
|--|---|---|--|
| Combining coculture directly | <ul style="list-style-type: none"> Logistically simple Even cellular mix distributed within the construct | <ul style="list-style-type: none"> Need to ensure cell survival in the same media type prior to seeding without alteration to monoculture cellular properties | <ol style="list-style-type: none"> (Unger <i>et al.</i> 2007) (Unger <i>et al.</i> 2010) (Hofmann <i>et al.</i> 2008) (Fuchs <i>et al.</i> 2007) (Henrich <i>et al.</i> 2009) (Seebach <i>et al.</i> 2010) (Villars <i>et al.</i> 2002) (Guillot <i>et al.</i> 2008) (Geuze <i>et al.</i> 2009) (Bidarra <i>et al.</i> 2011) (Melero-Martin <i>et al.</i> 2008) (Fuchs <i>et al.</i> 2009) (Rouwkema <i>et al.</i> 2009) (Koob <i>et al.</i> 2011) (Liu <i>et al.</i> 2012) |
| 2-step protocol (A) Seeding OB first, then EPC on same scaffold | <ul style="list-style-type: none"> Allow monocultures to develop optimally in their respective growth media, maintaining individual phenotypic characteristics | <ul style="list-style-type: none"> Uneven distribution of cells, where EPC are mostly attached to scaffold surfaces rather than within the scaffold core Prevascularises the EPC zones of the scaffold only, and might be difficult for vessels to infiltrate if osteogenic graft is highly confluent Minimal EPC/MSC interactions between coculture | <ol style="list-style-type: none"> (Dohle <i>et al.</i> 2010) (Fuchs <i>et al.</i> 2009) (Tsigkou <i>et al.</i> 2010) |
| (B) Seeding OB and EPC on different scaffolds which can be then combined together. | | | <ol style="list-style-type: none"> (Usami <i>et al.</i> 2009) |
| Coculture followed by dynamic stimulation | <ul style="list-style-type: none"> Improve metabolic and osteogenic activity Assist in maturation of graft | <ul style="list-style-type: none"> Logistically more challenging | <ol style="list-style-type: none"> (Grellier <i>et al.</i> 2009) |

In summation, few groups have investigated coculture systems in conjunction with bioreactor technologies (Grellier *et al.* 2009) or under a hypoxic culture environment (Gawlitta *et al.* 2012). So far, Grellier and coworkers are the only team to have reported the dynamic culture for cell-encapsulated alginate microspheres prior to subsequent assays comparing its cocultures of human osteoprogenitors and HUVEC to its monocultures. There has been yet to be any reports on the influence of dynamic culture on osteoblast-endothelial cell cocultures for vascularised BTE towards aiding vascular and bone development.

While hypoxia is highly relevant in the natural physiology of the vascularised bone, few have investigated the effects of low oxygen tensions on a coculture system. A recent study investigated the effect of hypoxic cultures on EPC/MSC on the hypothesis that a hypoxic environment will contribute to prevascularisation. Results however, showed an impediment of vaculogenesis upon hypoxia stimulation as compared to their normoxic cultures which supported the formation of prevascularised structures (Gawlitta *et al.* 2012). More studies need to be done to be done to verify the importance of a hypoxic stimulus for the purpose of prevascularising tissue-engineered coculture constructs and facilitating bone regeneration and fracture repair response *in vivo*.

Chapter 3 – Materials and Methods

We are all faced with a series of great opportunities
brilliantly disguised as impossible situations ~ Charles R. Swindoll

Chapter 3 - Materials and Methods

3.1 Samples, Animals and Ethics

Human tissue collection for research purposes was approved by the Domain Specific Review Board of National University Hospital Systems (DSRB-D-06-154), in compliance with international guidelines regarding the use of fetal tissue for research as previously described (Zhang *et al.* 2010). In all cases, patients gave separate written consent for the use of the collected tissue. Fetal femurs were collected for isolation of hfMSC after clinically-indicated termination of pregnancy. In this study, a sample derived from a 17⁺³ weeks^{+days} gestation was used. Human UCB samples from newborns were collected from normal term deliveries.

Male non-obese diabetic severe combined immunodeficient (NOD SCID) mice (6-8 weeks old) were acquired from Animal Resources Centre (Canning Vale, Western Australia). All procedures were approved by the Institutional Animal Care and Use Committee at The National University of Singapore, and procedures performed in the Association for Assessment and Accreditation of Laboratory Animal Care International (AAALAC) accredited animal facilities.

3.2 Cells

3.2.1 Cell Isolation, Culture and Characterisation

3.2.1.1 Human Fetal Bone Marrow Derived Mesenchymal Stem Cells

hfMSC were isolated from bone marrow as previously described (Zhang *et al.* 2009). Briefly, single-cell suspensions were prepared by flushing the bone marrow cells from femurs using a 22-gauge needle, passed through a 70µm cell strainer (BD Falcon, USA) and plated on 10 cm diameter plates (NUNC, USA) at 10⁶ cells/ml.

Adherent spindle-shaped cells were recovered from the primary culture after 4 to 7 days. Non-adherent cells were removed with initial media changes every 2-3 days. At subconfluence, they were trypsinised and replated at 10^4 cells/ cm^2 . MSCs were cultured in Dulbecco modified Eagle media (DMEM)-Glutamax (GIBCO, USA) supplemented with 10% fetal bovine serum (FBS), 50U/mL penicillin and streptomycin (GIBCO, USA), thereafter referred to as D10 media. hfMSC were screened using flow cytometry for MSC markers such as CD73, CD90, CD105; hematopoietic and endothelial markers such as CD14, CD34, CD45 respectively using a human MSC phenotyping kit. Their tri-lineage differentiation capacity was also confirmed upon directing the cells towards adipogenic, chondrogenic and osteogenic lineage in the respective media. Cells from passage 2-4 were used and characterised as previously described (Zhang *et al.* 2010).

3.2.1.2 Human Umbilical Cord Blood Derived Endothelial Progenitor Cells

UCB-EPC were obtained as previously described (Yoder *et al.* 2007). Briefly, blood was diluted and overlaid onto Ficoll-Paque PLUS (Amersham, Piscataway, NJ). Mononuclear cells (MNC) from the buffy coat retrieved from UCB by low density centrifugation were resuspended in EGM (Cambrex, USA) supplemented with 10% FBS, thereafter referred to as EGM10, and then plated onto 10 cm diameter tissue culture dishes coated with Type I rat tail collagen (BD Biosciences, Bedford, MA) at 37°C, 5% CO₂ in a humidified incubator. Culture media was changed every 3 days subsequently. Typical cobblestone colonies appeared after two weeks, and were subcultured at subconfluence. Immunocytochemistry was used to screen EPC for Dil complex acetylated low density lipoprotein (Dil acLDL) (Dako, Denmark), CD31 (Millipore, USA), vWF (Millipore, USA) and VE Cadherin (Enzo Life Sciences, USA).

3.2.2 Lentiviral-Transduction of hfMSC and EPC

The lentiviral vectors were produced as described previously (Chan *et al.* 2005). Briefly, the transfer plasmids (PGK-H2BmCherry / pHIV-dTomato and pRRLSIN.cPPT.PGK-GFP.WPRE) were cotransfected with pMD2.G and pCMV.ΔR8.74 into HEK293T cells. The supernatant was collected at 48 and 72 hours following transfection and concentrated by two rounds of ultracentrifugation at 50,000 g for 2 hours and the final pellet was dissolved in a small volume of 1% BSA in PBS (1/100 of starting volume). The number of transducing units (TUs) of the vectors was determined by infecting 100,000 293T cells using serial dilution of the vector. The dilution resulting in <30% green fluorescent protein (GFP) or red fluorescent protein (RFP)-positive cells was used to calculate the number of TUs per ml. For transduction, cells were seeded at 0.5×10^4 cells/cm² in T-25 flasks, and exposed to lentivirus with 4 mg/mL polybrene at multiplicity of infection of 5. GFP labelled EPC and nuclear-mCherry labelled hfMSC at >90% transduction efficiencies were used in the experiments.

3.3 Flow Cytometry

MSC were trypsinised, spun down and enumerated. 1×10^6 cells were then suspended in buffer (PBS supplemented with 20% Goat Serum, 0.5% Bovine Serum Album, 2mM EDTA) and incubated with the MSC Phenotyping Cocktail (MACS, Germany) for 30 minutes in the dark at 4°C. Cells were washed before resuspending the cell pellet in buffer for analysis by flow cytometry. Flow cytometry was first carried out on an unstained sample, where the population of cells have been gated to exclude any debris. The gate was then applied to both the sample group stained with the marker of interest and its histogram was overlaid with that of the unstained group. The percentage of positively-stained cells were measured.

3.4 Multilineage Differentiation

3.4.1 Adipogenic Differentiation

To induce adipogenic differentiation, MSC were plated at $2 \times 10^4/\text{cm}^2$ and cultured in adipogenic differentiation medium (D10 medium supplemented with $5\mu\text{g}/\text{ml}$ Insulin, 10^{-6}M Dexamethasone and $0.6 \times 10^{-4}\text{M}$ Indomethacin) (Sigma Aldrich, USA) for up to 21 days with change of medium three times per week. The existence of lipid vacuoles was confirmed by Oil-Red O staining.

3.4.2 Chondrogenic Differentiation

To induce chondrogenic differentiation, MSC were pelleted and cultured in chondrogenic differentiation medium (DMEM medium supplemented with $0.1\mu\text{M}$ Dexamethasone, 0.17mM ascorbic acid, 1.0mM Sodium Pyruvate, 0.35mM L-Proline, 1% ITS (BD Pharmingen, USA), $1.25\text{ mg}/\text{ml}$ BSA, $5.33\mu\text{g}/\text{ml}$ Linoleic acid and $0.01\mu\text{g}/\text{ml}$ TGF-beta) (Sigma Aldrich, USA) for up to 28 days with change of medium three times per week. The spheroid cell masses were fixed, embedded and microtome cut before Alcian Blue staining.

3.4.3 Osteogenic Differentiation

To induce osteogenic differentiation, MSC were plated at $2 \times 10^4/\text{cm}^2$ and cultured in osteogenic differentiation medium (D10 medium supplemented with 10mM β -glycerophosphate, 10^{-8}M Dexamethasone and 0.2mM Ascorbic Acid) (Sigma Aldrich, USA) for up to 14 days, with change of medium three times per week. Evidence for extracellular accumulation of calcium was assayed by von Kossa staining.

3.5 Preparation of EPC Conditioned Media

To obtain EPC conditioned media (EPC^{CM}), EPC were cultured in EGM10 until confluence, washed thrice with PBS prior to the addition of BM. Media were collected

after 72 hours, centrifuged, filtered through a 0.22 μ m filter and further diluted in ratios of 1:1 and 1:10 with BM, thereafter referred to as EPC^{CM (1:1)} and EPC^{CM (1:10)} respectively.

3.6 Osteogenic Assays

3.6.1 Calcium Assay

Calcium deposition was assayed as previously described (Zhang *et al.* 2010). Briefly, each sample well (n=3) was incubated with 0.5N acetic acid overnight to dissolve calcium. A colorimetric calcium assay kit (BioAssay Systems, USA) was used to quantify calcium content spectrophotometrically at 612 nm according to manufacturer's instruction.

3.6.2 Alkaline Phosphatase Assay

Alkaline phosphatase (ALP) was assayed as previously described (Zhang *et al.* 2010). Briefly, samples (n=3) were gently rinsed twice with PBS, and incubated in 1mg/ml of Collagenase Type 1 (Sigma Aldrich, USA) dissolved in 0.1% Trypsin (Invitrogen, USA) solution and incubated at 37 °C for 2 hours to digest the extracellular matrix completely. After three cycles of freeze-thaw, the cell lysate solution was assayed for ALP activity using SensoLyte™ pNPP Alkaline Phosphatase Assay Kit (AnaSpec, USA) following the manufacturer's instruction.

3.6.3 Von Kossa Staining

Von Kossa staining was performed as previously described (Zhang *et al.* 2010). Briefly, samples were gently rinsed twice with PBS then fixed with 10% formalin for 1 hour, followed by 2 washes with distilled water and stained with freshly made 2% Silver nitrate (Sigma Aldrich, USA) in distilled water (w/v) for 10 minutes in the dark and expose to sunlight for 30 minutes.

3.7 Antibody Array and Microarray Scanning

Semi-quantitative G series antibody arrays 6, 7, 8 (Human Cytokine Antibody Array (RayBiotech, USA) were used to detect 174 cytokines as per manufacturer's instructions. Briefly, after blocking the arrays with blocking buffer for 30 minutes, they were incubated with either EPC^{CM} or BM for 2 hours at room temperature. Samples were decanted from each well and washed 3 times with Wash Buffer, incubated with Biotin-conjugated antibodies, and followed by Fluorescent dye-conjugated streptavidin for 2 hours each. Thereafter, arrays were washed, centrifuged and allowed to dry before scanning at an excitation frequency of 532nm (Axon Genepix 4000B, USA). Background signals obtained from the negative control, bovine serum albumin (BSA) were subsequently subtracted from median values and sample averages were normalised against the positive control, biotinylated protein as supplied by the manufacturer. Signals from EPC^{CM} were then subtracted from BM values and analysed.

3.8 Microarray Analysis of Gene Expression

Two microarray analyses were performed. In the first, total ribonucleic acid (RNA) was extracted from UCB-EPC grown to subconfluence in biological triplicates, using the RNeasy kit (Qiagen, Valencia, CA) as per the manufacturer's protocol. Ten micrograms total RNA were used to generate labeled cRNA and hybridised to Human Genome U133 Plus 2.0 arrays (Affymetrix, Santa Clara, CA). Data files were imported into GeneSpring GX 11 (Agilent Technologies, Palo Alto, CA). In the second microarray analysis, data files of UCB-EPC (gse508535) and adult peripheral blood-derived EPC (PB-EPC) (gsm508539-41) samples from Gene Expression Omnibus Series gse20283 (www.ncbi.nlm.nih.gov/geo) as published by Medina and colleagues (Medina *et al.* 2010) were imported into GeneSpring GX 11. Data files

from both microarray studies were subjected to normalisation, summarisation and Gene Ontology (GO) analysis with GeneSpring GX 11. Probe sets related to osteogenesis were identified by the related GO terms (GP:0001503 and children) (Ashburner *et al.* 2000). In the analysis of EPC transcriptome, selected probe sets were sorted in descending order of the mean expression of triplicate samples, and color-coded with the highest red, median (4.59) yellow and lowest blue. Further details are described in supporting information data.

3.9 Quantitative Polymerase Chain Reaction Analysis

mRNA derived from UCB-EPC (n=1) and adult PB-EPC samples (n=2) were obtained from Belfast, UK. Extracted total RNA of EPC derived from UCB and human adult peripheral blood were supplied by Belfast, UK. Briefly, 1 µg of RNA were converted to cDNA reverse-transcribed using the Superscript II First Strand cDNA synthesis kit (Life Technologies, USA) in a total volume of 19 µl. Quantitative Polymerase Chain Reaction (PCR) reactions were performed in triplicates for the following osteogenic genes: BMP1, BMP4, BMP6, COL1A1, TGFβ1, Osteonectin. 2µl of cDNA, 10µl of SYBR Green PCR Master Mix (Applied Biosystems, USA) and 1µl of 5µM primers formed the working solution which was topped up to a final volume of 20 µl. Thermal cycle conditions were 95°C for 10 min, then 45 cycles at 95°C for 15 sec, and 60°C for 1 min. Amplifications were monitored with the ABI Prism 7000 (Applied Biosystems, USA). Results were normalised against the housekeeping gene β-actin, and relative gene expression analysed with the 2-ddCt method. The 5'-3' forward (F) and reverse (R) primers of the respective genes are as follows:

| | |
|------|-------------------------|
| BMP1 | F: ATCGACCTTGCGGCTCGGGA |
| | R: GCGACCCACGTAGGAGCAGC |
| BMP4 | F: GCCAAGCGTAGCCCTAAGC |
| | R: GTGGCGCCGGCAGTT |
| BMP6 | F: CGGTGCACTAGCCCCCTTCC |

COL1A1 R: CTGCCCAGCAAACCCGCTCG
 F: CAGCTGCACCCCTACCACAGC
 R: CCCACATCTCCCCTCTTCGCA
 TGFβ1 F: GGCAGTGGTTGAGCCGTGGA
 R: TGTTGGACAGCTGCTCCACCT
 Osteonectin F: CGCGGTCCTTCAGACTGCC
 R: AGGCCCTCATGGTGCTGGGA

3.10 Cellular Viability Assay

Cellular viability in scaffolds was analysed by fluorescein diacetate/propidium iodide (FDA/PI) live/dead staining. The scaffolds/cells constructs were first incubated with 4µg/ml FDA for 20 minutes at 37°C. The samples were then rinsed thrice in PBS, placed for 10 minutes in a 100µg/ml PI solution, rinsed again in PBS once and viewed under a confocal laser microscope. FDA stains viable cell cytoplasm green and PI stains necrotic and apoptotic cell nuclei red. Stained samples were then viewed under a confocal laser microscope.

3.11 Growth Kinetics and Colony-Forming Unit-Fibroblasts Assay

hfMSC were plated in well plates at 5000 cells/cm² and allowed to proliferate in D10 media under the appropriate oxygen tensions. Cells were trypsinised daily and their growth kinetics was assessed by enumerating the cell numbers using a haemocytometer (n=4). Colony-Forming Unit-Fibroblasts (CFU-F) assay was carried out by low density plating of hfMSC at 400 cells per 100mm dish (8 cells/cm²) in D10 for 14 days, unless otherwise specified. The cells were then stained with 3% Crystal Violet in 100% methanol for 5 minutes at room temperature. Colonies ≥2 mm in diameter were counted.

3.12 Preparation of Cellular-Scaffold Constructs

3.12.1 Scaffold Fabrication and Treatment

Macroporous PCL/TCP (80/20) scaffolds (Osteopore International, Singapore) with a lay-down pattern of 0/60/120°, and porosity of 70% were fabricated using a fused deposition modelling technique under Current Good Manufacturing Practices (cGMP) environment (ISO 13485; **Figure 3-1**). Scaffolds were cut into 4X4X4mm dimensions, treated with 5M NaOH for 3 hrs to enhance hydrophilicity and washed thoroughly with PBS thrice prior to ethanol sterilisation.

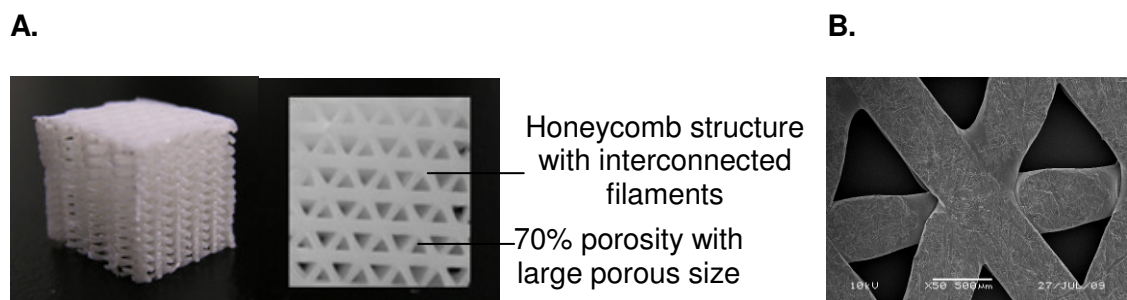


Figure 3-1: (A) Macroscopic view and (B) SEM imaging of the PCL/TCP scaffolds shows a high porosity with an approximate pore size of 500µm and honeycomb microarchitecture.

3.12.2 Cell Loading

EPC/hfMSC (1:1) and hfMSC were suspended in Tisseel Fibrin Sealant (Baxter, Switzerland). Thrombin was first dissolved in calcium chloride solution, while Tisseel was dissolved in sterile water. Tisseel solution was then added to the scaffold prior to seeding the coculture/fibrin mixture into the porous scaffolds, keeping the hfMSC density constant (at 3,000 cells per mm³). Fibrin mixture was allowed to polymerise for an hour in the incubator before adding BM.

3.13 Bioreactor Setup

The bioreactor set-up was as previously described in Zhang *et al* (Zhang *et al.* 2009). Briefly, the biaxial bioreactor consists of a spherical culture chamber, where the cellular scaffolds are anchored to the cap of bioreactor by pins, a medium reservoir and a perfusion system, which connects culture chamber and medium reservoir. The spherical culture chamber is designed to rotate in two perpendicular axes (Y and Z, pink block arrows) simultaneously and perfused with media flow circulating between culture chamber and medium reservoir (**Figure 3-2**). The bioreactor was then placed into the incubator that was equilibrated to atmospheric oxygen tension.

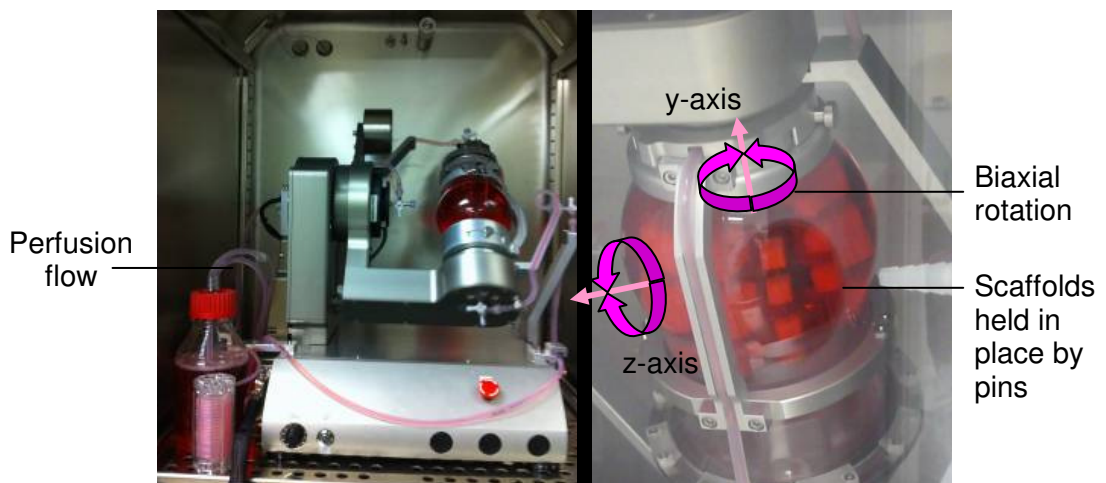


Figure 3-2: The perfusion biaxial bioreactor has two rotational axes (indicated by pink block arrows), with scaffolds pinned and fixed in place while the bioreactor rotates.

3.14 Imaging

3.14.1 Phase Contrast Light Microscopy

Cellular morphology, adhesion and extracellular matrix production were examined by phase contrast light microscopy (PCLM) daily and imaged at fixed time intervals using an attached camera unit.

3.14.2 Confocal Microscope

Monolayer and 3D cultures were viewed and scanned under a confocal laser microscope using laser wavelengths of 405nm (green), 594nm (red), 4',6-diamidino-2-phenylindole (DAPI) channel (blue) (Olympus, FV300 Fluoview, Japan).

3.14.3 Scanning Electron Microscope

Glutaldehyde-fixed scaffolds were then dehydrated, air-dried and gold sputtered with SCD 005 gold sputter machine (Bal-Tec, Liechtenstein) for 70s at 30mA under high vacuum before imaging on the Scanning Electron Microscope (SEM) (JSM 5660, JEOL, Japan).

3.14.4 Micro-Computed Tomography

The cellular-scaffold constructs were fixed in 10% formalin for one week prior to analysis of bone or vasculature network using the Micro-CT scanner (SMX-100CT X-ray CT Sys, Shimadzu, Japan). The scan settings were: X-ray voltage=45kV, X-ray current=100uA, detector size=9", scaling coefficient=50 and voxel resolution=0.008 mm. The scans were then reconstructed using VGStudioMax (Version 1.2, Volume Graphics, Germany) to create the 3D geometry and for quantitative histomorphometric analysis, with threshold values calibrated against its background.

3.15 Animal Work

3.15.1 Subcutaneous Implantations in Mice

Under general anaesthesia, cellular-scaffold constructs were implanted into subcutaneous pockets generated at the dorsal surface of each immunodeficient NOD/SCID mouse (**Figure 3-3**), and the skin closed with 5-O Vicryl sutures. Scaffolds were harvested at fixed time intervals for various assays such as histology and immunohistochemistry.

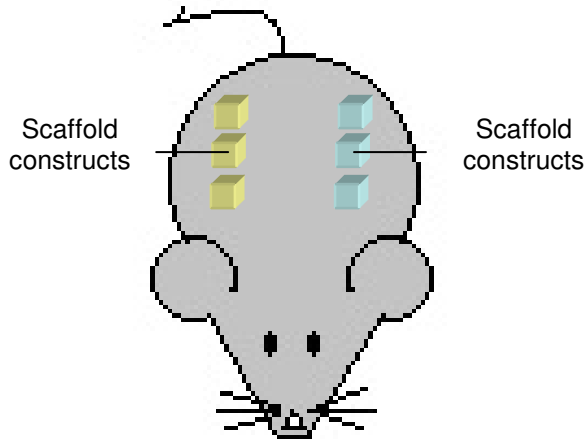


Figure 3-3: Diagrammatic representations of scaffold-constructs upon subcutaneous implantations at the dorsal surface of the NOD/SCID mice.

3.15.2 Microfil Perfusion

Visual observation of vascularisation was performed with the use of a vascular contrast, Microfil (MV-120, Flow Tech, USA). Briefly, mice were anaesthetised, laid supine and heparinised with 0.1ml of 500U *via* the tail vein before making a midline incision extending across the thorax and abdomen. Their left ventricles were cannulated and a perforation was made in the right atrial appendage before perfusion with 50ml of 10U heparinised saline. Upon exsanguination, 10ml of Microfil solution along with MV-curing agent (10% of total volume) were perfused via syringe. Animals were then stored at 4°C for 2h for the silicon compound to polymerise before scaffolds were harvested and fixed in 4% paraformaldehyde for a week prior to Micro-CT imaging (Zhang *et al.* 2010).

3.15.3 Histology

Cellular-scaffold constructs were placed on crushed dry ice for slow freezing, embedded in Optimal Cutting Temperature (OCT) compound and sectioned transversely with a Cryostat (CM 3050S, Leica, Germany). Sections of 50µm thickness were made for CD31 staining and all other sections were sectioned at

10µm thickness. Cryosections were then stained with Hematoxylin and Eosin stain (H&E) and Masson's Trichrome (MT) to visualise tissue morphology and evidence of new bone formation.

3.15.3.1 Capillary Density Analysis

Capillaries were quantified by evaluating the entire area of histological sections. Luminal structures perfused with red blood cells were identified as a capillary. The capillary density was calculated by dividing the total number of red blood cell-filled capillaries by the area of each section (vessels/mm²).

3.15.4 Immunohistochemistry

3.15.4.1 Human:Mouse Chimerism

Lamins A/C immunostaining was used to investigate chimerism of human cells in murine tissue. Cryosections from each sample were blocked with 5% normal goat serum for 1 hour, and left to react with monoclonal mouse anti-human Lamins A/C antibody (1:100, Vectorlabs, UK) overnight; sections were then incubated with goat anti-mouse secondary antibodies (1:100 Alexaflour 488, Life Technologies, New Zealand) for 1 hour, and counterstained with PI. Images were visualised using confocal microscopy.

3.15.4.2 Staining of CD31 Structures

Cryosections from each sample were blocked with 5% normal goat serum for 1 hour and left to react with monoclonal mouse anti-human lamin A/C (1:100, Vector Laboratories, U.K.), mouse anti-human CD31 (1:100, Millipore, USA), and rat antimouse CD31 (1:100, BD Pharmingen, USA) antibodies, respectively, overnight; sections were then incubated with goat anti-mouse secondary antibodies (1:100 Alexaflour 488/594, Life Technologies, New Zealand) for 90 minutes and

counterstained with PI or DAPI mounting media. Images were visualised using confocal microscopy.

3.15.4.3 Osteopontin Staining

The contribution of human cells to *in vivo* bone regeneration was delineated with human specific osteopontin staining (1:100, Abcam, UK) as previously described (Zhang *et al.* 2010).

3.15.5 Image Analysis

3.13.5.1 ImageJ Software

To enumerate the number of human and murine cells stained by Lamins A/C, ImageJ software was used to quantify the number of green and red staining in at least 3 different regions of the cryosections.

3.15.5.2 Imaris Software

Imaris was used to visualise the vessel formation from different angular perspectives as well as the vessel structures and cross sections at different depths.

3.16 Statistical Analysis

Parametric data are presented as mean \pm standard deviation and were analysed by t-test or analysis of variance (ANOVA). “*” ($p < 0.05$), “**” ($p < 0.01$), “***” ($p < 0.001$) indicate significant differences between samples.

**Chapter 4 - Coculture of Human Umbilical Cord Blood Endothelial Colony-
Forming Cells with Human Fetal Mesenchymal Stem Cells for the
Generation of Vascularised BTE Grafts**

If you can imagine it, you can achieve it; if you can dream it, you can become it.

~William Arthur Ward

Chapter 4 – Coculture of Human Umbilical Cord Blood Endothelial Colony-Forming Cells with Human Fetal Mesenchymal Stem Cells for the Generation of Vascularised BTE Grafts

4.1 Abstract

UCB-EPC show utility in neovascularisation, but their contribution to osteogenesis has not been defined. Cocultures of UCB-EPC with hfMSC resulted in earlier induction of ALP (Day 7 versus 10) and increased mineralisation (1.9 fold; $p < 0.001$) compared to hfMSC monocultures. This effect was mediated through soluble factors in EPC-conditioned media, leading to 1.8-2.2 fold higher ALP levels and a 1.4-1.5 fold increase in calcium deposition ($p < 0.01$) in a dose dependent manner. Transcriptomic and protein array studies demonstrated high basal levels of osteogenic (BMPs and TGF- β s) and angiogenic (VEGF and Angiopoietins) regulators. Comparison of defined UCB and adult PB-EPC showed higher osteogenic and angiogenic gene expression in UCB-EPC. Subcutaneous implantation of UCB-EPC with hfMSC in immunodeficient mice resulted in the formation of chimeric human vessels, with a 2.2 fold increase in host neovascularisation compared to hfMSC-only implants ($p = 0.001$). This study shows that UCB-EPC have potential in therapeutic angiogenesis and osteogenic applications in conjunction with MSC. It is speculated that UCB-EPC play an important role in skeletal and vascular development during perinatal development, but less so in later life when expression of key osteogenesis and angiogenesis genes in EPC is lower.

4.2 Introduction

Circulating EPC isolated from human PB have been implicated in the process of neovascularisation (Asahara *et al.* 1997) and investigated in various vascular paradigms. Numerous clinical trials using EPC have been performed, largely for treatment of limb ischemia (Tateishi-Yuyama *et al.* 2002) and myocardial infarction (Dimmeler and Zeiher 2009). However, unlike preclinical rodent models, only modest benefits have been observed; for example, left ventricular ejection fraction improved only 2-8%, with no reduction in death or stroke (Dimmeler and Zeiher 2009). A major problem confronting this field is the inconsistency in defining what constitutes an EPC, with the use of CD34+, CD133+ and VEGFR2+ among others as markers of EPC, leading to high levels of contamination with haemopoietic stem and progenitor cell types, and few studies providing evidence of functional differentiation *in vitro* or *in vivo* (Richardson and Yoder 2011). Furthermore, few protocols exist which can reliably expand these putative EPC into clinically-useful numbers.

Recently, the use of a stringent culture system for deriving PB or UCB-EPC has allowed the reliable isolation and expansion of cells which are clonogenic, have a well-defined immunophenotype and the ability to engraft functionally as blood vessels in murine models (Yoder *et al.* 2007; Richardson and Yoder 2011). These EPC are relatively pure and uncontaminated by haemopoietic lineages, being CD45 negative, and can be reliably isolated and expanded, raising the possibility of their use in regenerative medicine.

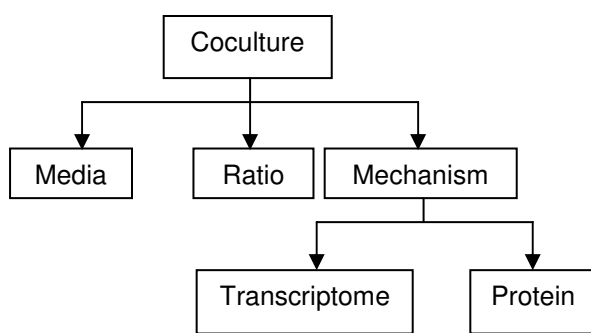
In previous work, the superiority of hfMSC over other MSC sources for generation of highly osteogenic tissue-engineered bone grafts utilising bioresorbable osteoinductive macroporous scaffolds has been shown (Zhang *et al.* 2010). Here, I propose the use of EPC in coculture with hfMSC to generate an osteogenic graft with

enhanced vasculogenic potential. This study will be of relevance to not only bone, but to other fields of tissue engineering where voluminous grafts are required.

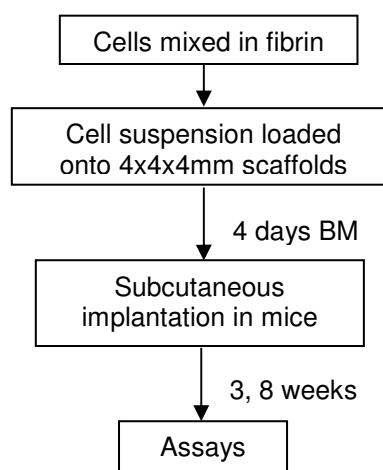
4.3 Experimental Approach

In this project, the interactions of well-characterised UCB-EPC with hfMSC are examined through a series of *in vitro* and *in vivo* transplantation assays, with the overall goal of defining the use of EPC in the generation of vascularised grafts.

In vitro



In vivo



4.4 Results

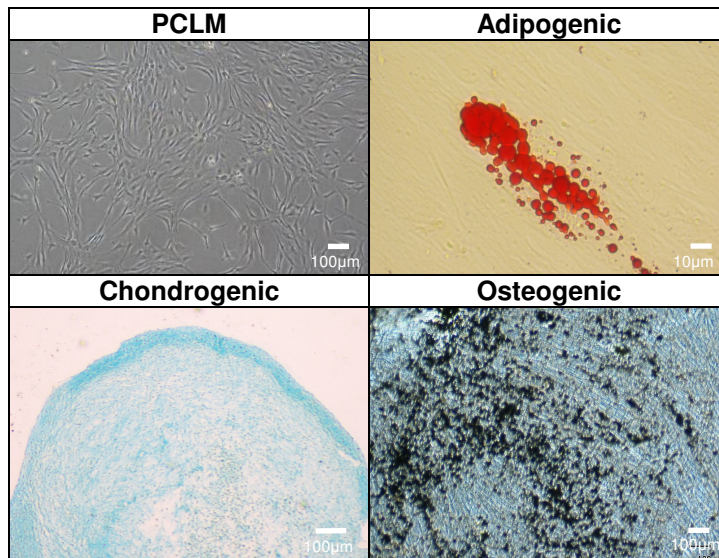
4.4.1 Cell Characterisation

4.4.1.1 Human Fetal Mesenchymal Stem Cells

hfMSC have a spindle morphology and underwent tri-lineage differentiation into adipogenic, chondrogenic and osteogenic lineage when differentiated in their respective media (**Figure 4-1A**). The cells were screened by flow cytometry, where the histogram of the cells stained with the marker of interest (green plots) was overlaid with that of the unstained cells (control; red plots). Plots that laid within the region of the control group were considered negative for the marker of interest, whereas those that laid towards its right indicated positive staining for the marker of

interest. Here, hfMSC were found to be negative for haemopoietic and endothelial markers (CD34, CD45 and CD31), expressing low levels within the range of ~1%. MSC markers such as CD73, CD105, CD90 were positive and showed a high level of expression (**Figure 4-1B**).

A. Phase Contrast Microscopy



B. Flow Cytometry

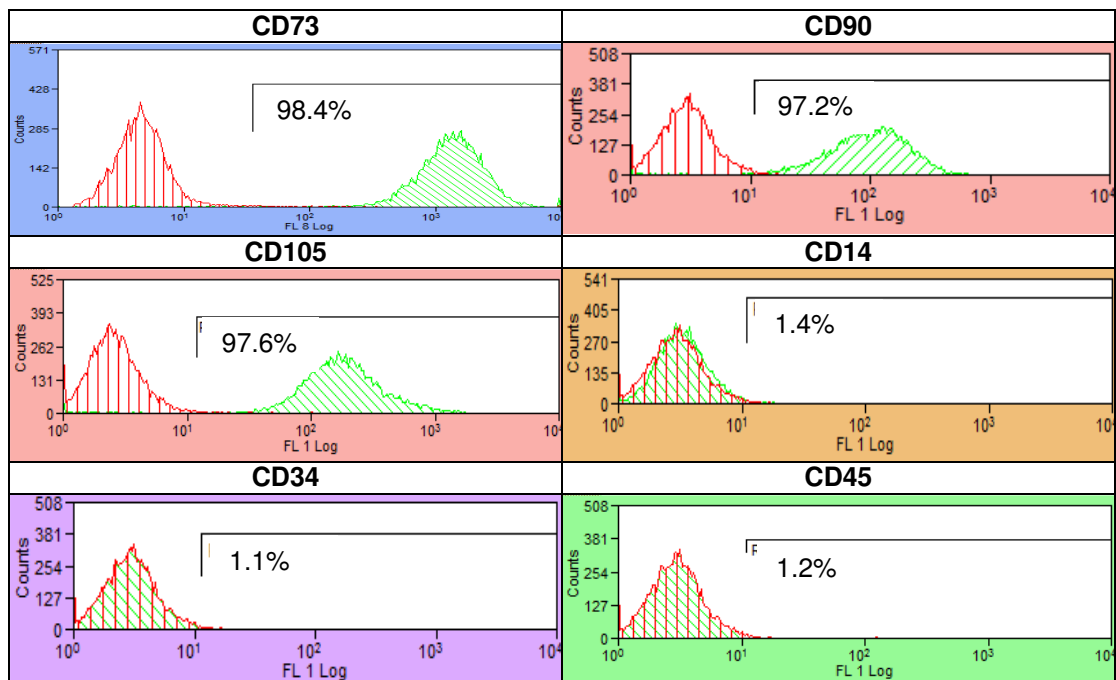


Figure 4-1: (A) hfMSC had a spindle-like morphology and underwent tri-lineage differentiation. This was confirmed by Oil-red-O staining for intracytoplasmic

vacuoles of neutral fat; Alcian Blue staining showed the presence of glycosaminoglycan in cartilages upon culture in a micro-mass pellet form; von Kossa stains (black) for extracellular calcium deposition. (B) Immunophenotypic characterisation of hfMSC using flow cytometry showed high expression of MSC markers such as (A-C) CD73, CD90, CD105 and did not express hematopoietic and endothelial markers such as (D-F) CD14, CD34 and CD45.

4.4.1.2 Endothelial Progenitor Cells

UCB-EPC emerged as polygonal cells in a cobblestone pattern and differentiated into tube-like networks when plated on Matrigel. Their immunophenotypic characteristics were demonstrated by its expression of Dil acLDL uptake, CD31, vWF and VE Cadherin, with cell nuclei counterstained with PI and DAPI accordingly (Figure 4-2) (Chong *et al.* 2009).

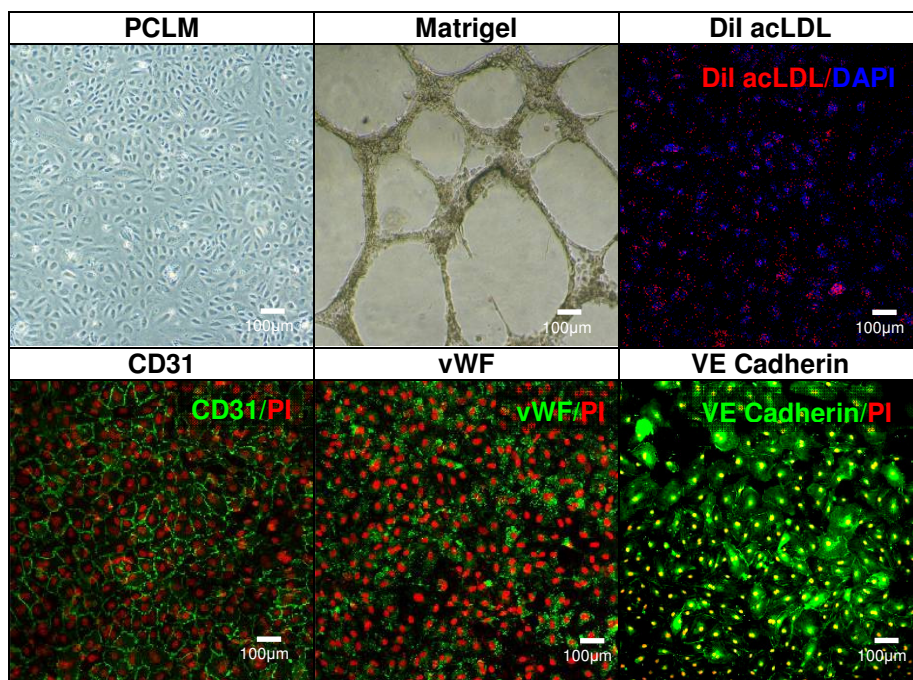


Figure 4-2: Characterisation of UCB-EPC. (Top row from left to right) PCLM of EPC demonstrated typical cobblestone morphology of endothelial cells. EPC differentiated and formed networks when plated on Matrigel. Immunostaining demonstrated expression of (Bottom row from left to right) CD31, von Willebrand Factor, acLDL uptake (red) and VE Cadherin, indicating endothelial phenotype and function. Cell nuclei were counterstained with PI (red) and DAPI (blue) accordingly.

4.4.2 Optimal Media for Osteogenic Differentiation of Coculture *In Vitro*

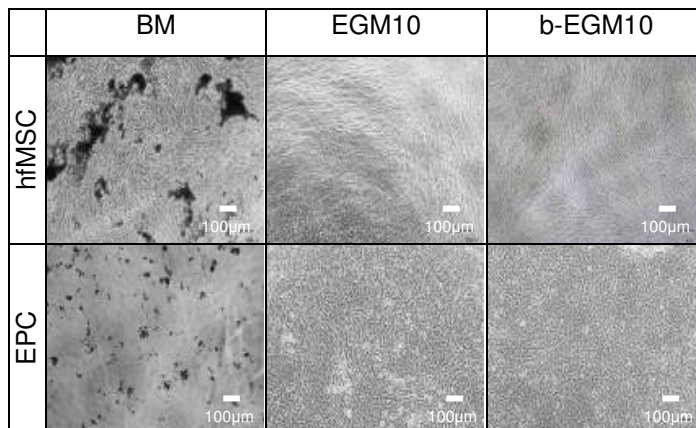
To determine suitable culture conditions for stimulating osteogenic differentiation, EPC and hfMSC were cultured separately in BM, EGM10 and EGM10 supplemented with bone inducing elements (b-EGM10). Various media types and their composition, as well as the rationale for their use in this study are summarised in **Table 4-1**.

Table 4-1: The different media types and their respective constituents are used for identifying the optimal media for directing osteogenic differentiation of the coculture.

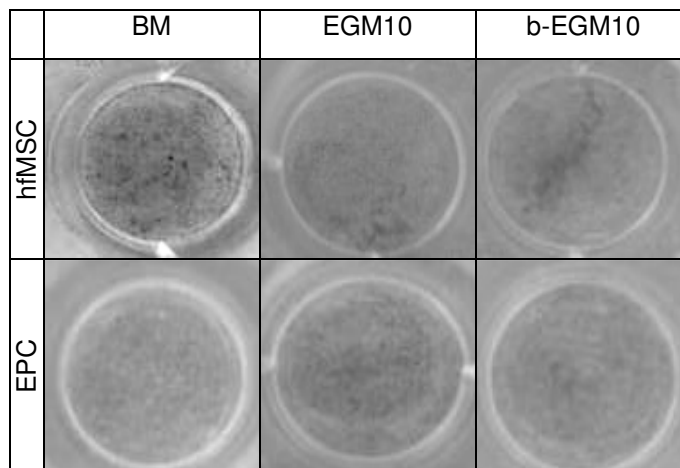
| Media | Media components | Rationale for use |
|---------|---|---|
| BM | <ul style="list-style-type: none"> • DMEM + 10% FBS • Bone inductive components (glycerophosphate, dexamethasone, ascorbic acid) | <ul style="list-style-type: none"> • Well-defined media for osteogenic differentiation • Intended as a control group |
| EGM10 | <ul style="list-style-type: none"> • EBM + 10% FBS • Bullet kit of growth factors (EGF, bFGF, VEGF, IGF) | <ul style="list-style-type: none"> • EGM10 to maintain cellular viability of EPC • Intended as a control group |
| b-EGM10 | <ul style="list-style-type: none"> • EBM + 10% FBS • Bullet kit of growth factors (EGF, bFGF, VEGF, IGF) • Bone inductive component (glycerophosphate, dexamethasone, ascorbic acid) | <ul style="list-style-type: none"> • EGM10 to maintain cellular viability of EPC • Bone inductive components to direct osteogenic differentiation |

Only BM, and not EGM10 or b-EGM10 induced osteogenic differentiation of hfMSC, seen as extracellular crystals under PCLM (**Figure 4-3A**), and confirmed by Von Kossa staining (**Figure 4-3B**). Quantitatively, BM induced high levels of calcium deposition in hfMSC (24.1µg/well), but not in EPC (0.1µg/well; $p < 0.001$) cultured in BM, while no calcium was deposited in either cell type when cultured in EGM10 or b-EGM10 (**Figure 4-3C**).

A. Phase Contrast Microscopy



B. Von Kossa Staining



C. Calcium Content Assay

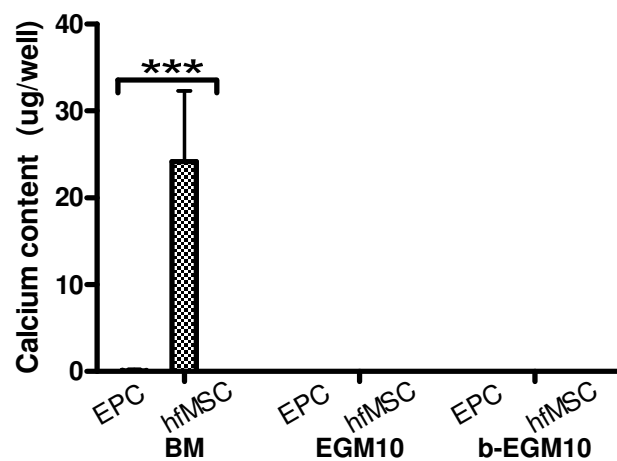


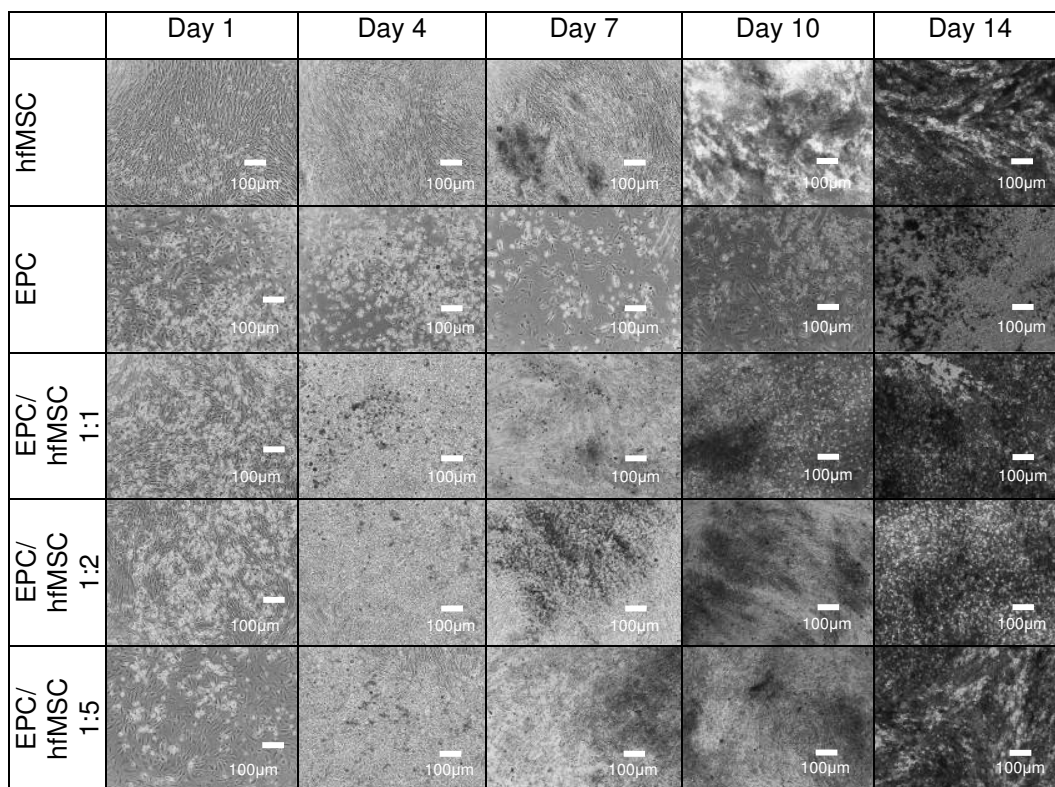
Figure 4-3: BM is necessary to induce osteogenic differentiation of hfMSC. (A) hfMSC laid down extracellular minerals when cultured in BM, while cell debris was observed with EPC in BM. Cells cultured in EGM10 and b-EGM10 did not demonstrate mineralisation. (B) hfMSC cultured in BM showed dark Von Kossa stains for calcium crystals but none in the other study groups. (C) This was

confirmed by quantitative calcium assays with only hfMSC grown in BM laying down significant amounts of calcium. All assays were performed on Day 14.

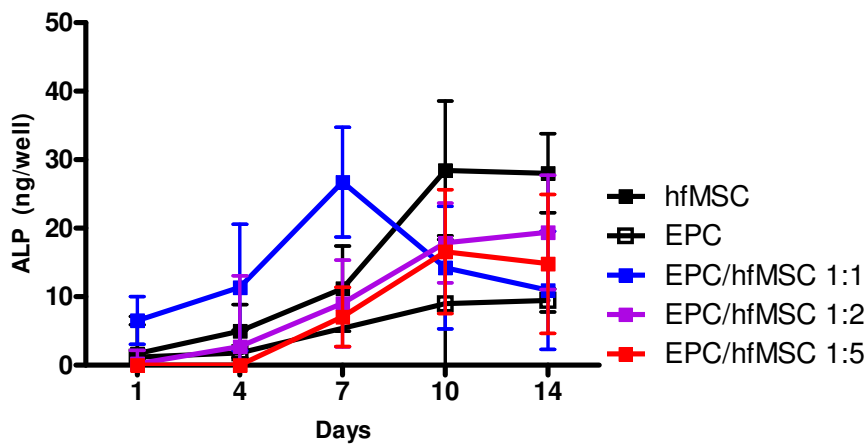
4.4.3 Optimal Coculture Ratio for Osteogenic Differentiation *In Vitro*

To determine the optimal cell-ratio for osteogenic induction, EPC and hfMSC were cocultured at different ratios but a constant hfMSC seeding density (20,000 cells/cm²). Cocultured EPC/hfMSC resulted in earlier mineralisation compared to hfMSC alone, with extracellular crystals seen by Day 4 in coculture groups compared with Day 7 in hfMSC-only cultures (**Figure 4-4A**). EPC/hfMSC cocultured in a 1:1 ratio achieved the earliest ALP peak on Day 7 compared to other groups (**Figure 4-4B**), and a 1.9 fold higher calcium deposition on Day 14 compared to hfMSC cultures (p=0.001, n=3 replicates) (**Figure 4-4C**), indicating enhanced osteogenic differentiation.

A. Phase Contrast Microscopy



B. Alkaline Phosphatase Assay



C. Calcium Content Assay

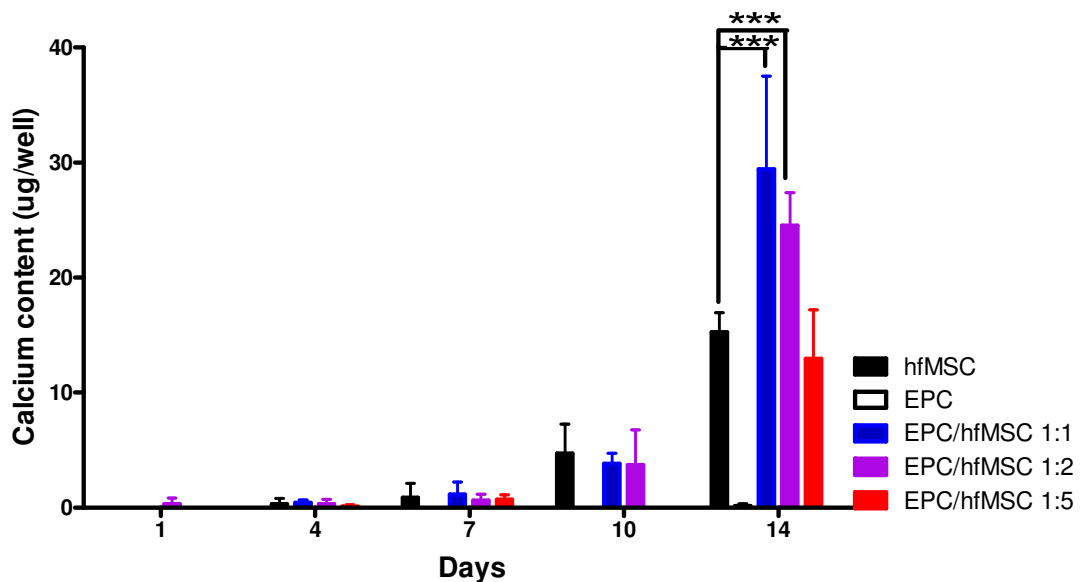


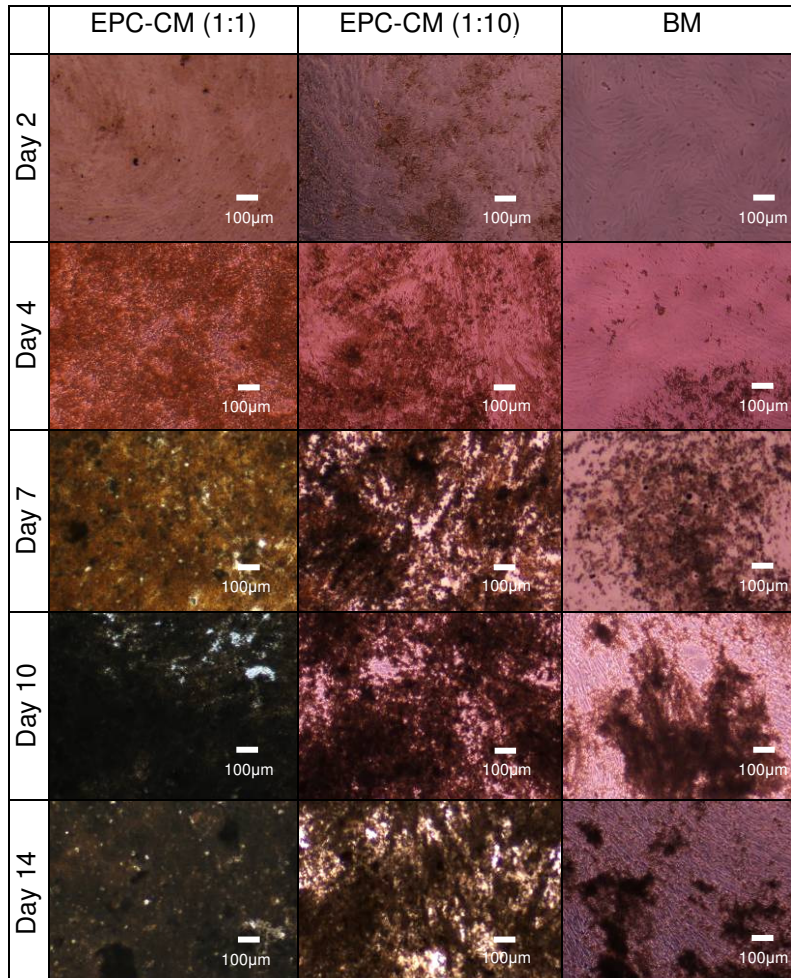
Figure 4-4: EPC/hfMSC in coculture induces earlier osteogenic differentiation of hfMSC. (A) EPC/hfMSC groups in varying ratios displayed earlier mineralisation compared to EPC and hfMSC monocultures. (B) Quantitative ALP measurements with EPC/hfMSC (1:1) demonstrated the earliest ALP peak activity on Day 7. (C) EPC/hfMSC (1:1) cocultures laid down the most calcium on Day 14. “***” ($p < 0.001$).

4.4.4 Mechanism of Action of EPC for Osteogenic Potentiation

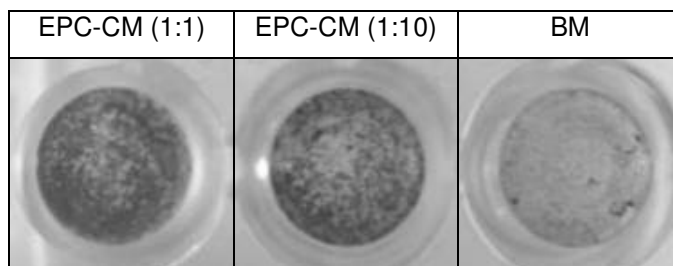
To investigate the mechanism for the observed osteogenic enhancement of hfMSC, EPC conditioned media (EPC^{CM}) was added directly into hfMSC cultures. This resulted in more extracellular crystals being deposited than in hfMSC cultured in BM alone, as seen on light microscopy (**Figure 4-5A**). This was confirmed by increased von Kossa staining on Day 14 in EPC^{CM (1:1)} and EPC^{CM (1:10)} cultures compared to BM cultures (**Figure 4-5B**). Quantitatively, ALP activity peaked earlier in the EPC^{CM (1:1)} group at Day 7 compared to Day 10 for EPC^{CM (1:10)} and BM groups, with peak values being 2.2 and 1.8 fold higher when cultured in EPC^{CM (1:1)} and EPC^{CM (1:10)} respectively compared to BM (**Figure 4-5C**). Correspondingly, 1.3 fold more calcium was deposited in the EPC^{CM (1:1)} compared to BM by Day 14 ($p < 0.05$) (**Figure 4-5D**). Collectively, these results suggest that soluble factors secreted by EPC play a role in potentiating osteogenic differentiation of hfMSC in a dose dependent manner.

Next, I assessed the ability of EPC themselves in the absence of bone inducing components to induce osteogenic programming of hfMSC upon direct contact. hfMSC and EPC/hfMSC groups cultured in BM showed 2 ($p < 0.01$) and 2.5 fold ($p < 0.001$) higher ALP activity respectively compared to culture in basal D10 media (**Figure 4-5E**). Similarly, calcium deposition was found only in BM cultures, but not D10 cultures for either hfMSC and EPC/hfMSC as assayed by Von Kossa staining and quantitated (**Figure 4-5F-G**), suggesting that the addition of EPC to hfMSC in basal D10 media does not induce osteogenic programming in hfMSC, but rather, EPC potentiates osteogenic differentiation of hfMSC cultured in BM.

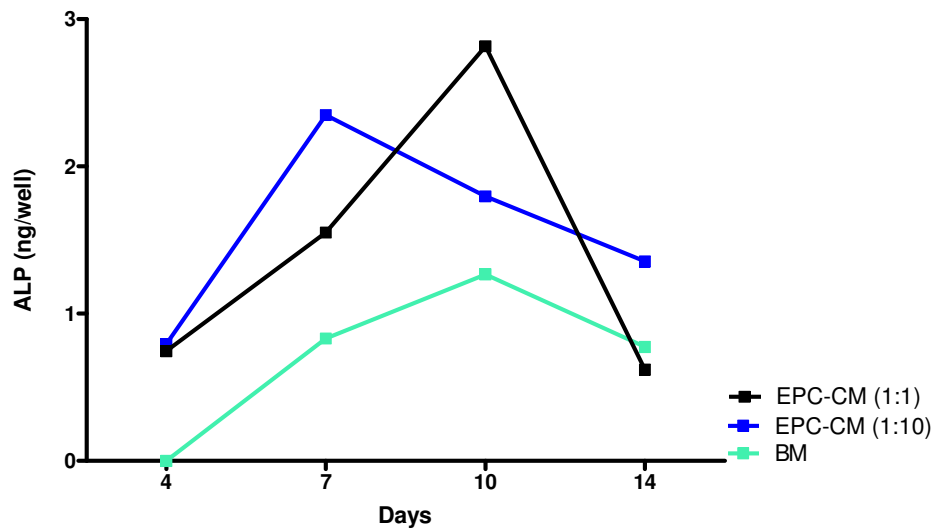
A. Phase Contrast Microscopy



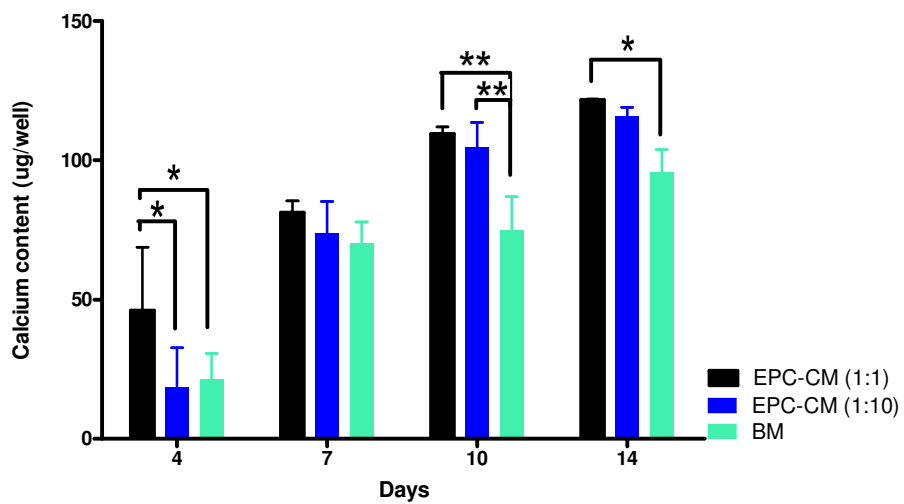
B. Von Kossa Staining



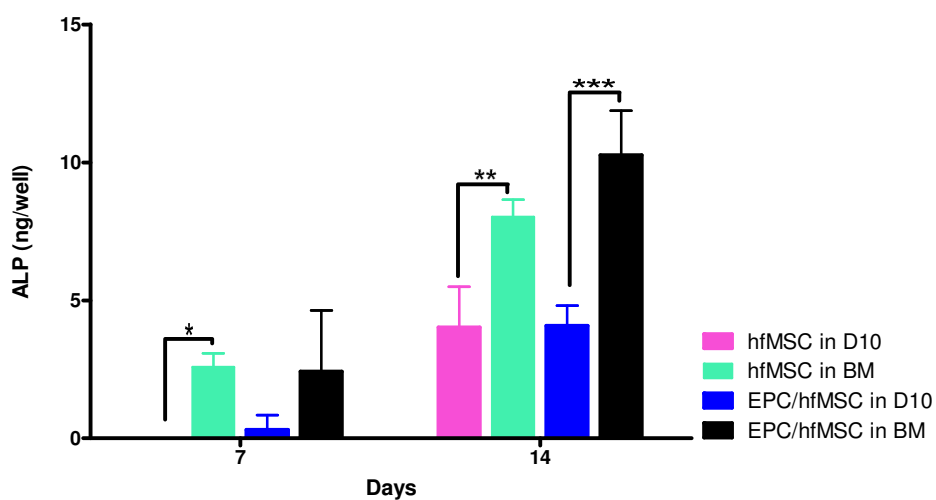
C. Alkaline Phosphatase Assay (CM)



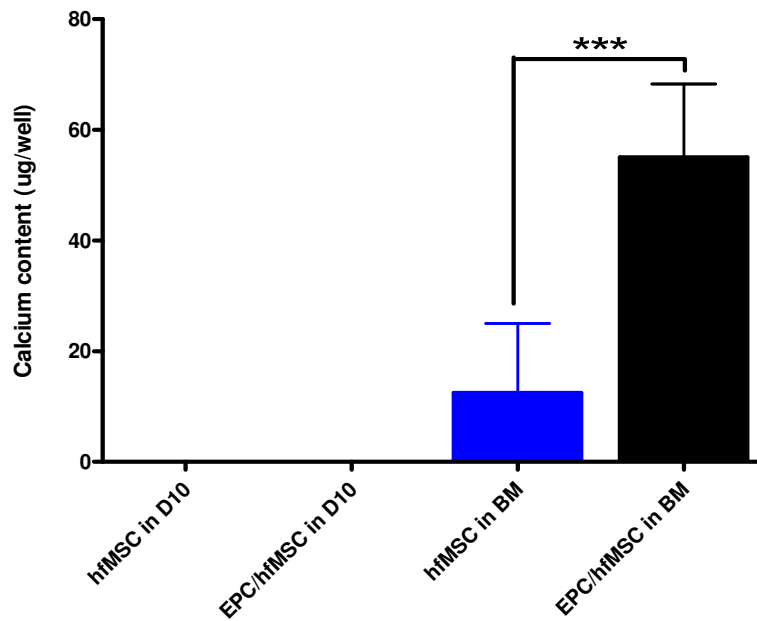
D. Calcium Content Assay (CM)



E. Alkaline Phosphatase Assay (Coculture)



F. Calcium content assay (Coculture)



G. Von Kossa Staining

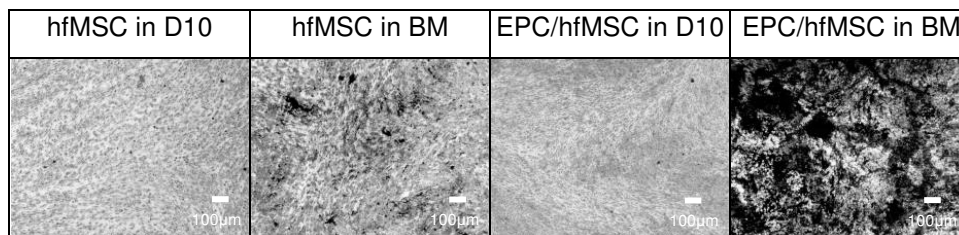


Figure 4-5: Dose dependent effect of soluble factors in EPC^{CM} enhanced osteogenic differentiation of hfMSC. (A) hfMSC cultured in EPC^{CM} (1:1) and EPC^{CM} (1:10) demonstrated earlier and more extensive mineralisation than when cultured in BM. (B) Greater Von Kossa staining were observed in EPC^{CM} (1:1) and EPC^{CM} (1:10) compared to BM at Day 14 of osteogenic differentiation. (C) EPC^{CM} (1:1) and EPC^{CM} (1:10) displayed higher (2.2 fold and 1.8 fold respectively) peak of ALP activity than BM. (D) Calcium deposited in EPC^{CM} (1:1) and EPC^{CM} (1:10) was consistently higher (1.5 fold and 1.4 fold respectively) than BM in all time points. (E) ALP levels were consistently higher in BM than in basal media, D10, with the coculture displaying highest levels on Day 14. (F) Both hfMSC and EPC/hfMSC cocultures required osteogenic supplements to induce osteogenic differentiation, which was potentiated with coculture, with deposition of calcium after 14 days of induction, further confirmed by Von Kossa staining (G). “****” ($p < 0.001$)

4.4.5 Identity of EPC Secretome

Two approaches were adopted to interrogate the identity of secreted proteins in EPC^{CM} responsible for the enhanced osteogenic differentiation of hfMSC. Firstly, I

used a transcriptomic approach to find that EPC highly expressed a range of genes associated with angiogenesis, as well genes associated with osteogenesis such as members of the TGF-beta pathway including SMAD1,2,3 and 5 and Bone Morphogenetic Proteins, BMP-1,2,3,6,7 and 8 (**Supplementary Table S1A-B, 2-3**).

Next, a semi-quantitative antibody array (**Figure 4-6**) was used to assay the secretome of EPC found in EPC^{CM}. EPC secreted several inflammatory cytokines, angiogenic factors, as well as bone-related proteins, all of which play an important role in regulating the biological processes involved in fracture healing. High levels of secreted proteins such as Angiogenin, Ang-2, GRO, IL-6, IL-8, MCP-1, MIP-3a, PDGF-BB and TIMP-2 were identified (**Table 4-2**). In addition, I confirmed the transcriptomic observations identifying bone related proteins, BMP-5, BMP-6, BMP-7, TGF- β 1, TGF- β 2 from the TGF- β superfamily secreted into EPC^{CM}. These, along with bFGF, Endoglin, FGF-4, IGF-1, MCP-1, Oncostatin, Osteoprotegerin, PDGF and VEGF found in the EPC^{CM}, may have contributed directly or indirectly to the observed enhancement in osteogenesis (**Supplementary Table S4**).

A. Human Cytokine Antibody Array

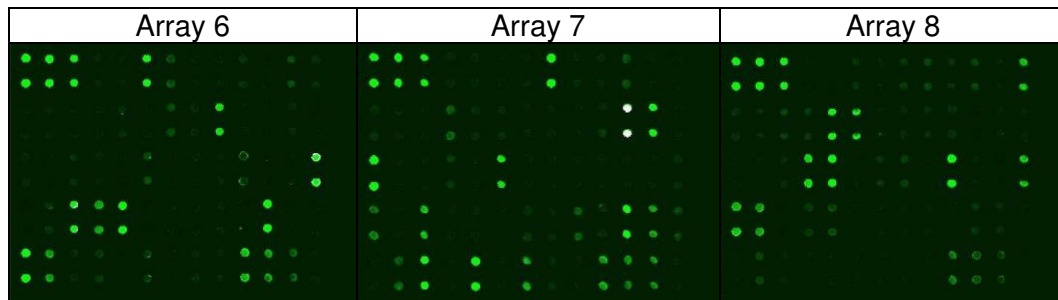


Figure 4-6: Semi-quantitative analysis of EPC^{CM} using the Human Cytokine Antibody Array, where 118 secreted proteins found within EPC^{CM}.

Table 4-2: (A) Top highest concentration of proteins found within EPC^{CM}, of which angiogenic cytokines and other (B) bone related morphogens belonging to the TGF- β superfamily are featured prominently.

A. Secreted Proteins in High Concentrations in EPC^{CM}

| Cytokine | Normalised value |
|----------------|------------------|
| Angiogenin | 1.09 |
| Angiopoietin-2 | 2.72 |
| GRO | 4.66 |
| IL-6 | 5.47 |
| IL-8 | 1.73 |
| MCP-1 | 5.48 |
| MIP-3a | 1.14 |
| PDGF-BB | 1.28 |
| TIMP-2 | 1.64 |

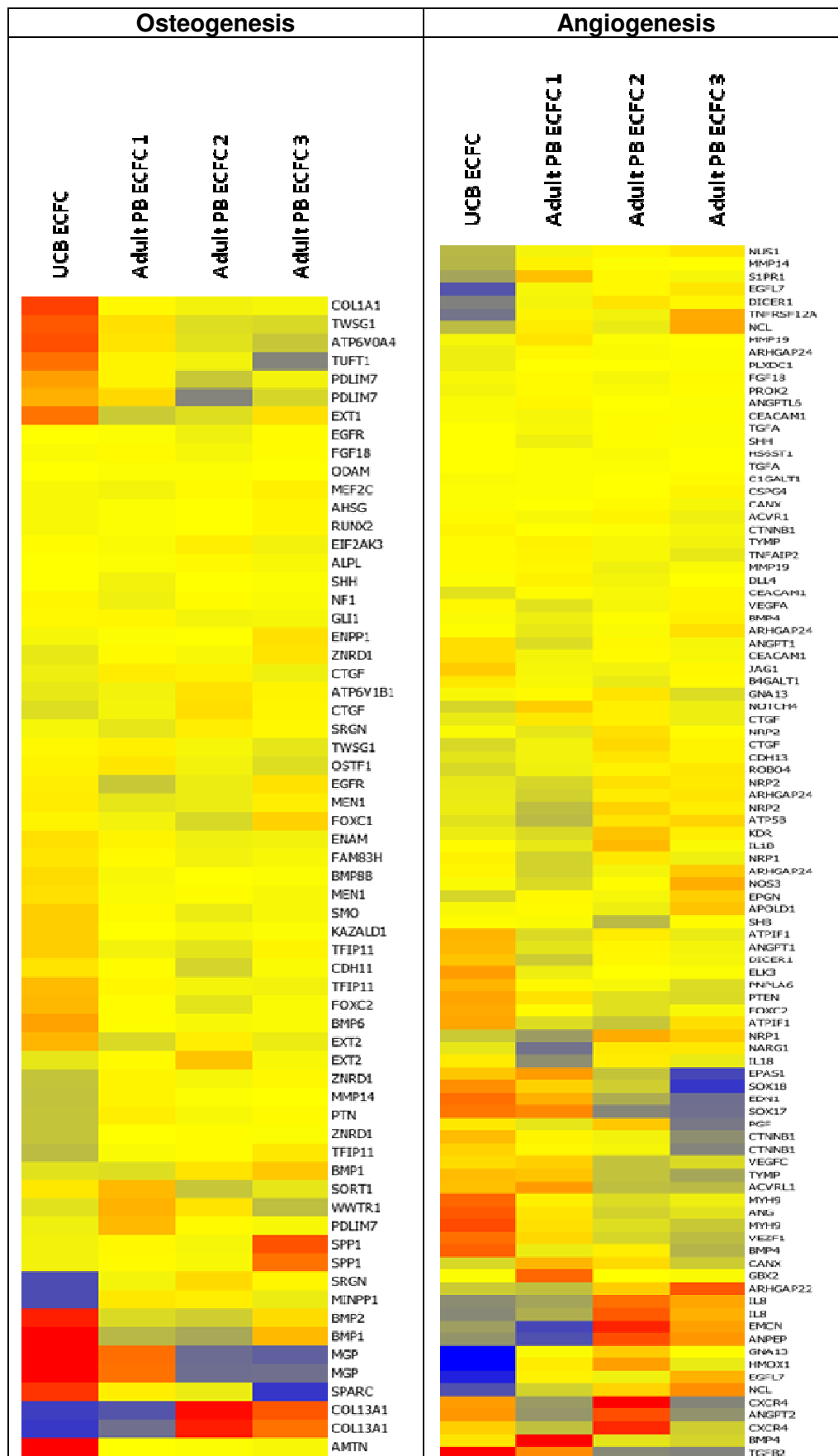
B. Members of TGF- β Superfamily Secreted in EPC^{CM}

| Bone-related cytokines | Normalised value |
|------------------------|-----------------------|
| BMP-5 | 2.56×10^{-2} |
| BMP-6 | 7.42×10^{-3} |
| BMP-7 | 8.74×10^{-3} |
| TGF beta2 | 1.04×10^{-2} |
| TGF-b1 | 9.66×10^{-3} |

4.4.6 Osteogenic and Angiogenic Capacity of UCB versus PB-EPC

To validate this, transcriptomic data from a previously-published study was reanalysed. The effect of EPC on osteogenesis and angiogenesis processes was reported separately for well characterised UCB-EPC and adult PB-EPC (**Figure 4-7A**) (Medina *et al.* 2010). Results showed that UCB-EPC expressed BMP-1 (4.1 fold), BMP-2 (2.9 fold), BMP-4 (2.4 fold), BMP-6 (1.5 fold), TGF- β 2 (11.0 fold) and COL1A1 (2.4 fold) among others at higher levels than in adult PB-EPC. By using different samples of UCB (n=1) and adult PB-EPC (n=2), I validated some of these genes through quantitative PCR to show that BMP1, BMP4, BMP6, COL1A1, TGF β 1 and osteonectin were upregulated in UCB over adult PB-EPC (**Figure 4-7B**). Similarly, UCB-EPC expressed key angiogenesis genes at higher levels (**Figure 4-7A and Supplementary Table S5-6**).

A. Microarray Analysis



B. Quantitative Real-Time PCR

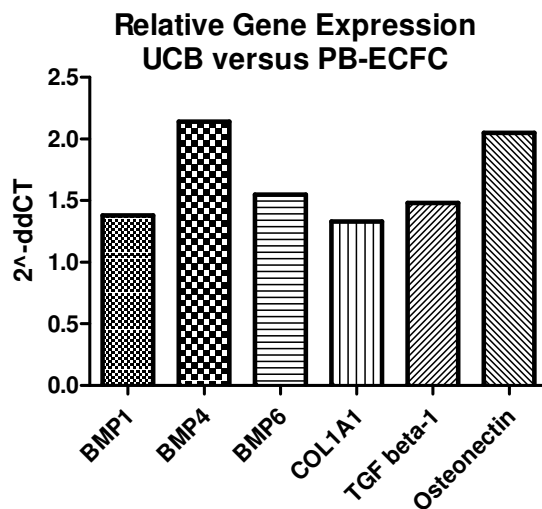


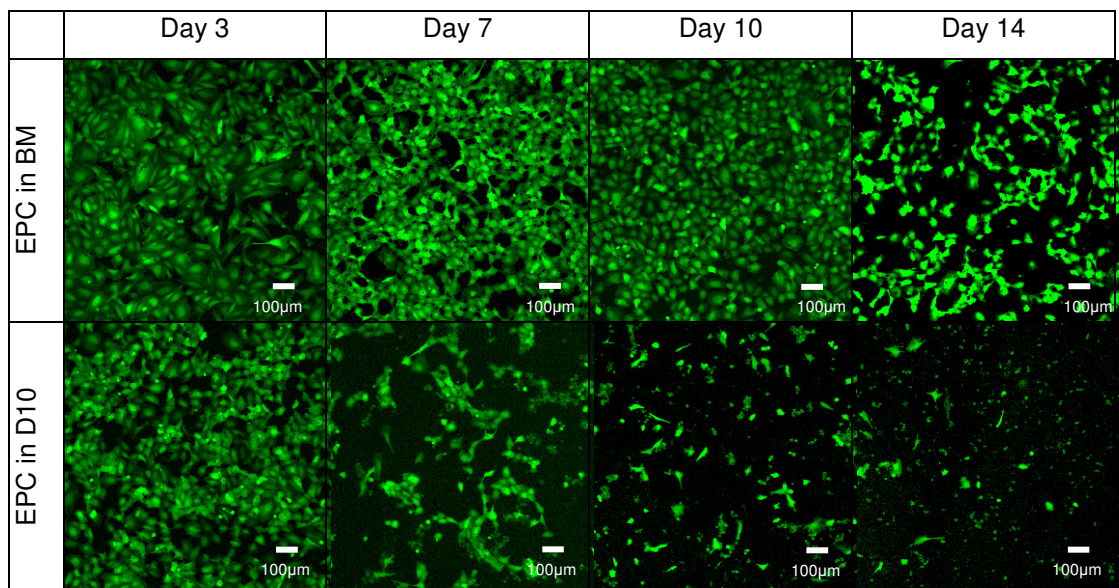
Figure 4-7: UCB versus adult PB-EPC taken from Medina *et al* (Medina *et al.* 2010) demonstrated higher expression levels of key osteogenic and angiogenic genes using (A) Transcriptomic microarray analysis and (B) qPCR.

4.4.7 *In Vitro* Vessel Forming Ability of EPC/hfMSC Cocultures

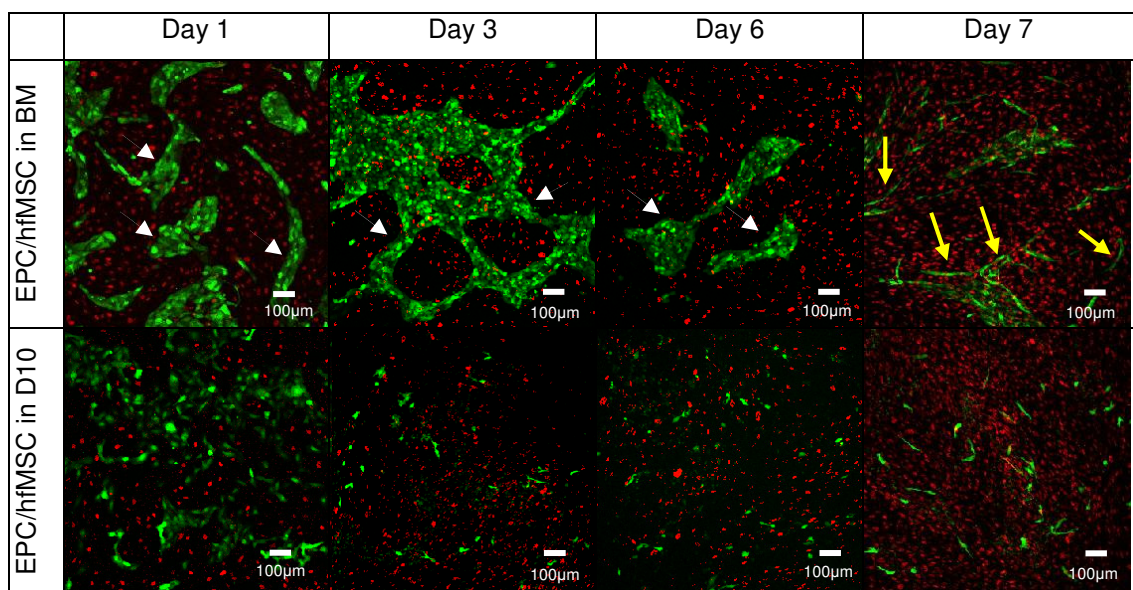
By labelling EPC with GFP, a poor viability of EPC when cultured in D10 over 14 days was observed, whereas the addition of the standard osteogenic inducing agents dexamethasone, ascorbate and β -glycerophosphate, improved their viability markedly (**Figure 4-8A**). Coculture of GFP-labelled EPC with nuclear RFP-labelled hfMSC, resulted in formation of EPC-derived islets which evolved by Day 7 into tube-like structures when cultured in BM, but not when cultured in D10 (**Figure 4-8B**).

Next, I looked at the ability of this coculture system to induce tube-like structures in a 3D culture system within a macroporous scaffold. Cocultured GFP-EPC and hfMSC embedded in fibrin and loaded onto these scaffolds proliferated and occupied the porous scaffold over time, with complex tubular structures with multiple branch-points seen throughout the scaffold by Day 14 (**Figure 4-8C**).

A. Viability of EPC Cultures in BM and D10 in 2D



B. Confocal Imaging of Coculture Distribution in 2D



C. EPC Vascular Network in Coculture with hfMSC in 3D at Day 14 of *In Vitro* Culture

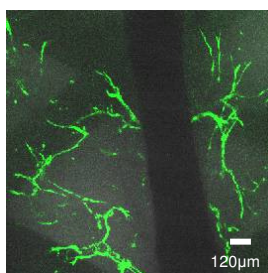


Figure 4-8: EPC potentiate osteogenic programming of hfMSC and *in vitro* tubule formation in the presence of bone inducing components (A) GFP-labelled EPC showed better survival when cultured in BM than in D10. (B) Coculture of GFP-EPC

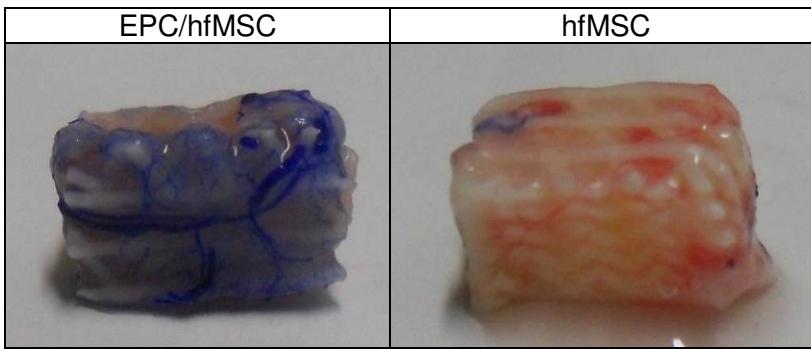
and H2B-RFP-hfMSC (Red fluorescence nuclear staining) resulted in the formation of EPC islets (white arrowheads), leading eventually to the development of tubular structures (yellow arrows) by Day 7 (C) Formation of GFP-EPC vessel-like structures with complex branching points was observed when EPC/hfMSC were cocultured over 14 days within a 3D culture system within a macroporous scaffold.

4.4.8 *In Vivo* Vasculogenesis of EPC/hfMSC Cocultures

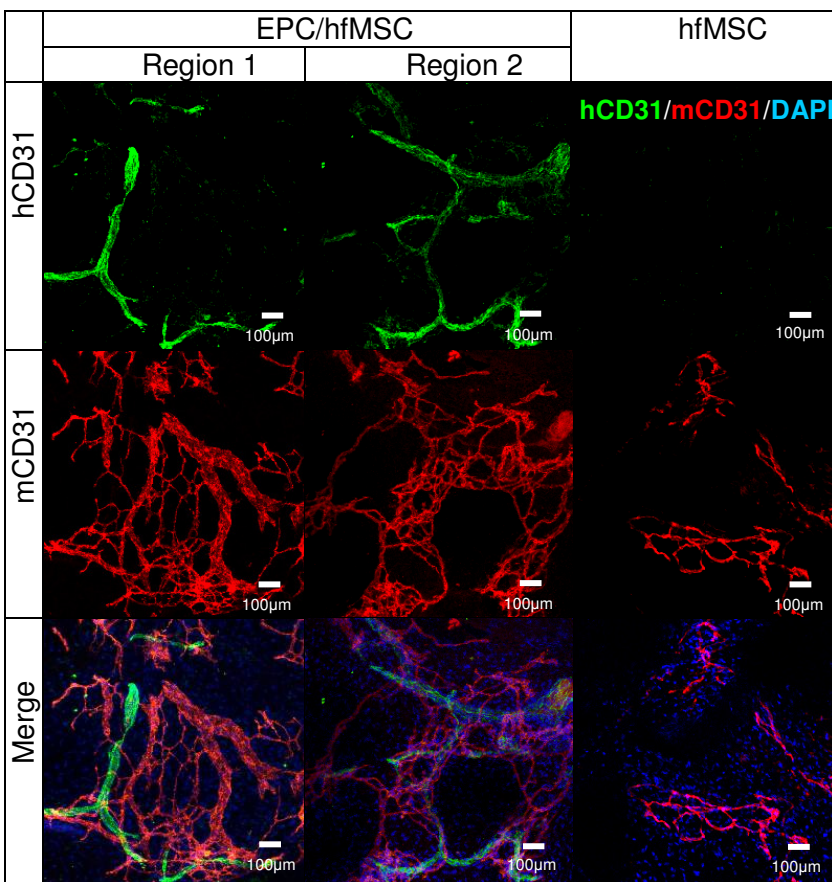
Following the robust formation of vascular structures within 3D EPC/hfMSC cocultures *in vitro*, I implanted EPC/hfMSC and hfMSC-loaded scaffolds subcutaneously into immunodeficient mice (**Figure 3-3**). Three weeks after implantation, perfusion of a vascular contrast agent showed an extensive network of vessels surrounding the harvested EPC/hfMSC scaffolds, while comparatively few vessels were seen on hfMSC-only scaffolds (**Figure 4-9A**).

By Week 8, human CD31 positive blood vessels with complex networks could be seen coursing through EPC/hfMSC scaffolds but not hfMSC-only scaffolds (**Figure 4-9B**). These human vessels were seen to form chimeric vessels, joining with host-derived vessels stained with murine-specific CD31 antibodies (white arrows in **Figure 4-9C**) at multiple levels throughout the scaffold (**Figure 4-9B-C**). By staining for murine specific CD31 positive blood vessels (red), EPC/hfMSC scaffolds were found to develop 2.2 fold greater area of murine-specific CD31 per μm^2 than hfMSC-only scaffolds ($p=0.001$), suggesting a higher degree of host-derived neovascularisation (**Figure 4-9D**). In EPC/hfMSC scaffolds, human vessels accounted for 30.2% of all vessels within the scaffold core (**Figure 4-9E**). This observation was supported by a lower degree of human cell chimerism in the EPC/hfMSC scaffolds compared to hfMSC-only scaffolds (55.9 ± 4.7 versus $74.8\pm 12.3\%$, $p>0.05$) (**Figure 4-9F**), and may reflect a higher degree of host-derived cellular infiltrate.

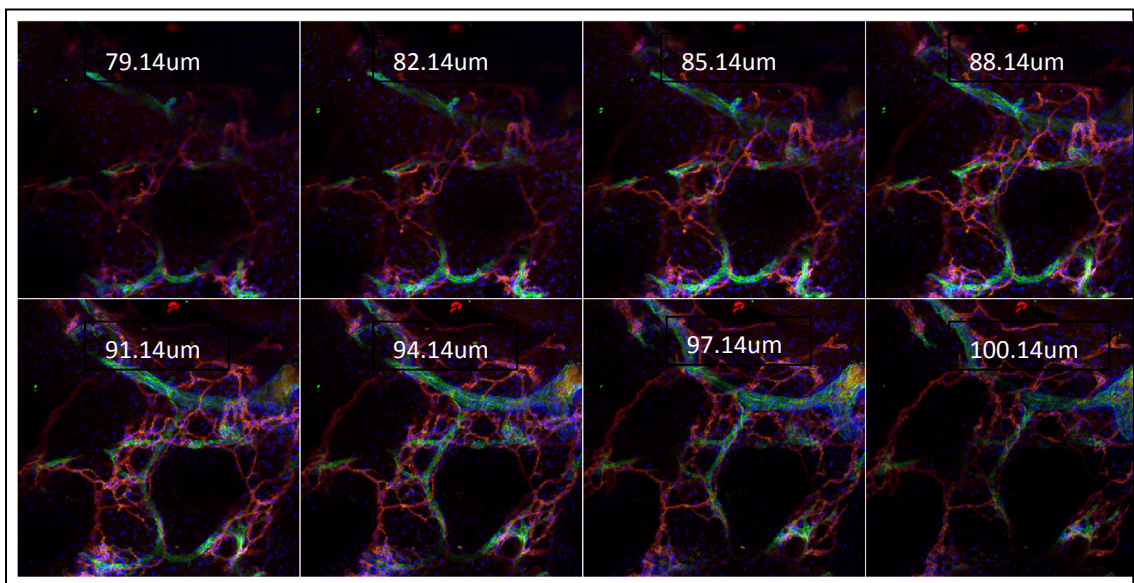
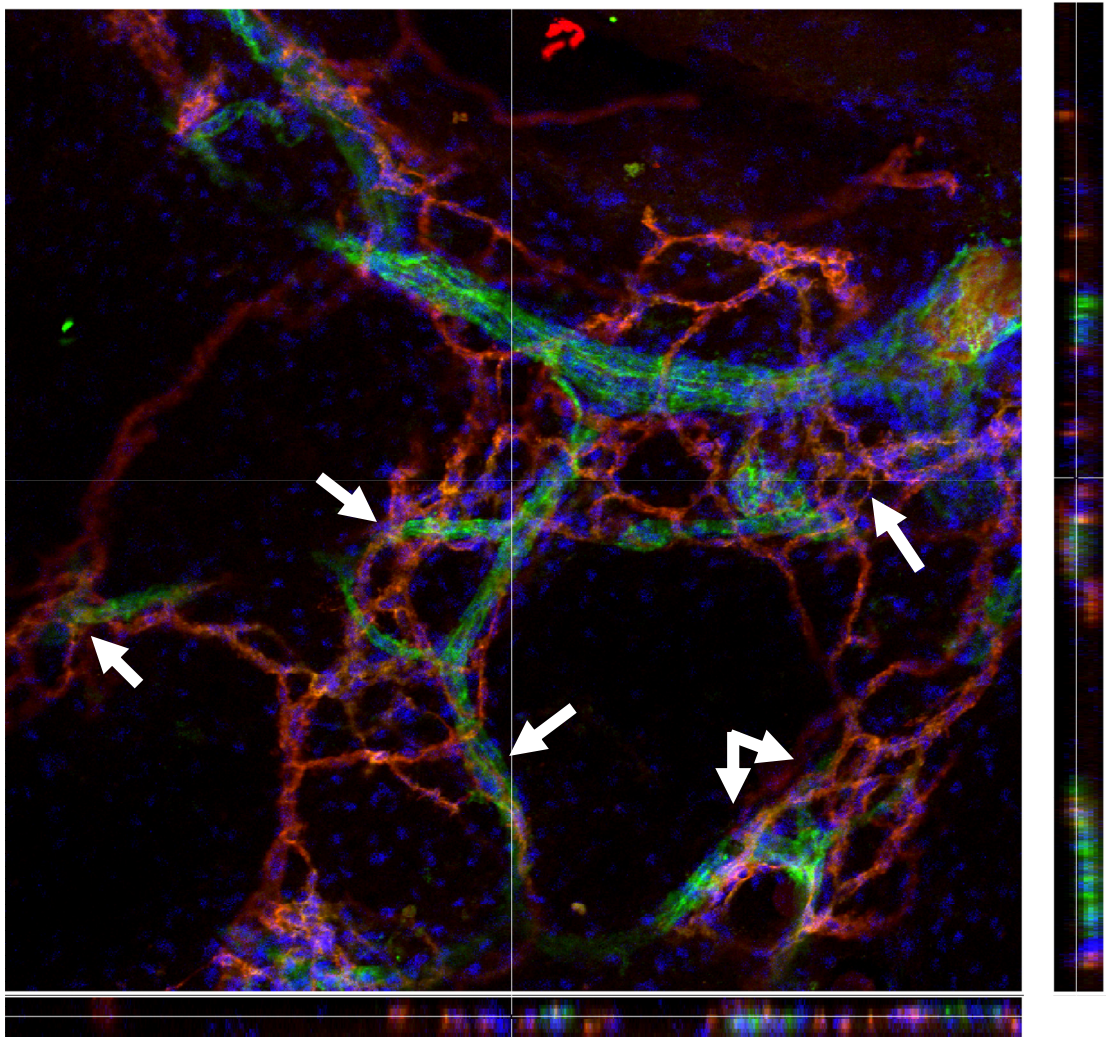
A. Vascularisation in Scaffolds



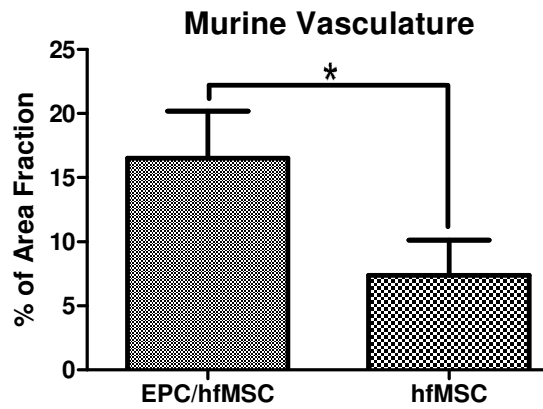
B. Human and Mouse Specific CD31 Vessel Networks in Scaffolds



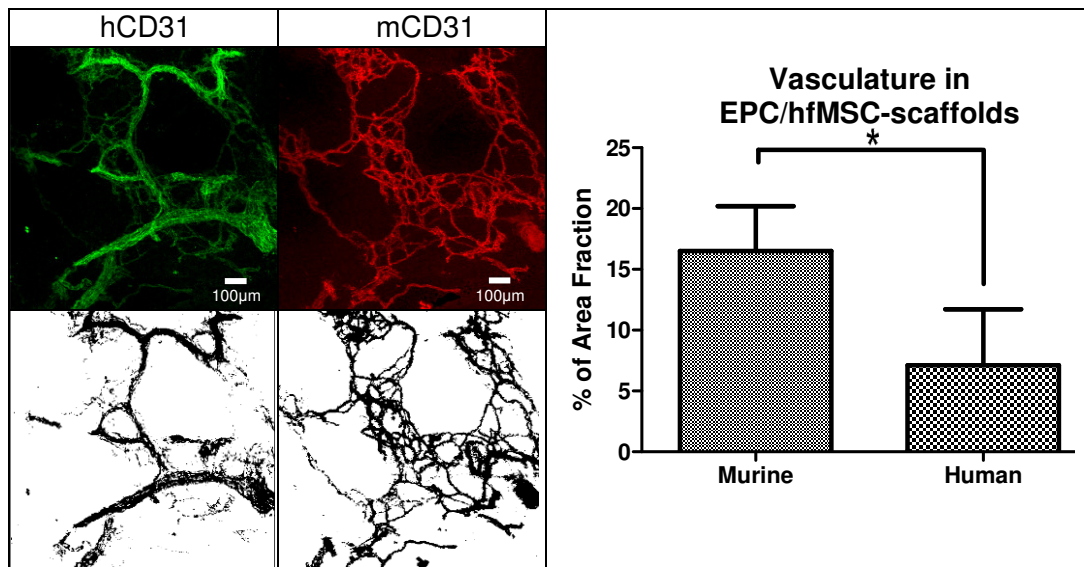
C. Cross Sectional View of Slide



D. Identification and Quantification of Murine Vessel Structures



E: Quantification of Human and Murine Vasculature in EPC/hfMSC Scaffolds



F. Human : Mouse Chimerism

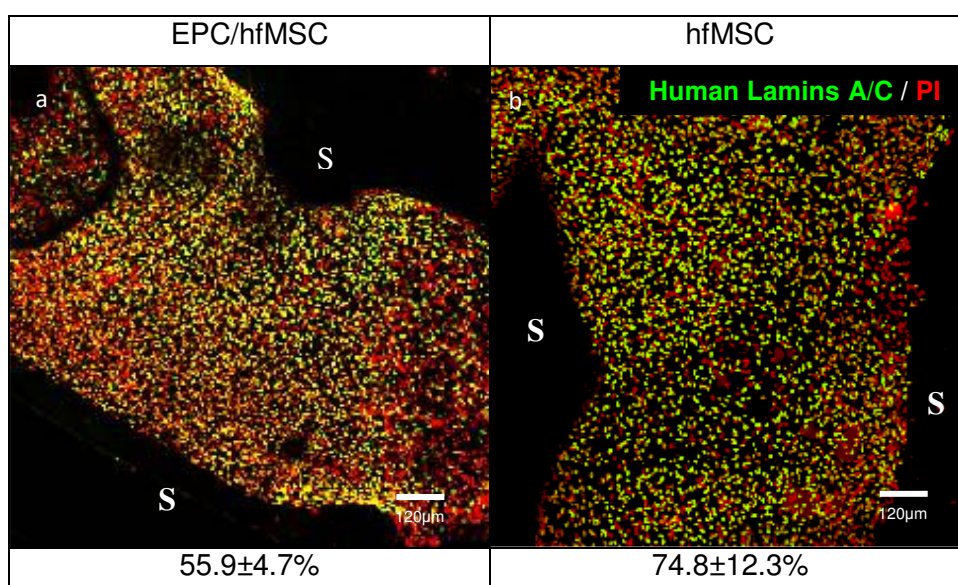
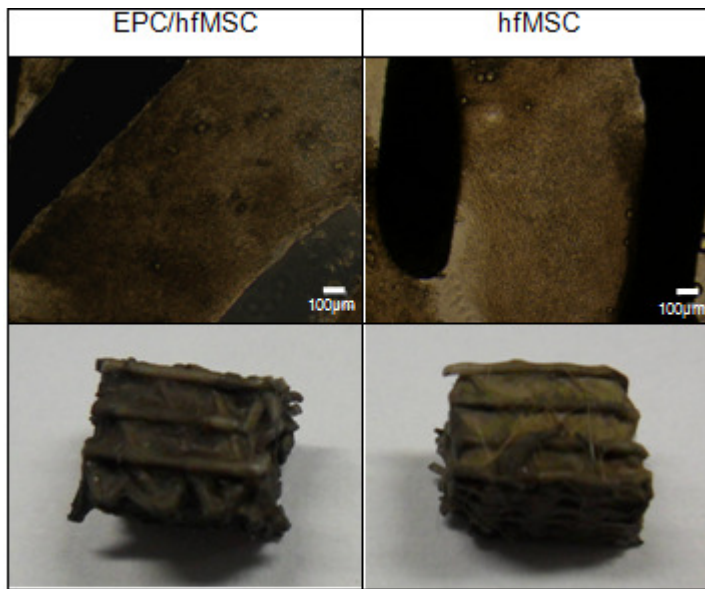


Figure 4-9: *In vivo* neovascularisation and ectopic bone formation. A) Increased vascularisation of the EPC/hfMSC scaffolds evident three weeks after implantation, as seen after Microfil perfusion (blue vessels). (B) At eight weeks, human blood vessels stained with human specific CD31 (green) were seen coursing through EPC/hfMSC scaffolds but not hfMSC scaffolds. These human vessels can be seen enmeshed with murine vessels (stained red with murine CD31 antibody) as evident in a 50 µm section [merged and stacked confocal images (C)]. EPC/hfMSC scaffolds contained a 2.2 fold ($p=0.001$) higher density of host-derived murine-CD31 positive vessels (red) compared to hfMSC scaffolds (arrows indicating area of human-murine vasculature junctures (D), while human vessels constituted 30.2% of the total vessel area within the construct (E). (F) Immunostaining with human Lamins A/C demonstrated high levels of chimerism in both scaffolds, with a trend towards lower human cell chimerism in EPC/hfMSC scaffolds compared with hfMSC scaffolds.

4.4.9 Ectopic Bone Forming Ability of EPC/hfMSC Cocultures

Von Kossa staining revealed darker staining in EPC/hfMSC scaffolds (**Figure 4-10A**), suggesting greater osteogenic differentiation was induced in the cocultured scaffolds. This was verified by the calcium quantification which showed a trend towards greater ectopic bone formation in the coculture group (**Figure 4-10B**), implicating the increased vascularisation in enhancing osteogenic differentiation *in vivo*.

A. Ectopic Bone Formation



B. Calcium Content Assay

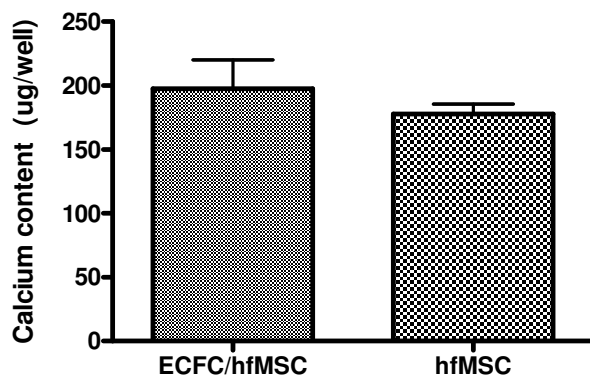


Figure 4-10: (A-B) Von Kossa staining of the implants showed darker level of staining (Scaffold regions has been denoted as S) and a slightly higher level of calcium deposited in EPC/hfMSC scaffolds compared to hfMSC scaffold. “**” ($p < 0.05$)

4.5 Discussion

Several groups have cocultured putative EPC with MSC or osteoblast-like cell types on the premise that this strategy will generate prevascular networks within bone tissue-engineered grafts to aid bone repair (Fuchs *et al.* 2007; Melero-Martin *et al.* 2008; Fuchs *et al.* 2009; Usami *et al.* 2009; Seebach *et al.* 2010; Tsigkou *et al.* 2010). However, the majority of studies used EC (Kaigler *et al.* 2005; Unger *et al.* 2007;

Unger *et al.* 2010; Koob *et al.* 2011; Saleh *et al.* 2011), rather than EPC. In this project, well-characterised UCB-EPC were cocultured with hfMSC (Zhang *et al.* 2009) chosen primarily for their ability to undergo a well-defined osteogenic differentiation pathway (Frank *et al.* 2002; Guillot *et al.* 2008; Zhang *et al.* 2009) and superiority in osteogenic differentiation over adult counterparts (Guillot *et al.* 2008; Zhang *et al.* 2009) for bone tissue engineering applications. I unexpectedly found a 2 fold enhancement in the osteogenic differentiation of hfMSC when cocultured with UCB-EPC, and showed that this effect was at least in part through paracrine signalling involving secreted members of the TGF β superfamily. In addition, the addition of UCB-EPC to hfMSC led to the formation of tube-like network of endothelial structures *in vitro*, with the generation of chimeric human-murine blood vessels and enhancement of host-neovascularisation *in vivo*. Further, I provided evidence that there is an ontological advantage in skeletal morphogenesis and angiogenesis of the more primitive UCB derived EPC over adult sources.

EPC were first identified in peripheral blood (Asahara *et al.* 1997) and subsequently isolated from other sources including bone marrow, fetal liver and umbilical cord blood (Richardson and Yoder 2011). However, the isolation of EPC from umbilical cord blood is still favoured over other sites due to its plentiful supply and non-invasive collection process. In addition, EPC in UCB are found at higher frequencies and have higher proliferative and vasculogenic capacity than adult PB-EPC (Ingram *et al.* 2004).

Studies of EPC have largely focused on their vasculogenic potential, with evidence of efficacy in augmenting neovascularisation in several different ischemic models. Recently, there has been increasing interest in the use of EPC populations for bone repair in mice (Matsumoto *et al.* 2008), rat (Atesok *et al.* 2010) and ovine models (Rozen *et al.* 2009). The key finding was a potentiated osteogenic response of

hfMSC *in vitro* via paracrine signaling, where soluble factors present in EPC conditioned media exerted a profound effect on osteogenic differentiation of hfMSC. The probable mechanism mediating the enhanced osteogenic effect is likely to be soluble factors secreted by EPC when cocultured in BM, given the lack of osteogenic induction when the coculture was performed in basal hfMSC growth media. Bone inductive components in BM could have been responsible for inducing osteo-inductive secretions in EPC as detected by the protein array blot which identified a milieu of secreted factors present in EPC conditioned media, with negligible levels of these proteins found in BM alone (data not shown). The bone-related morphogens detected included BMP-5, BMP-6, BMP-7, TGF- β 1, TGF- β 2, which are known key facilitators or inducers of osteogenic programming in MSC. BMPs and TGF β s of the TGF β superfamily are produced by osteoblasts and other bone cells incorporated into mineralised matrix, thus contributing to osteoblast differentiation *in vitro* (Cho *et al.* 2002). *In vivo*, such growth factors participate actively in various stages of intramembranous and endochondral bone ossification for bone formation and remodelling (Reddi 1981). In particular, the potent osteo-inductive abilities of BMPs have been widely demonstrated in various animal and clinical studies (Luginbuehl *et al.* 2004) and more recently, BMP-2 has also been used as an adjunct to the standard of care in the BMP-2 Evaluation in Surgery for Tibial Trauma (BESTT) study involving 450 patients with diaphyseal open tibial fractures (Nordsletten 2006). Despite the low relative levels of BMP detected, EPC conditioned media was still able to induce a significant increase in osteogenic differentiation of MSC in a dose-dependent manner. In addition, VEGF detected in EPC conditioned media may have contributed significantly to the observed phenomena. VEGF has been reported to induce ALP activity in osteoblasts (Midy and Plouet 1994) and enhance osteoblast differentiation (Deckers *et al.* 2000). Behr *et al.* also demonstrated that VEGF-A promotes osteogenic and endothelial differentiation (Behr *et al.* 2011), thus playing a significant role in skeletal repair (Peng *et al.* 2002). Other bone-morphogenic factors

such as FGFs, PDGF, oncostatin M, and endoglin have also been reported to induce osteoblast differentiation. The effects of multiple osteogenic factors secreted by EPC could have acted in synergy to enhance the potency of osteogenic differentiation of MSC, leading to the strong enhancement in mineralisation observed *in vitro*.

Few groups have investigated the mechanism behind these enhanced osteogenic effects. Dohle and colleagues, through a study of primary osteoblast and adult peripheral blood late endothelial outgrowth cocultures implicated the sonic hedgehog (Shh) pathway as a key modulator in EPC-enhanced osteogenesis through supplementation of Shh and its inhibitor (Dohle *et al.* 2010). Saleh *et al.* in demonstrating enhanced proliferation and osteogenic differentiation of human MSC exposed to conditioned media from HUVECs alluded to the possibility of FGF, Wnt, BMP and Notch pathways as possible regulators of this phenomenon (Saleh *et al.* 2011), albeit without identifying these putative regulators directly. Wang and colleagues showed that cocultured HUVECs augmented osteogenic differentiation of adipose-derived MSC, with BMP-2 being identified in HUVEC conditioned media, although they did not test its paracrine activity (Wang *et al.* 2011). In contrast to my suggested mechanism of paracrine signalling, several other groups failed to show osteogenic enhancement when MSC were cultured in the conditioned media of endothelial cells (Villars *et al.* 2000), instead suggesting direct cell-cell contact *via* gap junction communication was required to mediate the osteogenic enhancement effect (Villars *et al.* 2002; Kaigler *et al.* 2005). These groups however, employed mature human endothelial cells in coculture with osteoblast-like cells, which although they have shown promise in generating a prevascularised network (Tsigkou *et al.* 2010; Unger *et al.* 2010) and/or enhancing osteogenesis (Villars *et al.* 2000; Villars *et al.* 2002; Kaigler *et al.* 2005; Rouwkema *et al.* 2006; Grellier *et al.* 2009; Koob *et al.* 2011), their biological phenotype depends upon the site of the endothelium from which they were harvested from (Aird 2007).

The use of BM to stimulate osteogenic differentiation of MSC, while maintaining high survivability of EPC without altering phenotypic stability (Fuchs *et al.* 2007) is essential for the observed enhanced osteogenic differentiation. EPC survived in monoculture at high levels of confluence in BM while maintaining their cobblestone morphology in the absence of any standard endothelial growth factors supplements (VEGF, EGF, bFGF, IGF-1, ascorbic acid, hydrocortisone and heparin). This is likely due to the presence of dexamethasone in BM, a potent synthetic glucocorticoid critical for EPC survival as an alternative to the hydrocortisone supplemented in EGM. In contrast to my findings, others have suggested that growth factor supplements are necessary to sustain EPC survival. Usami and colleagues attributed the difficulties of coculturing EPC and MSC in direct contact to the inability of EPCs to survive in osteogenic media, and resorted to culturing the cells on Polylactide-coated collagen fiber mesh separately in their respective growth media prior to coimplantation *in vivo* (Usami *et al.* 2009). Other similar studies maintained cocultures in EGM instead (Fuchs *et al.* 2007; Fuchs *et al.* 2009; Rouwkema *et al.* 2009). In this study, UCB-EPC were unable to induce osteogenic differentiation on hfMSC in the absence of bone inductive components of dexamethasone, ascorbate and β -glycerophosphate.

By comparing the transcriptome of well-defined EPC populations derived from primitive UCB with mature adult PB-EPC from a previous study (Medina *et al.* 2010), both osteogenic and vasculogenic genes were significantly more expressed in UCB compared to adult PB-EPC. While the higher vasculogenic potential of UCB-derived EPC is largely expected, the higher expression of osteogenesis-related genes here may reflect the intense skeletal development occurring during neonatal life as compared to the mature adult. These circulating EPC are found at higher frequencies during neonatal life compared to adult life (Murohara *et al.* 2000), with increased mobilisation in the event of bony injury (Laing *et al.* 2007; Fujio *et al.* 2011).

In cocultures, EPC organised into islets that with decreasing cluster sizes from Day 7 onwards, formed tubular structures which increased branching complexity over time during MSC coculture, while on their own, EPC monocultures were unable to form vascular networks on a collagen matrix. Establishment of more complex vessel-like networks was seen when EPC/hfMSC were cocultured within 3D macroporous scaffolds in BM culture. This suggests that MSC have a critical support function on endothelial cell survival and sprouting *in vitro*, in agreement with findings from other groups (Au *et al.* 2008; Tsigkou *et al.* 2010). Subcutaneous implants of these coculture constructs in mice further supported the observations *in vitro*, with more extensive neovascularisation of the scaffolds at three and eight weeks post implantation compared to MSC alone. Human-murine chimeric vessels were seen on confocal sections and species-specific immunohistochemistry only in EPC/hfMSC cocultures, with human specific CD31 positive structures arranged in a lumen-like fashion. This finding is consistent with previous reports (Au *et al.* 2008; Melero-Martin *et al.* 2008; Fuchs *et al.* 2009; Rouwkema *et al.* 2009; Unger *et al.* 2010).

By probing the transcriptome and secretome of UCB-EPC, I identified several pro-inflammatory and angiogenic cytokines, in particularly Angiogenin, Angiopoietin-2 and PDGF-BB that were found in relatively high concentrations which could have contributed to this *in vivo* observation of increased angiogenesis. Inflammatory cytokines such as IL-1, IL-6 and TNF- α , and other angiogenic protagonists such as VEGF, bFGF, angiopoietins, PDGF-BB - angiogenin, IL-8, bFGF, FGF-4, TGF- β , VEGF (Kanczler and Oreffo 2008), have a direct stimulatory effect on angiogenesis *in vivo*. Such increase in vascularisation could make a direct contribution to bone formation, as evident in the increased ectopic bone formed in the EPC/MS constructs, suggesting an interdependent relationship between vascularisation and bone formation. Usami *et al* found a 1.6 fold higher capillary score formation on both the surface and central regions of canine-EPC/MS scaffolds, accompanied by a 1.3

fold increase in bone area regenerated in subcutaneous implants (Usami *et al.* 2009), while Seebach *et al.* demonstrated increased early vascularisation in the first four weeks with improved bone regeneration and healing in a rat critical-sized femoral defect model after EPC/MSC implantation compared to MSC alone (Seebach *et al.* 2010).

4.6 Conclusion

In addition to their vasculogenic potential, circulating EPC in late fetal/neonatal life have significant osteogenic-inducing capacity, which they effect through secretion of potent osteogenic regulators from the TGF β superfamily. The interaction of UCB-EPC with hfMSC allows both the generation of stable functional blood vessels and the direct potentiation of hfMSC osteogenic differentiation through secreted factors. These effects alone or in combination are likely to lend themselves towards applications in regenerative medicine and tissue engineering.